BAR-ILAN UNIVERSITY

Nonlinear Optical Response of Periodic Structures in the X-ray Regime

Ron Cohen

Submitted in partial fulfillment of the requirements for the
Master's Degree in the Department of Physics, Bar-Ilan
University

Ramat Gan, Israel 2019

This work was carried out under the supervision of

Prof. Sharon Shwartz

Department of Physics, Bar-Ilan University

Acknowledgments

I would like to express my sincere gratitude and appreciation to my supervisor Prof. Sharon Shwartz, from whom I have learned greatly about physics and what it entails to do research. I would also like to thank Prof. Shwartz for guiding and supporting me during my MSc studies.

I would like to thank Dr. Emanuele G. Dalla Torre, and Prof. Efrat Shimshoni for inspiring and useful discussion.

I would like to thank Mrs. Hila Schwartz for her support and assistance during my time in the group.

I would like to thank my group members (past and present): Dr. Aviad Schori, Dr. Eli Schwartz, Dr. Denis Borodin, Mr. Shimon Yudovich, Mr. Edward Strizhevsky, Mr. Yonathan Frohlich, Mr. Sarig Namer, Mrs. Shiran Tsalisher-Levy, Mr. Eviatar Minerbi, Mr. Yishay Klein, Mr. Sason Sofer, Mr. Or Sefi, Mr. Sergey Volkovich, Mr. Amram Malkosh, Mr. Haim Aknin and Mr. Adi Ben Yehuda for supporting, teaching and inspiring me during my studies.

I would like to express my sincere appreciation to the administrative staff of the physics department, Rachel Rothberg, Rita Golender, and Dr. Yossi Ben-Zion for their help and assistance.

Finally, I would like to thank my family and friends for supporting me during my studies.

Contents

Abstract

In this work, I have developed a theoretical description for the nonlinear optical response of crystals. The nonlinear optical response described in this work involves the mixing of two radiation fields. As a specific example I have focused on the process of Spontaneous Parametric Down-Conversion (SPDC) of x-ray into optical radiation. I have examined the nonlinear optical response dependence on the band structure, fields polarizations and inter-molecular interactions. In addition, I have examined a specific case of two bands, illustrated the spectral dependence and also considered an estimation on the contribution from inter-molecular interactions. The nonlinear response depends on the interaction between the radiation fields and intrinsic properties of the medium such as the band structure and other related properties. These types of interactions can be used to reveal microscopic information on fundamental properties of crystalline bulk materials.

The theoretical approach uses perturbation theory in the density matrix formalism. Since this approach relies on statistical parameters, it provides access to investigate statistical properties, such as temperature dependence, Fermi energy, population probabilities and density of states.

Previous descriptions of the nonlinearity in this spectral region, considered the periodicity of the crystal, but not the band structure. The previous works showed that it is possible to relate the nonlinearity to microscopic information on the valence electrons at the atomic scale resolution. In contrast, my work suggests that the nonlinear interactions also contain information that is related to the periodic potential of the crystal, such as the band structure, and describes the conditions for which the two contributions are separable. My theory also predicts a new polarization dependence, which can be used to probe different terms of the interaction, and thus can provide additional information. The key results of this thesis work were recently published [1].

Recent experimental results were found to be in agreement with some of the

theoretical predictions of my work. In particular, recent experiments showed an enhancement at the band gap energy [2, 3]. Another experiment, by S. Sofer et al., showed a new polarization dependence. The strong dependence on the joint-density of states as well as the new polarization dependence, are both in agreement with these experimental results respectively.

Since the theory suggests that the interaction arises from both band structure properties and atomic-scale interactions, it can pave the way to utilize nonlinear effects of x rays and long wavelengths to reveal a very broad band spectroscopic information and structural information of valence electrons.

1 Introduction

The possibility to utilize nonlinear interactions between x rays and radiation at wavelengths ranging from infrared (IR) to ultraviolet (UV) as an atomic-scale probe for inter-molecular interactions and for properties of valence electrons has been discussed in several publications [2–10]. The prospect of utilizing nonlinear effects to develop such a probe, relies on on the atomic scale wavelengths of the x-rays, which provide the high resolution, while the longer wavelengths (UV/optical) are used to enhance the interactions with the valence electrons, which are usually weak for x rays.

Recent experimental evidence of spontaneous parametric down conversion (SPDC) of x rays into UV [2, 3, 6, 10–12] suggests that nonlinear interactions between x rays and longer wavelengths can be used also as new spectroscopy tools for the investigation of phenomena that traditionally are probed by using long wavelength radiation with the advantage of providing microscopic atomic-scale information. Furthermore, in contrast to electron or ion scattering techniques, x-rays penetrate into materials more than electrons and therefore can provide bulk properties.

Nonlinear mixing effects between x ray and optical/UV are weak, and therefore the measurement of such effects produces a challenge. To overcome the challenge of measuring such effects, experiments are performed with crystals where the periodic structure is used to enhance the signal in analogy to Bragg scattering, in which the reciprocal lattice vector is used to achieve momentum conservation (phase matching). The use of the reciprocal lattice vector also provides the atomic scale resolution, which can be achieved by measuring the efficiencies of the effect for many reciprocal lattice vectors and by using Fourier analysis [6]. Since the goal of the measurements is to probe microscopic information, the use of crystals introduces a new challenge for the interpretation of the results since the measured signal depends not just on the atomic or inter unit cell interactions between the valence electrons but also on the properties related to the periodic potential of the materials, such as the band structure. It is therefore essential to develop a formalism that enables the separation of the two contributions. The theoretical formalism presented in this work, shows how the nonlinear response depends on both inter-molecular interactions and the band structure, and present the conditions in which these two contributions are separable.

To date, most theoretical models that have been considered for the description of nonlinear interactions between x rays and longer wavelengths have focused on the ability to observe microscopic information and on the estimation of the strength of the effects [5–9, 13–16]. However, they have not addressed the challenge of the separation of the inter unit cell information from the periodic information. I note that Freund and Levine and also Jha and colleagues [13–15, 17–21] have considered the periodic structure but not the influence of the electronic band structure on the nonlinear interactions, which can be significant for valence electrons with binding energies that are weaker or on the order of the periodic potential.

In several recent experimental papers, the experimental results were fitted to the theory by using the band gap rather than the atomic binding energy, but although good agreements were obtained for transparent materials, this approach is phenomenological and failed for energies near or above the band gap [2]. In this work, I illustrate how the nonlinear interaction between x-rays and longer wavelengths depends on the band structure and related properties by using perturbation theory in the density matrix formalism. As an example I describe explicitly the dependence of the nonlinear interactions on the joint density of states of interband transitions. In addition, I analyze the polarization dependencies of the nonlinear interactions and predict that it is not trivial.

2 Background

In this section I will review the theoretical background this work is based on. First, I will introduce the concept of optical response, and the physical characteristics of it, I will then review the theoretical framework I used to describe the optical response in a periodic system and conclude with a brief introduction to the process of Spontaneous Parametric Down-Conversion (SPDC), for which the nonlinear optical response is being investigated in this work.

2.1 Nonlinear optical response

The focus of this work is on the second order nonlinearity, which can be used to describe many nonlinear optical effects such as sum-frequency generation (SFG) and SPDC. Schematic diagrams for these processes are presented in Fig. 1.

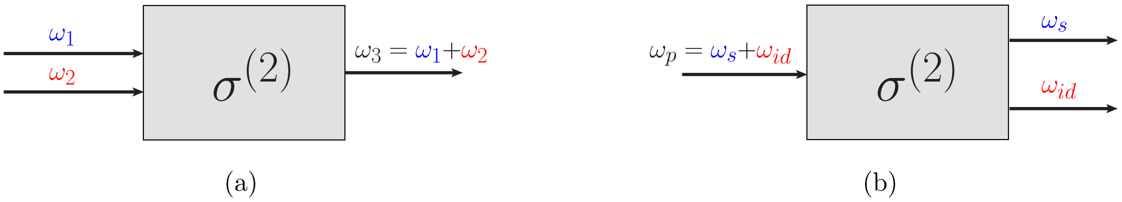

Figure 1: Schematic diagrams for the nonlinear processes of SFG and SPDC. (a) SFG: two input photons at frequencies ω_1 and ω_2 are converted to a photon at frequency $\omega_3 = \omega_1 + \omega_2$. (b) SPDC: an input pump photon at frequency ω_p interacts with the vacuum field, to produce a converted photon pair at frequencies ω_s and ω_{id}.

The optical response of a system is characterized by the interactions between incident electromagnetic (EM) fields and a medium. The incident fields induce currents in the medium, which act as sources for radiation, which can interact with the incident fields and so forth.

These induced currents are introduced as a source in the wave equation for the fields. The EM wave equation for the electric field, can be written as

$$\left(\nabla^2 - \frac{1}{c^2}\frac{\partial^2}{\partial t^2}\right)\mathbf{E} = \mu_0 \frac{\partial \boldsymbol{j}}{\partial t}, \tag{2.1.1}$$

where $\mathbf{E}$ is the electric field, and $\boldsymbol{j}$ is the current density. The current density describes the optical response of a system, but it can also be described by its associated conductivity via the tensor form of Ohm's law.

Under the assumption that the electric field is a sum of monochromatic waves, the resultant current density is also a sum of monochromatic waves, namely

$$\mathbf{E}(\boldsymbol{x}, t) = \sum_n \left[\boldsymbol{\varepsilon}(\omega_n) e^{-i\omega_n t} + \text{c.c.}\right], \quad \boldsymbol{j}(\boldsymbol{x}, t) = \sum_n \left[\boldsymbol{j}(\boldsymbol{x}; \omega_n) e^{-i\omega_n t} + \text{c.c.}\right], \tag{2.1.2}$$

where $\boldsymbol{\varepsilon}(\omega_n)$ and $\boldsymbol{j}(\boldsymbol{x}; \omega_n)$ are the electric field and current density amplitudes of mode ω_n, and c.c. stands for the complex conjugate of the neighboring term.

In this case, Ohm's law relates between the Fourier coefficients of the current density and the electric field, for the linear case according to

$$\boldsymbol{j}^{(1)}(\boldsymbol{x}; \omega_n) \cdot \hat{e}_i = \sum_j \sigma_{ij}^{(1)}(\boldsymbol{x}; \omega_n)(\boldsymbol{\varepsilon}(\omega_n) \cdot \hat{e}_j), \tag{2.1.3}$$

where $\boldsymbol{j}^{(1)}(\boldsymbol{x}; \omega_n)$ and $\sigma_{ij}^{(1)}(\boldsymbol{x}; \omega_n)$ are the linear current density field amplitude and the linear conductivity at mode ω_n respectively, $\hat{e}_i$ is a unit vector in the i-th direction, and $\{i, j\}$ indicates Cartesian coordinates.

This relation can be extended for nonlinear response to various orders.

The second order nonlinear current density Fourier component is associated to the second order conductivity in the following way

$$\begin{aligned}
&\boldsymbol{j}^{(2)}(\boldsymbol{x};\omega_l+\omega_{l'})\cdot\hat{e}_i\\
&=\sum_{j,k=1}^{3}\sigma^{(2)}_{ijk}(\boldsymbol{x};\omega_l+\omega_{l'},\omega_l,\omega_{l'})\left(\boldsymbol{\varepsilon}(\omega_l)\cdot\hat{e}_j\right)\left(\boldsymbol{\varepsilon}(\omega_{l'})\cdot\hat{e}_k\right)\\
&+\sum_{j,k=1}^{3}\sigma^{(2)}_{ijk}(\boldsymbol{x};\omega_{l'}+\omega_l,\omega_{l'},\omega_l)\left(\boldsymbol{\varepsilon}(\omega_{l'})\cdot\hat{e}_j\right)\left(\boldsymbol{\varepsilon}(\omega_l)\cdot\hat{e}_k\right)\\
&=\sum_{j,k=1}^{3}\Big[\sigma^{(2)}_{ijk}(\boldsymbol{x};\omega_l+\omega_{l'},\omega_l,\omega_{l'})+\sigma^{(2)}_{ikj}(\boldsymbol{x};\omega_{l'}+\omega_l,\omega_{l'},\omega_l)\Big]\left(\boldsymbol{\varepsilon}(\omega_l)\cdot\hat{e}_j\right)\left(\boldsymbol{\varepsilon}(\omega_{l'})\cdot\hat{e}_k\right)\\
&=\sum_{j,k=1}^{3}\;\sigma^{(2)}_{ijk}(\boldsymbol{x};\omega_l+\omega_{l'})\left(\boldsymbol{\varepsilon}(\omega_l)\cdot\hat{e}_j\right)\left(\boldsymbol{\varepsilon}(\omega_{l'})\cdot\hat{e}_k\right).
\end{aligned}\tag{2.1.4}$$

Note that this form of the conductivity

$$\sigma^{(2)}_{ijk}(\boldsymbol{x};\omega_l+\omega_{l'})=\sigma^{(2)}_{ijk}(\boldsymbol{x};\omega_l+\omega_{l'},\omega_l,\omega_{l'})+\sigma^{(2)}_{ikj}(\boldsymbol{x};\omega_{l'}+\omega_l,\omega_{l'},\omega_l),\tag{2.1.5}$$

assures that it conserves intrinsic permutation symmetry, namely

$$\sigma^{(2)}_{ijk}(\boldsymbol{x};\omega_l+\omega_{l'})=\sigma^{(2)}_{ikj}(\boldsymbol{x};\omega_{l'}+\omega_l).\tag{2.1.6}$$

To conclude, it is sufficient to characterize the optical response of the material by its associated conductivity, since one can easily reconstruct from it the wave equation for the optical process of interest.

2.2 Hamiltonian

Since the goal is to find the optical response of a periodic structure, I first need to characterize the medium.

The Hamiltonian used to describe the medium is the one electron Bloch Hamiltonian $\mathcal{H}_0$ and it describes an electron bounded by a periodic potential.

$$\mathcal{H}_0=\frac{\mathbf{p}^2}{2m}+V(\boldsymbol{x}),\tag{2.2.1}$$

where the electron mass is m and the momentum operator is $\mathbf{p}$.

The potential $V(\boldsymbol{x}) = V(\boldsymbol{x}+\mathbf{R})$ is periodic with respect to translation by a lattice vector, where $\mathbf{R}$ is any lattice vector.

The solutions of the Hamiltonian $\mathcal{H}_0$ are given by the Bloch states

$$\mathcal{H}_0 \left| n\, \mathbf{q} \right\rangle = \varepsilon_n(\mathbf{q}) \left| n\, \mathbf{q} \right\rangle , \tag{2.2.2}$$

with eigenvalues $\varepsilon_n(\mathbf{q})$, where n is the band number and $\mathbf{q}$ is the wave vector associated with the Bloch state.

To describe the interaction between the electron and the electromagnetic field, I used the minimal coupling interaction term, so that the full Hamiltonian is of the form

$$\mathcal{H} = \mathcal{H}_0 + \mathcal{H}_{\text{int}} = \frac{(\mathbf{p}+e\mathbf{A})^2}{2m} + V(\boldsymbol{x}), \tag{2.2.3}$$

and the interaction Hamiltonian is

$$\mathcal{H}_{\text{int}} = \frac{e}{2m}\left(\mathbf{p}\cdot\mathbf{A} + \mathbf{A}\cdot\mathbf{p}\right) + \frac{e^2}{2m}\mathbf{A}^2, \tag{2.2.4}$$

where $\mathbf{A}$ is the electromagnetic vector potential, and $-e$ is the electron charge.

In this work the vector potential was assumed to be in the coulomb gauge ($\boldsymbol{\nabla}\cdot\mathbf{A} = 0$), and the scalar potential is zero. This choice was taken since the vector potential is sufficient to describe the external field. Under this gauge choice, the relation between the vector potential and the electric field is

$$\mathbf{E} = -\frac{\partial \mathbf{A}}{\partial t}. \tag{2.2.5}$$

Under the assumption that the field is comprised of a sum of monochromatic waves (Eq. 2.1.2), the vector potential can be expressed in terms of the electric field amplitudes in the following way

$$\mathbf{A}(\boldsymbol{x},t) = \sum_l \left[\frac{\boldsymbol{\varepsilon}(\omega_l)}{i\omega_l} e^{-i\omega_l t} + c.c.\right]. \tag{2.2.6}$$

Expressing the vector potential in this manner is convenient for the purpose of evaluating the conductivity, according to Ohm's law (Eqs. 2.1.3, 2.1.4).

2.3 Density matrix formalism

To evaluate the current density from which the conductivity will be derived, I used the density matrix formalism. This formalism is used to describe the interaction between the medium and the EM fields.

The density matrix is used to describe an ensemble of identical quantum systems. This formalism takes into account the statistical uncertainties of a real system and therefore is very useful for practical purposes. The density matrix ρ, is governed by the equation [22]

$$i\hbar\frac{\partial\rho_{nm}}{\partial t} = [\mathcal{H}_0 + \mathcal{H}_{\text{int}}, \rho]_{nm} - i\hbar\gamma_{nm}\left(\rho_{nm} - \rho^{(0)}_{nm}\right), \tag{2.3.1}$$

where $\rho_{nm} = \langle n|\,\rho\,|m\rangle$, the commutator $[\mathcal{H}_0 + \mathcal{H}_{\text{int}}, \rho]_{nm} = \langle n|\,[\mathcal{H}_0 + \mathcal{H}_{\text{int}}, \rho]\,|m\rangle$ and the states denoted by the quantum numbers n and m, are the eigenstates of the unperturbed Hamiltonian $\mathcal{H}_0$. The phenomenological damping coefficients are denoted by γ_{nm} and $\rho^{(0)} = f_0(\mathcal{H}_0)$ is the relaxed density matrix which is the normalized Fermi-Dirac distribution, such that $\text{tr}\big(\rho^{(0)}\big) = 1$.

The diagonal elements ρ_{nn} give the probability of occupying a quantum state $|n\rangle$ and therefore are referred to as populations. The off-diagonal elements ρ_{nm} describes the evolution of coherent superpositions and are referred to as coherences. Under the assumption that $\mathcal{H}_{int}$ is a small perturbation, one can use perturbation theory.

2.3.1 Perturbation theory

To develop a perturbative scheme one can expand the density matrix in the following form

$$\rho_{nm} = \sum_k \lambda^k \rho_{nm}^{(k)} = \rho_{nm}^{(0)} + \lambda \rho_{nm}^{(1)} + \lambda^2 \rho_{nm}^{(2)} + \cdots \tag{2.3.2}$$

by replacing the perturbation Hamiltonian $\mathcal{H}_{\text{int}} \to \lambda \mathcal{H}_{\text{int}}$, where $\rho_{nm}^{(k)}$ is the perturbation theory solution of the density matrix of order k. This leads to a set of iterative equations [22].

$$\frac{\partial \rho_{nm}^{(k)}}{\partial t} = -(i\omega_{nm} + \gamma_{nm})\rho_{nm}^{(k)} - \frac{i}{\hbar}\left[\mathcal{H}_{\text{int}}, \rho_{nm}^{(k-1)}\right]_{nm}, \tag{2.3.3}$$

where $\omega_{nm} = \frac{\langle n|\mathcal{H}_0|n\rangle - \langle m|\mathcal{H}_0|m\rangle}{\hbar} = \frac{\epsilon_n - \epsilon_m}{\hbar}$. (this scheme is developed in the eigenbasis of $\mathcal{H}_0$, and $\{n, m\}$ represent the quantum numbers of the system.)

Solving these differential equations up to the desired order concludes the scheme. For the solution presented by Eq. (2.3.2) to represent physical reality, I set $\lambda = 1$ at the end of the procedure.

The full density matrix $\rho(t)$, can then be expressed as a power series in the field $\mathbf{A}$

$$\rho(t) = \rho^{(0)} + \rho^{(A)} + \rho^{(AA)} + \cdots , \tag{2.3.4}$$

where the first term on the right hand side is the relaxed density matrix in the absence of the field, the second term is linear with the field amplitude, the third term is square in the field amplitude and so on.

After obtaining the solution for the density matrix it is possible to calculate observables and in particular to calculate the expectation value of the current density $\langle \boldsymbol{j} \rangle$.

2.3.2 Current density

In the density matrix formalism, calculation of an observable average $\langle O \rangle$ is given by

$$\langle O \rangle = \mathrm{tr}(\rho O), \tag{2.3.5}$$

where O is any physical operator of interest.

In the presence of an EM field, the current density operator [23] is

$$\boldsymbol{j}_{\mathrm{op}}(\boldsymbol{x},t) = \frac{-e}{2m}\left[|\boldsymbol{x}\rangle \langle \boldsymbol{x}| \left(\mathbf{p} + e\mathbf{A}\right) + \left(\mathbf{p} + e\mathbf{A}\right) |\boldsymbol{x}\rangle \langle \boldsymbol{x}| \right], \tag{2.3.6}$$

and thus the current density expectation value is given by

$$\langle \boldsymbol{j} \rangle (\boldsymbol{x},t) = \mathrm{tr}\big(\rho(t)\boldsymbol{j}_{\mathrm{op}}(\boldsymbol{x},t)\big). \tag{2.3.7}$$

Once attaing the current density, the evalution of the conductivity is done using Ohm's law (Eqs. 2.1.3, 2.1.4).

2.4 X-ray spontaneous parametric down-conversion

This subsection includes a brief introduction to the process of X-ray spontaneous parametric down-conversion.

2.4.1 Literature review

Spontaneous parametric down-conversion (SPDC) is a second order nonlinear process, where an incident photon called pump (with frequency ω_p) converts into two photons conventionally called signal and idler (with frequencies ω_s and ω_{id} respectively), such that $\omega_p = \omega_s + \omega_{id}$. The conversion occurs in the nonlinear medium and it is a quantum process since it is stimulated by vacuum fluctuations [19].

The effect of SPDC was first observed experimentally and described theoretically in the 1960's in the visible region [24–31]. Freund's work on nonlinear diffraction [17] offered to use a reciprocal lattice vector to meet phase-matching conditions which led to the development of SPDC in the x-ray region [13, 19]. The first experimental observation of SPDC in the x-ray region was done in 1971 by Eisenberger and McCall [32], where they used Mo target x-ray tube as a source for the pump photons at 17 keV, hitting a beryllium crystal, producing degenerate photon pairs with energy of 8.5 keV. In 1972 Freund suggested the possibility of experimental determination of the valence electron charge density using SPDC of x-rays into a lower energy x-ray and UV [15]. The proposed method was to select the UV energy to be between the UV band gap and the lowest absorption edge of the inner shell electrons, where the nonlinearity is dominated by the charge distribution of the valence electrons. Following that work, in 1981 Freund and Danino observed SPDC of an x-ray pump (produced from Cu-Kα $\sim$8.04keV) into x-ray (signal - 7.7keV) and extreme ultraviolet (idler - 335eV) [4]. In that paper they reiterated that a direct determination of valence electron charge distributions is possible. In 2007 Tamasaku et al. investigated theoretically and experimentally the effect of SPDC of x-ray into extreme ultraviolet taking into account Compton scattering and suggested the possibility of interference between the two processes [11, 33]. Later they demonstrated that x-ray SPDC is observable indirectly via the Fano effect and were able to determine the second order susceptibility [5]. Following that work, Tamasaku et al. demonstrated the x-ray SPDC into UV effect with high resolution and calculated the first and second order susceptibilities [6]. In a recent work by our group, Borodin et al. first reported the high energy-resolution measurement of SPDC of x-ray into UV in diamond and in lithium fluoride crystals, using an x-ray tube source [12]. Subsequently, Schori et al. first reported the experimental observation of SPDC of x rays to optical wave-lengths [2]. Later on, Borodin et al. reported the observation of collective effects in x-ray into UV in diamond crystal [10]. The authors proposed an interpretation which includes nonlinear interactions with plasmons. In a recently accepted publication by our group, Sofer et al. reported the observation of SPDC of x rays into UV in gallium arsenide and lithium niobate crystals [3]. The authors used crystals with no center of symmetry, and measured the effect with efficiencies that are about 4 orders of magnitude stronger than in any material studied before.

2.4.2 Kinematics

For the SPDC process to be efficient, phase-matching condition is required. This condition reflects conservation of momentum, and when it is met, the efficiency of the process is maximal. In the x-ray region, reciprocal lattice vectors are used to achieve phase-matching. This is possible since the reciprocal lattice vectors and the pump wave vector are on the same order of magnitude. The phase-matching condition for x-ray SPDC is shown by the diagram presented in Fig. 2, and can be written as

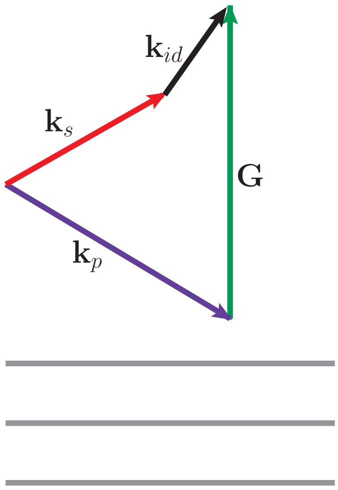

Figure 2: Phase-matching diagram. $\mathbf{k}_s$, $\mathbf{k}_{id}$ and $\mathbf{k}_p$ are the wave vectors of the signal, idler and pump fields, respectively. $\mathbf{G}$ is the reciprocal lattice vector.

$$\mathbf{k}_p + \mathbf{G} = \mathbf{k}_s + \mathbf{k}_{id}. \tag{2.4.1}$$

This condition along with the conservation of energy $\omega_p = \omega_s + \omega_{id}$, is taken into account in the wave equations for the process, thus is also enforced in the associated conductivity for the process.

3 Nonlinear optical response for crystals

In this section I follow the scheme presented in the background, and present my calculation for the general second order optical response of of periodic structures in the x-ray regime. It is important to note, that the scheme I used, to evaluate the current density, is very similar to the one presented by Jha and Warke [18].

I will begin with the evaluation of the density matrix up to second order and discuss the different terms and their origin. The next step will be the evaluation of the current density from the obtained density matrix. In this part I first find the temporal Fourier coefficients of the current density and then derive the conductivity. In the final step, I focus on the spatial Fourier coefficient of the conductivity. Since the Hamiltonian of the unperturbed system is of a periodic structure, the conductivity is also periodic and thus Fourier synthesis is possible.

3.1 Density matrix

In this section to evaluate the density matrix, I follow perturbation theory [18, 22]. For convenience of notation, the quantum numbers will be written by single number, such that the states, the Bloch wave functions and the energies will be written in the following way

$$\begin{aligned}
&|n\,\mathbf{q}\rangle \Rightarrow |n\rangle\,, \\
&\langle \boldsymbol{x}|n\,\mathbf{q}\rangle = \psi_{n\,\mathbf{q}}(\boldsymbol{x}) \Rightarrow \langle \boldsymbol{x}|n\rangle = \psi_n(\boldsymbol{x}), \\
&\langle n\,\mathbf{q}|\,\mathcal{H}_0\,|n\,\mathbf{q}\rangle = \varepsilon_n(\mathbf{q}) \Rightarrow \langle n|\,\mathcal{H}_0\,|n\rangle = \epsilon_n.
\end{aligned} \tag{3.1.1}$$

In later sections, where it will be important, the quantum numbers, states and energies will be written explicitly. In the scheme presented in the theoretical background, each perturbation theory order of the density matrix corresponds to the previous order by Eq. (2.3.3). I am interested in the effect of the perturbation in the long time limit, and so I assume that the perturbation was turned on at $t = -\infty$, and get the following solution

$$\rho_{nm}^{(k)}(t) = \rho_{nm}^{(0)}\delta_{k,0} - (1-\delta_{k,0})i\hbar^{-1}e^{-(i\omega_{nm}+\gamma_{nm})t}\int\limits_{-\infty}^{t} d\tau\, e^{(i\omega_{nm}+\gamma_{nm})\tau}\left[\mathcal{H}_{\text{int}}, \rho^{(k-1)}\right]_{nm}(\tau). \tag{3.1.2}$$

Since the relaxed density matrix is of the form $\rho^{(0)} = f_0(\mathcal{H}_0)$, it contains only diagonal elements. This also means that the perturbation will only add off-diagonal terms.

It is important to note that the perturbation consists of two terms, with one being linear with the field, and the other term being nonlinear with the field, such that it can be written as

$$\mathcal{H}_{\text{int}} = \mathcal{H}^A + \mathcal{H}^{AA}. \tag{3.1.3}$$

I denote the linear term as $\mathcal{H}^A$ and the other term, which is of second order in the field as $\mathcal{H}^{AA}$, and they are given by

$$\begin{aligned} \mathcal{H}^A &= \frac{e}{2m}\left(\mathbf{p}\cdot\mathbf{A} + \mathbf{A}\cdot\mathbf{p}\right) = \frac{e}{m}\mathbf{A}\cdot\mathbf{p}, \\ \mathcal{H}^{AA} &= \frac{e^2}{2m}\mathbf{A}^2, \end{aligned} \tag{3.1.4}$$

where $[\mathbf{p}, \mathbf{A}] = -i\hbar\boldsymbol{\nabla}\boldsymbol{\cdot}\mathbf{A} = 0$ was used in the first equation and the vector potential is a sum of plane waves, such that amplitude in Eq. (2.2.6) is $\boldsymbol{\varepsilon}(\omega_l) = \boldsymbol{\varepsilon}_l e^{i\mathbf{k}_l\cdot\boldsymbol{x}}$. This fact, along with the iterative solution given by Eq. (3.1.2), leads to that each order of the density matrix $\rho^{(k)}$, may contain several terms, with each term having different field dependence.

To put it simply, the density matrix of order k can be written as

$$\rho^{(k)} = \delta_{k,0}\rho^{(0)} + \sum_{j=1}\rho^{(k,A^j)}, \tag{3.1.5}$$

where $\rho^{(k,A^j)}$, is the k-th order density matrix with j-th order field dependence. The zeroth order having no field dependence, and the first two orders can be written as

$$\rho^{(1)} = \rho^{(1,A)} + \rho^{(1,A^2)}, \quad \rho^{(2)} = \rho^{(2,A^2)} + \rho^{(2,A^3)} + \rho^{(2,A^4)}. \tag{3.1.6}$$

This also means that if I use Eq. (2.3.4), I get

$$\rho^{(A)} = \rho^{(1,A)}, \qquad \rho^{(AA)} = \rho^{(1,A^2)} + \rho^{(2,A^2)}. \tag{3.1.7}$$

The solution given by Eq. (3.1.2) depends on matrix elements of the perturbation. These matrix elements can be Fourier expanded, since the field is a sum of plane waves.

$$\begin{aligned}
\mathcal{H}^A_{nm} &= \langle n| \mathcal{H}^A |m\rangle = \sum_l \left[\mathcal{H}^A(n,m,l)e^{-i\omega_l t} + c.c.\right], \\
\mathcal{H}^{AA}_{nm} &= \langle n| \mathcal{H}^{AA} |m\rangle = \sum_{l,l'} \left[\mathcal{H}^{AA}(n,m,l,l')e^{-i(\omega_l+\omega_{l'})t} + c.c.\right].
\end{aligned} \tag{3.1.8}$$

and the Fourier coefficients are given by

$$\mathcal{H}^A(n,m,l) = \frac{e}{im\omega_l}\boldsymbol{\varepsilon}_l \cdot \langle n| e^{i\mathbf{k}_l\cdot\boldsymbol{x}}\mathbf{p} |m\rangle = \frac{e}{im\omega_l}e^{-i\mathbf{k}_l\cdot\boldsymbol{x}}\sum_{h=1}^{3}\boldsymbol{\varepsilon}(\omega_l)\cdot\hat{e}_h \langle n| e^{i\mathbf{k}_l\cdot\boldsymbol{x}}\mathbf{p}\cdot\hat{e}_h |m\rangle,$$

$$\begin{aligned}
\mathcal{H}^{AA}(n,m,l,l') &= \frac{-e^2}{2m\omega_l\omega_{l'}}\boldsymbol{\varepsilon}_l \cdot \boldsymbol{\varepsilon}_{l'} \langle n| e^{i(\mathbf{k}_l+\mathbf{k}_{l'})\cdot\boldsymbol{x}} |m\rangle \\
&= \frac{-e^2}{2m\omega_l\omega_{l'}}e^{-i(\mathbf{k}_l+\mathbf{k}_{l'})\cdot\boldsymbol{x}}\sum_{h=1}^{3}\boldsymbol{\varepsilon}(\omega_l)\cdot\hat{e}_h\boldsymbol{\varepsilon}(\omega_{l'})\cdot\hat{e}_h \langle n| e^{i(\mathbf{k}_l+\mathbf{k}_{l'})\cdot\boldsymbol{x}} |m\rangle.
\end{aligned} \tag{3.1.9}$$

Using these definitions along with the solution given by Eq. (3.1.2) I find that

$$\begin{aligned}
\rho^{(A)}_{nm}(t) &= -i\hbar^{-1}\left(f_0(\epsilon_m) - f_0(\epsilon_n)\right)\sum_l \frac{\mathcal{H}^A(n,m,l)}{i(\omega_{nm}-\omega_l)+\gamma_{nm}}e^{-i\omega_l t} \\
\rho^{(1,A^2)}_{nm}(t) &= -i\hbar^{-1}\left(f_0(\epsilon_m) - f_0(\epsilon_n)\right)\sum_{l,l'} \frac{\mathcal{H}^{AA}(n,m,l,l')}{i(\omega_{nm}-\omega_l-\omega_{l'})+\gamma_{nm}}e^{-i(\omega_l+\omega_{l'})t}
\end{aligned} \tag{3.1.10}$$

where $f_0(\epsilon_n) = \langle n| f_0(\mathcal{H}_0) |n\rangle$ was used. These solutions can be rewritten in the following way

$$\begin{aligned}
\rho^{(A)}_{nm}(t) &= \sum_l \rho^{(A)}(n,m,l)e^{-i\omega_l t}, \\
\rho^{(1,A^2)}_{nm}(t) &= \sum_{l,l'} \rho^{(1,A^2)}(n,m,l,l')e^{-i(\omega_l+\omega_{l'})t},
\end{aligned} \tag{3.1.11}$$

where

$$\begin{aligned}\rho^{(A)}(n,m,l) &= \frac{-i\hbar^{-1}\left(f_0(\epsilon_m)-f_0(\epsilon_n)\right)\mathcal{H}^A(n,m,l)}{i(\omega_{nm}-\omega_l)+\gamma_{nm}},\\ \rho^{(1,A^2)}(n,m,l,l') &= \frac{-i\hbar^{-1}\left(f_0(\epsilon_m)-f_0(\epsilon_n)\right)\mathcal{H}^{AA}(n,m,l,l')}{i(\omega_{nm}-\omega_l-\omega_{l'})+\gamma_{nm}}.\end{aligned} \tag{3.1.12}$$

Using the iterative solution given by Eq. (3.1.2), I find

$$\rho^{(2,A^2)}_{nm}(t) = -i\hbar^{-1}\sum_{r,l,l'}\frac{\left[\mathcal{H}^A(n,r,l)\rho^{(A)}(r,m,l')-\rho^{(A)}(n,r,l')\mathcal{H}^A(r,m,l)\right]}{i(\omega_{nm}-\omega_l-\omega_{l'})+\gamma_{nm}}e^{-i(\omega_l+\omega_{l'})t}. \tag{3.1.13}$$

Note that the sum index r runs over the quantum numbers of the unperturbed Hamiltonian, and the indices l,l' corresponds to the external field modes.

Following the expansion described by Eq. (2.3.4). I will summarize the result for each term.

$$\begin{aligned}\rho^{(0)}_{nm} &= \delta_{nm}f_0(\epsilon_n),\\ \rho^{(A)}_{nm}(t) &= -i\hbar^{-1}\left(f_0(\epsilon_m)-f_0(\epsilon_n)\right)\sum_l\frac{\mathcal{H}^A(n,m,l)}{i(\omega_{nm}-\omega_l)+\gamma_{nm}}e^{-i\omega_l t},\\ \rho^{(AA)}_{nm}(t) &= -i\hbar^{-1}\sum_{l,l'}\left[\frac{\left(f_0(\epsilon_m)-f_0(\epsilon_n)\right)\mathcal{H}^{AA}(n,m,l,l')}{i(\omega_{nm}-\omega_l-\omega_{l'})+\gamma_{nm}}\right.\\ &\quad\left.+\sum_r\frac{\left[\mathcal{H}^A(n,r,l)\rho^{(A)}(r,m,l')-\rho^{(A)}(n,r,l')\mathcal{H}^A(r,m,l)\right]}{i(\omega_{nm}-\omega_l-\omega_{l'})+\gamma_{nm}}\right]e^{-i(\omega_l+\omega_{l'})t}.\end{aligned} \tag{3.1.14}$$

The contribution to $\rho^{(A)}$ comes only from $\mathcal{H}^A$ and for $\rho^{(AA)}$ there are two contributions: one from the first order perturbation theory, which comes from $\mathcal{H}^{AA}$ whereas the second term comes from the second order perturbation theory, which comes from $\mathcal{H}^A$. Both $\rho^{(A)}$ and $\rho^{(AA)}$ contribute to the second order current density, as will be shown in the next section.

3.2 Current density

In this section, I describe my derivation of the second order current density. I start by noting that the current density operator given by Eq. (2.3.6), can be written in a more convenient form by first defining the charge density operator $D_{\text{op}}(\boldsymbol{x})$, to be

$$D_{\text{op}}(\boldsymbol{x}) = -e \left|\boldsymbol{x}\right\rangle \left\langle\boldsymbol{x}\right| . \tag{3.2.1}$$

The current density operator

$$\begin{aligned} \boldsymbol{j}_{\text{op}}(\boldsymbol{x},t) &= \boldsymbol{j}^{\boldsymbol{p}}_{\text{op}}(\boldsymbol{x}) + \boldsymbol{j}^{\mathbf{A}}_{\text{op}}(\boldsymbol{x},t), \\ &= \frac{1}{2m}\left\{D_{\text{op}}(\boldsymbol{x}), \mathbf{p}\right\} + \frac{e}{m} D_{\text{op}}(\boldsymbol{x})\mathbf{A}(\boldsymbol{x},t), \end{aligned} \tag{3.2.2}$$

where the first term being the momentum current density

$$\boldsymbol{j}^{\boldsymbol{p}}_{\text{op}}(\boldsymbol{x}) = \frac{1}{2m}\left\{D_{\text{op}}(\boldsymbol{x}), \mathbf{p}\right\}, \tag{3.2.3}$$

and the second term is the so called gauge current density

$$\boldsymbol{j}^{\mathbf{A}}_{\text{op}}(\boldsymbol{x},t) = \frac{e}{m} D_{\text{op}}(\boldsymbol{x})\mathbf{A}(\boldsymbol{x},t). \tag{3.2.4}$$

The average current density is given by Eq. (2.3.7), can be written as

$$\left\langle\boldsymbol{j}\right\rangle(\boldsymbol{x},t) = \sum_n \left\langle\boldsymbol{j}\right\rangle^{(n)} = \left\langle\boldsymbol{j}\right\rangle^{(0)}(\boldsymbol{x}) + \left\langle\boldsymbol{j}\right\rangle^{(1)}(\boldsymbol{x},t) + \left\langle\boldsymbol{j}\right\rangle^{(2)}(\boldsymbol{x},t) + \cdots, \tag{3.2.5}$$

where n signifies the order in which the current density depends on the field. Following Eq. (2.3.4) I find that the second order current density is comprised of two parts

$$\left\langle\boldsymbol{j}\right\rangle^{(2)}(\boldsymbol{x},t) = \left\langle\boldsymbol{j}\right\rangle^{(2,\boldsymbol{p})} + \left\langle\boldsymbol{j}\right\rangle^{(2,\mathbf{A})}, \tag{3.2.6}$$

where $\left\langle\boldsymbol{j}\right\rangle^{(2,\boldsymbol{p})}$ is the second order current density that arises from the momentum part and $\left\langle\boldsymbol{j}\right\rangle^{(2,\mathbf{A})}$ is the second order current density that arises from the gauge part of the current density operator. These terms are given by

$$\begin{aligned} \left\langle\boldsymbol{j}\right\rangle^{(2,\boldsymbol{p})} &= \text{tr}\big(\rho^{(AA)}\, \boldsymbol{j}^{\boldsymbol{p}}_{\text{op}}(\boldsymbol{x})\big) \\ \left\langle\boldsymbol{j}\right\rangle^{(2,\mathbf{A})} &= \text{tr}\big(\rho^{(A)}\, \boldsymbol{j}^{\mathbf{A}}_{\text{op}}(\boldsymbol{x},t)\big) \end{aligned} \tag{3.2.7}$$

The distinction between the two parts will be useful later to relate between the conductivity which arises from $\boldsymbol{j}^{\mathbf{A}}_{\text{op}}$, and the induced charge density tensor.

To find $\langle\boldsymbol{j}\rangle^{(2)}(\boldsymbol{x},t)$ using Eq. (2.3.7), I first need to find the current density operator matrix elements, in the basis of the unperturbed Hamiltonian, namely

$$\langle n|\,\boldsymbol{j}_{\mathrm{op}}(\boldsymbol{x})\,|m\rangle = \boldsymbol{j}_{\mathrm{op}}(\boldsymbol{x})_{nm} = \boldsymbol{j}^{\boldsymbol{p}}_{\mathrm{op}}(\boldsymbol{x})_{nm} + \boldsymbol{j}^{\mathbf{A}}_{\mathrm{op}}(\boldsymbol{x},t)_{nm}, \tag{3.2.8}$$

and I get

$$\begin{aligned} \boldsymbol{j}^{\mathbf{A}}_{\mathrm{op}}(\boldsymbol{x},t)_{nm} &= -\frac{e^2}{m}\psi^*_n(\boldsymbol{x})\psi_m(\boldsymbol{x})\mathbf{A}(\boldsymbol{x},t), \\ \boldsymbol{j}^{\boldsymbol{p}}_{\mathrm{op}}(\boldsymbol{x})_{nm} &= -\frac{e}{2m}\left\{\psi^*_n(\boldsymbol{x})\left(-i\hbar\boldsymbol{\nabla}\right)\psi_m(\boldsymbol{x}) - \psi_m(\boldsymbol{x})\left(-i\hbar\boldsymbol{\nabla}\right)\psi^*_n(\boldsymbol{x})\right\}, \end{aligned} \tag{3.2.9}$$

and thus $\langle\boldsymbol{j}\rangle^{(2)}(\boldsymbol{x},t)$ is given by

$$\begin{aligned} \langle\boldsymbol{j}\rangle^{(2)}(\boldsymbol{x},t) &= \mathrm{tr}\big(\rho^{(A)}(t)\boldsymbol{j}^{\mathbf{A}}_{\mathrm{op}}(\boldsymbol{x},t)\big) + \mathrm{tr}\big(\rho^{(AA)}(t)\boldsymbol{j}^{\boldsymbol{p}}_{\mathrm{op}}(\boldsymbol{x})\big) \\ &= \sum_{nm}\Big[\rho^{(A)}_{nm}(t)\boldsymbol{j}^{\mathbf{A}}_{\mathrm{op}_{mn}}(\boldsymbol{x},t) + \rho^{(AA)}_{nm}(t)\boldsymbol{j}^{\boldsymbol{p}}_{\mathrm{op}_{mn}}(\boldsymbol{x})\Big]. \end{aligned} \tag{3.2.10}$$

Using Eqs. (3.1.14, 3.2.9) I get

$$\begin{aligned} &\langle\boldsymbol{j}\rangle^{(2)}(\boldsymbol{x},t) \\ &= -\frac{e^2}{m}\sum_{n,m,l}\frac{-i\hbar^{-1}\left(f_0(\epsilon_m)-f_0(\epsilon_n)\right)\mathcal{H}^A(n,m,l)}{i(\omega_{nm}-\omega_l)+\gamma_{nm}}e^{-i\omega_l t}\psi^*_m(\boldsymbol{x})\psi_n(\boldsymbol{x})\mathbf{A}(\boldsymbol{x},t) \\ &+ \frac{e}{2m}\sum_{n,m,l,l'}\frac{\left(f_0(\epsilon_m)-f_0(\epsilon_n)\right)\mathcal{H}^{AA}(n,m,l,l')}{i(\omega_{nm}-\omega_l-\omega_{l'})+\gamma_{nm}}e^{-i(\omega_l+\omega_{l'})t} \\ &\times\left\{\psi^*_m(\boldsymbol{x})\left(\boldsymbol{\nabla}\psi_n(\boldsymbol{x})\right)-\psi_n(\boldsymbol{x})\left(\boldsymbol{\nabla}\psi^*_m(\boldsymbol{x})\right)\right\} \\ &- \frac{ie}{2\hbar m}\sum_{n,m,r,l,l'}\left\{\psi^*_m(\boldsymbol{x})\left(\boldsymbol{\nabla}\psi_n(\boldsymbol{x})\right)-\psi_n(\boldsymbol{x})\left(\boldsymbol{\nabla}\psi^*_m(\boldsymbol{x})\right)\right\}e^{-i(\omega_l+\omega_{l'})t} \\ &\times\left[\frac{\mathcal{H}^A(n,r,l)\mathcal{H}^A(r,m,l')\left(f_0(\epsilon_m)-f_0(\epsilon_r)\right)}{\left[i(\omega_{nm}-\omega_l-\omega_{l'})+\gamma_{nm}\right]\left[i(\omega_{rm}-\omega_{l'})+\gamma_{rm}\right]}\right. \\ &-\left.\frac{\mathcal{H}^A(n,r,l')\mathcal{H}^A(r,m,l)\left(f_0(\epsilon_r)-f_0(\epsilon_n)\right)}{\left[i(\omega_{nm}-\omega_l-\omega_{l'})+\gamma_{nm}\right]\left[i(\omega_{nr}-\omega_{l'})+\gamma_{nr}\right]}\right] \end{aligned} \tag{3.2.11}$$

where the summation indices $\{r,n,m\}$ are on the states quantum numbers and $\{l,l'\}$ are on the field modes.

To display this result explicitly in terms of the matrix elements of the perturbation and full quantum numbers, I use Eq. (3.1.9), and make the following substitutions

$$\begin{aligned}
&n \Rightarrow n_1\,\mathbf{q}_1, \quad m \Rightarrow n_2\,\mathbf{q}_2, \quad r \Rightarrow n_3\,\mathbf{q}_3, \\
&\omega_{nm} \Rightarrow \omega_{n_1\,\mathbf{q}_1,n_2\,\mathbf{q}_2}, \quad \omega_{nr} \Rightarrow \omega_{n_1\,\mathbf{q}_1,n_3\,\mathbf{q}_3}, \quad \omega_{rm} \Rightarrow \omega_{n_3\,\mathbf{q}_3,n_2\,\mathbf{q}_2}, \\
&\gamma_{nm} \Rightarrow \gamma_{n_1\,\mathbf{q}_1,n_2\,\mathbf{q}_2}, \quad \gamma_{nr} \Rightarrow \gamma_{n_1\,\mathbf{q}_1,n_3\,\mathbf{q}_3}, \quad \gamma_{rm} \Rightarrow \gamma_{n_3\,\mathbf{q}_3,n_2\,\mathbf{q}_2}, \\
&\epsilon_n \Rightarrow \varepsilon_{n_1}(\mathbf{q}_1), \quad \epsilon_m \Rightarrow \varepsilon_{n_2}(\mathbf{q}_2), \quad \epsilon_r \Rightarrow \varepsilon_{n_3}(\mathbf{q}_3),
\end{aligned} \tag{3.2.12}$$

and get

$$\begin{aligned}
&\langle \boldsymbol{j} \rangle^{(2)}(\boldsymbol{x},t) = \\
&\sum_{n_1\,\mathbf{q}_1,n_2\,\mathbf{q}_2} \sum_{l,l'} \sum_{h=1}^{3} \frac{e^3}{im^2\omega_l\omega_{l'}\hbar} \frac{\left(f_0(\varepsilon_{n_2}(\mathbf{q}_2)) - f_0(\varepsilon_{n_1}(\mathbf{q}_1))\right) \langle n_1\,\mathbf{q}_1 | e^{i\mathbf{k}_l\cdot\boldsymbol{x}} \mathbf{p}\cdot\hat{e}_h | n_2\,\mathbf{q}_2\rangle}{i(\omega_{n_1\,\mathbf{q}_1,n_2\,\mathbf{q}_2} - \omega_l) + \gamma_{n_1\,\mathbf{q}_1,n_2\,\mathbf{q}_2}} \\
&\psi^*_{n_2\,\mathbf{q}_2}(\boldsymbol{x})\psi_{n_1\,\mathbf{q}_1}(\boldsymbol{x}) e^{-i\mathbf{k}_l\cdot\boldsymbol{x}} (\boldsymbol{\varepsilon}(\omega_l)\cdot\hat{e}_h)\boldsymbol{\varepsilon}(\omega_{l'}) e^{-i(\omega_l+\omega_{l'})t} \\
&- \sum_{n_1\,\mathbf{q}_1,n_2\,\mathbf{q}_2} \sum_{l,l'} \sum_{h=1}^{3} \frac{e^3}{4m^2\omega_l\omega_{l'}} \frac{\left(f_0(\varepsilon_{n_2}(\mathbf{q}_2)) - f_0(\varepsilon_{n_1}(\mathbf{q}_1))\right) \langle n_1\,\mathbf{q}_1 | e^{i(\mathbf{k}_l+\mathbf{k}_{l'})\cdot\boldsymbol{x}} | n_2\,\mathbf{q}_2\rangle}{i(\omega_{n_1\,\mathbf{q}_1,n_2\,\mathbf{q}_2} - \omega_l - \omega_{l'}) + \gamma_{n_1\,\mathbf{q}_1,n_2\,\mathbf{q}_2}} \\
&\times \left\{ \psi^*_{n_2\,\mathbf{q}_2}(\boldsymbol{x}) \left(\boldsymbol{\nabla}\psi_{n_1\,\mathbf{q}_1}(\boldsymbol{x})\right) - \psi_{n_1\,\mathbf{q}_1}(\boldsymbol{x}) \left(\boldsymbol{\nabla}\psi^*_{n_2\,\mathbf{q}_2}(\boldsymbol{x})\right) \right\} e^{-i(\mathbf{k}_l+\mathbf{k}_{l'})\cdot\boldsymbol{x}} \\
&\times (\boldsymbol{\varepsilon}(\omega_l)\cdot\hat{e}_h)(\boldsymbol{\varepsilon}(\omega_{l'})\cdot\hat{e}_h) e^{-i(\omega_l+\omega_{l'})t} \\
&+ \sum_{n_1\,\mathbf{q}_1,n_2\,\mathbf{q}_2,n_3\,\mathbf{q}_3} \sum_{l,l'} \sum_{h=1,h'=1}^{3} \frac{ie^3}{2m^3\omega_l\omega_{l'}\hbar} \\
&\times \left\{ \psi^*_{n_2\,\mathbf{q}_2}(\boldsymbol{x}) \left(\boldsymbol{\nabla}\psi_{n_1\,\mathbf{q}_1}(\boldsymbol{x})\right) - \psi_{n_1\,\mathbf{q}_1}(\boldsymbol{x}) \left(\boldsymbol{\nabla}\psi^*_{n_2\,\mathbf{q}_2}(\boldsymbol{x})\right) \right\} e^{-i(\mathbf{k}_l+\mathbf{k}_{l'})\cdot\boldsymbol{x}} \\
&\times \Bigg[\frac{\langle n_1\,\mathbf{q}_1 | e^{i\mathbf{k}_l\cdot\boldsymbol{x}} \mathbf{p}\cdot\hat{e}_h | n_3\,\mathbf{q}_3\rangle \langle n_3\,\mathbf{q}_3 | e^{i\mathbf{k}_{l'}\cdot\boldsymbol{x}} \mathbf{p}\cdot\hat{e}_{h'} | n_2\,\mathbf{q}_2\rangle \left(f_0(\varepsilon_{n_2}(\mathbf{q}_2)) - f_0(\varepsilon_{n_3}(\mathbf{q}_3))\right)}{\left[i(\omega_{n_1\,\mathbf{q}_1,n_2\,\mathbf{q}_2} - \omega_l - \omega_{l'}) + \gamma_{n_1\,\mathbf{q}_1,n_2\,\mathbf{q}_2}\right] \left[i(\omega_{n_3\,\mathbf{q}_3,n_2\,\mathbf{q}_2} - \omega_{l'}) + \gamma_{n_3\,\mathbf{q}_3,n_2\,\mathbf{q}_2}\right]} \\
&- \frac{\langle n_1\,\mathbf{q}_1 | e^{i\mathbf{k}_{l'}\cdot\boldsymbol{x}} \mathbf{p}\cdot\hat{e}_{h'} | n_3\,\mathbf{q}_3\rangle \langle n_3\,\mathbf{q}_3 | e^{i\mathbf{k}_l\cdot\boldsymbol{x}} \mathbf{p}\cdot\hat{e}_h | n_2\,\mathbf{q}_2\rangle \left(f_0(\varepsilon_{n_3}(\mathbf{q}_3)) - f_0(\varepsilon_{n_1}(\mathbf{q}_1))\right)}{\left[i(\omega_{n_1\,\mathbf{q}_1,n_2\,\mathbf{q}_2} - \omega_l - \omega_{l'}) + \gamma_{n_1\,\mathbf{q}_1,n_2\,\mathbf{q}_2}\right] \left[i(\omega_{n_1\,\mathbf{q}_1,n_3\,\mathbf{q}_3} - \omega_{l'}) + \gamma_{n_1\,\mathbf{q}_1,n_3\,\mathbf{q}_3}\right]} \Bigg] \\
&\times (\boldsymbol{\varepsilon}(\omega_l)\cdot\hat{e}_h)(\boldsymbol{\varepsilon}(\omega_{l'})\cdot\hat{e}_{h'}) e^{-i(\omega_l+\omega_{l'})t}
\end{aligned} \tag{3.2.13}$$

3.2.1 Current density temporal Fourier components

To proceed with the calculation, I first need to find the Fourier components of the current density.

The current density can be written as

$$\begin{aligned} \langle \boldsymbol{j} \rangle^{(2)}(\boldsymbol{x},t) &= \sum_{l,l'} \left[\langle \boldsymbol{j} \rangle^{(2)}(\boldsymbol{x};\omega_l+\omega_{l'},\omega_l,\omega_{l'}) e^{-i(\omega_l+\omega_{l'})t} + \text{c.c.} \right], \\ \langle \boldsymbol{j} \rangle^{(2)}(\boldsymbol{x};\omega_l+\omega_{l'}) &= \langle \boldsymbol{j} \rangle^{(2)}(\boldsymbol{x};\omega_l+\omega_{l'},\omega_l,\omega_{l'}) + \langle \boldsymbol{j} \rangle^{(2)}(\boldsymbol{x};\omega_{l'}+\omega_l,\omega_{l'},\omega_l). \end{aligned} \tag{3.2.14}$$

This form corresponds with the result of Eq. (3.2.13), having two different terms when exchanging between l and l'.

For our purposes, it is sufficient to find $\langle \boldsymbol{j} \rangle^{(2)}(\boldsymbol{x};\omega_l+\omega_{l'},\omega_l,\omega_{l'})$, and when evaluating the conductivity, both terms must be taken, namely $\langle \boldsymbol{j} \rangle^{(2)}(\boldsymbol{x};\omega_l+\omega_{l'})$.

I project the current density onto an arbitrary direction, denoted by $\hat{e}_i$ and find that the current density Fourier component is given by

$$
\begin{aligned}
&\langle \boldsymbol{j} \rangle^{(2)} (\boldsymbol{x}; \omega_l + \omega_{l'}, \omega_l, \omega_{l'}) \cdot \hat{e}_i = \\
&\sum_{n_1\,\mathbf{q}_1, n_2\,\mathbf{q}_2} \sum_{h=1}^{3} \frac{e^3}{i m^2 \omega_l \omega_{l'} \hbar} \frac{\left(f_0(\varepsilon_{n_2}(\mathbf{q}_2)) - f_0(\varepsilon_{n_1}(\mathbf{q}_1))\right) \langle n_1\,\mathbf{q}_1 | \, e^{i\mathbf{k}_l \cdot \boldsymbol{x}} \mathbf{p} \cdot \hat{e}_h \, | n_2\,\mathbf{q}_2 \rangle}{i(\omega_{n_1\,\mathbf{q}_1, n_2\,\mathbf{q}_2} - \omega_l) + \gamma_{n_1\,\mathbf{q}_1, n_2\,\mathbf{q}_2}} \\
&\psi^*_{n_2\,\mathbf{q}_2}(\boldsymbol{x}) \psi_{n_1\,\mathbf{q}_1}(\boldsymbol{x}) e^{-i\mathbf{k}_l \cdot \boldsymbol{x}} (\boldsymbol{\varepsilon}(\omega_l) \cdot \hat{e}_h)(\boldsymbol{\varepsilon}(\omega_{l'}) \cdot \hat{e}_i) \\
&- \sum_{n_1\,\mathbf{q}_1, n_2\,\mathbf{q}_2} \sum_{h=1}^{3} \frac{e^3}{4 m^2 \omega_l \omega_{l'}} \frac{\left(f_0(\varepsilon_{n_2}(\mathbf{q}_2)) - f_0(\varepsilon_{n_1}(\mathbf{q}_1))\right) \langle n_1\,\mathbf{q}_1 | \, e^{i(\mathbf{k}_l + \mathbf{k}_{l'}) \cdot \boldsymbol{x}} \, | n_2\,\mathbf{q}_2 \rangle}{i(\omega_{n_1\,\mathbf{q}_1, n_2\,\mathbf{q}_2} - \omega_l - \omega_{l'}) + \gamma_{n_1\,\mathbf{q}_1, n_2\,\mathbf{q}_2}} \\
&\times \left\{ \psi^*_{n_2\,\mathbf{q}_2}(\boldsymbol{x}) \left(\boldsymbol{\nabla} \psi_{n_1\,\mathbf{q}_1}(\boldsymbol{x}) \right) - \psi_{n_1\,\mathbf{q}_1}(\boldsymbol{x}) \left(\boldsymbol{\nabla} \psi^*_{n_2\,\mathbf{q}_2}(\boldsymbol{x}) \right) \right\} \cdot \hat{e}_i e^{-i(\mathbf{k}_l + \mathbf{k}_{l'}) \cdot \boldsymbol{x}} \\
&\times (\boldsymbol{\varepsilon}(\omega_l) \cdot \hat{e}_h)(\boldsymbol{\varepsilon}(\omega_{l'}) \cdot \hat{e}_h) \\
&+ \sum_{n_1\,\mathbf{q}_1, n_2\,\mathbf{q}_2, n_3\,\mathbf{q}_3} \sum_{h=1, h'=1}^{3} \frac{i e^3}{2 m^3 \omega_l \omega_{l'} \hbar} \\
&\times \left\{ \psi^*_{n_2\,\mathbf{q}_2}(\boldsymbol{x}) \left(\boldsymbol{\nabla} \psi_{n_1\,\mathbf{q}_1}(\boldsymbol{x}) \right) - \psi_{n_1\,\mathbf{q}_1}(\boldsymbol{x}) \left(\boldsymbol{\nabla} \psi^*_{n_2\,\mathbf{q}_2}(\boldsymbol{x}) \right) \right\} \cdot \hat{e}_i e^{-i(\mathbf{k}_l + \mathbf{k}_{l'}) \cdot \boldsymbol{x}} \\
&\times \left[\frac{\langle n_1\,\mathbf{q}_1 | \, e^{i\mathbf{k}_l \cdot \boldsymbol{x}} \mathbf{p} \cdot \hat{e}_h \, | n_3\,\mathbf{q}_3 \rangle \langle n_3\,\mathbf{q}_3 | \, e^{i\mathbf{k}_{l'} \cdot \boldsymbol{x}} \mathbf{p} \cdot \hat{e}_{h'} \, | n_2\,\mathbf{q}_2 \rangle \left(f_0(\varepsilon_{n_2}(\mathbf{q}_2)) - f_0(\varepsilon_{n_3}(\mathbf{q}_3))\right)}{\left[i(\omega_{n_1\,\mathbf{q}_1, n_2\,\mathbf{q}_2} - \omega_l - \omega_{l'}) + \gamma_{n_1\,\mathbf{q}_1, n_2\,\mathbf{q}_2}\right] \left[i(\omega_{n_3\,\mathbf{q}_3, n_2\,\mathbf{q}_2} - \omega_{l'}) + \gamma_{n_3\,\mathbf{q}_3, n_2\,\mathbf{q}_2}\right]} \right. \\
&\left. - \frac{\langle n_1\,\mathbf{q}_1 | \, e^{i\mathbf{k}_{l'} \cdot \boldsymbol{x}} \mathbf{p} \cdot \hat{e}_{h'} \, | n_3\,\mathbf{q}_3 \rangle \langle n_3\,\mathbf{q}_3 | \, e^{i\mathbf{k}_l \cdot \boldsymbol{x}} \mathbf{p} \cdot \hat{e}_h \, | n_2\,\mathbf{q}_2 \rangle \left(f_0(\varepsilon_{n_3}(\mathbf{q}_3)) - f_0(\varepsilon_{n_1}(\mathbf{q}_1))\right)}{\left[i(\omega_{n_1\,\mathbf{q}_1, n_2\,\mathbf{q}_2} - \omega_l - \omega_{l'}) + \gamma_{n_1\,\mathbf{q}_1, n_2\,\mathbf{q}_2}\right] \left[i(\omega_{n_1\,\mathbf{q}_1, n_3\,\mathbf{q}_3} - \omega_{l'}) + \gamma_{n_1\,\mathbf{q}_1, n_3\,\mathbf{q}_3}\right]} \right] \\
&\times (\boldsymbol{\varepsilon}(\omega_l) \cdot \hat{e}_h)(\boldsymbol{\varepsilon}(\omega_{l'}) \cdot \hat{e}_{h'})
\end{aligned}
\tag{3.2.15}
$$

3.3 Second order conductivity

In this section I describe my derivation of the second order conductivity from the current density. I relate $\langle \boldsymbol{j} \rangle^{(2)} (\boldsymbol{x}; \omega_l + \omega_{l'}, \omega_l, \omega_{l'}) \cdot \hat{e}_i$ to the conductivity, by using the relation

$$
\langle \boldsymbol{j} \rangle^{(2)} (\boldsymbol{x}; \omega_l + \omega_{l'}, \omega_l, \omega_{l'}) \cdot \hat{e}_i = \sum_{j,k=1}^{3} \sigma^{(2)}_{ijk}(\boldsymbol{x}; \omega_l + \omega_{l'}, \omega_l, \omega_{l'}) \left(\boldsymbol{\varepsilon}(\omega_l) \cdot \hat{e}_j\right) \left(\boldsymbol{\varepsilon}(\omega_{l'}) \cdot \hat{e}_k\right). \tag{3.3.1}
$$

I note that the full conductivity $\sigma^{(2)}_{ijk}(\boldsymbol{x}; \omega_l + \omega_{l'})$, is attainable using Eqs. (2.1.4)-(2.1.6), for which intrinsic permutation symmetry holds. Using Eqs. (3.3.1, 3.2.15), I find

$$
\begin{aligned}
&\sigma^{(2)}_{ijk}(\boldsymbol{x};\omega_l+\omega_{l'},\omega_l,\omega_{l'}) = \\
&\sum_{n_1\,\mathbf{q}_1,n_2\,\mathbf{q}_2} \frac{e^3}{im^2\omega_l\omega_{l'}\hbar} \frac{\left(f_0(\varepsilon_{n_2}(\mathbf{q}_2)) - f_0(\varepsilon_{n_1}(\mathbf{q}_1))\right) \langle n_1\,\mathbf{q}_1|\, e^{i\mathbf{k}_l\cdot\boldsymbol{x}}\mathbf{p}\cdot\hat{e}_j\,|n_2\,\mathbf{q}_2\rangle}{i(\omega_{n_1\,\mathbf{q}_1,n_2\,\mathbf{q}_2}-\omega_l)+\gamma_{n_1\,\mathbf{q}_1,n_2\,\mathbf{q}_2}} \\
&\psi^*_{n_2\,\mathbf{q}_2}(\boldsymbol{x})\psi_{n_1\,\mathbf{q}_1}(\boldsymbol{x})e^{-i\mathbf{k}_l\cdot\boldsymbol{x}}\delta_{i,k} \\
&-\sum_{n_1\,\mathbf{q}_1,n_2\,\mathbf{q}_2} \frac{e^3}{4m^2\omega_l\omega_{l'}} \frac{\left(f_0(\varepsilon_{n_2}(\mathbf{q}_2)) - f_0(\varepsilon_{n_1}(\mathbf{q}_1))\right) \langle n_1\,\mathbf{q}_1|\, e^{i(\mathbf{k}_l+\mathbf{k}_{l'})\cdot\boldsymbol{x}}\,|n_2\,\mathbf{q}_2\rangle}{i(\omega_{n_1\,\mathbf{q}_1,n_2\,\mathbf{q}_2}-\omega_l-\omega_{l'})+\gamma_{n_1\,\mathbf{q}_1,n_2\,\mathbf{q}_2}} \\
&\times\left\{\psi^*_{n_2\,\mathbf{q}_2}(\boldsymbol{x})\left(\boldsymbol{\nabla}\psi_{n_1\,\mathbf{q}_1}(\boldsymbol{x})\right) - \psi_{n_1\,\mathbf{q}_1}(\boldsymbol{x})\left(\boldsymbol{\nabla}\psi^*_{n_2\,\mathbf{q}_2}(\boldsymbol{x})\right)\right\}\cdot\hat{e}_i e^{-i(\mathbf{k}_l+\mathbf{k}_{l'})\cdot\boldsymbol{x}}\delta_{j,k} \\
&+\sum_{n_1\,\mathbf{q}_1,n_2\,\mathbf{q}_2,n_3\,\mathbf{q}_3} \frac{ie^3}{2m^3\omega_l\omega_{l'}\hbar} \\
&\times\left\{\psi^*_{n_2\,\mathbf{q}_2}(\boldsymbol{x})\left(\boldsymbol{\nabla}\psi_{n_1\,\mathbf{q}_1}(\boldsymbol{x})\right) - \psi_{n_1\,\mathbf{q}_1}(\boldsymbol{x})\left(\boldsymbol{\nabla}\psi^*_{n_2\,\mathbf{q}_2}(\boldsymbol{x})\right)\right\}\cdot\hat{e}_i e^{-i(\mathbf{k}_l+\mathbf{k}_{l'})\cdot\boldsymbol{x}} \\
&\times\left[\frac{\langle n_1\,\mathbf{q}_1|\, e^{i\mathbf{k}_l\cdot\boldsymbol{x}}\mathbf{p}\cdot\hat{e}_j\,|n_3\,\mathbf{q}_3\rangle\langle n_3\,\mathbf{q}_3|\, e^{i\mathbf{k}_{l'}\cdot\boldsymbol{x}}\mathbf{p}\cdot\hat{e}_k\,|n_2\,\mathbf{q}_2\rangle\left(f_0(\varepsilon_{n_2}(\mathbf{q}_2)) - f_0(\varepsilon_{n_3}(\mathbf{q}_3))\right)}{\left[i(\omega_{n_1\,\mathbf{q}_1,n_2\,\mathbf{q}_2}-\omega_l-\omega_{l'})+\gamma_{n_1\,\mathbf{q}_1,n_2\,\mathbf{q}_2}\right]\left[i(\omega_{n_3\,\mathbf{q}_3,n_2\,\mathbf{q}_2}-\omega_{l'})+\gamma_{n_3\,\mathbf{q}_3,n_2\,\mathbf{q}_2}\right]}\right. \\
&-\left.\frac{\langle n_1\,\mathbf{q}_1|\, e^{i\mathbf{k}_{l'}\cdot\boldsymbol{x}}\mathbf{p}\cdot\hat{e}_k\,|n_3\,\mathbf{q}_3\rangle\langle n_3\,\mathbf{q}_3|\, e^{i\mathbf{k}_l\cdot\boldsymbol{x}}\mathbf{p}\cdot\hat{e}_j\,|n_2\,\mathbf{q}_2\rangle\left(f_0(\varepsilon_{n_3}(\mathbf{q}_3)) - f_0(\varepsilon_{n_1}(\mathbf{q}_1))\right)}{\left[i(\omega_{n_1\,\mathbf{q}_1,n_2\,\mathbf{q}_2}-\omega_l-\omega_{l'})+\gamma_{n_1\,\mathbf{q}_1,n_2\,\mathbf{q}_2}\right]\left[i(\omega_{n_1\,\mathbf{q}_1,n_3\,\mathbf{q}_3}-\omega_{l'})+\gamma_{n_1\,\mathbf{q}_1,n_3\,\mathbf{q}_3}\right]}\right]
\end{aligned}
\tag{3.3.2}
$$

3.3.1 Second order conductivity spatial Fourier components

Since the unperturbed Hamiltonian is symmetric under translation by a lattice vector, the conductivity also preserves this symmetry. Therefore, it can be written in the following form

$$
\sigma^{(2)}_{ijk}(\boldsymbol{x};\omega_l+\omega_{l'},\omega_l,\omega_{l'}) = \sum_{\mathbf{G}}\sigma^{(2)}_{ijk}(\omega_l+\omega_{l'},\omega_l,\omega_{l'};\mathbf{G})e^{i\mathbf{G}\cdot\boldsymbol{x}}, \tag{3.3.3}
$$

where $\mathbf{G}$ is the reciprocal lattice vector and V is the crystal volume. This also means

$$
\sigma^{(2)}_{ijk}(\omega_l+\omega_{l'},\omega_l,\omega_{l'};\mathbf{G}) = \frac{1}{V}\int_V d\boldsymbol{x}\,\sigma^{(2)}_{ijk}(\boldsymbol{x};\omega_l+\omega_{l'},\omega_l,\omega_{l'})e^{-i\mathbf{G}\cdot\boldsymbol{x}}. \tag{3.3.4}
$$

Note that for $\mathbf{G} = 0$, one obtains the average macroscopic conductivity.

To find $\sigma^{(2)}_{ijk}(\omega_l + \omega_{l'}, \omega_l, \omega_{l'}; \mathbf{G})$, I use Eq. (3.3.4) and get

$$
\begin{aligned}
&\sigma^{(2)}_{ijk}(\omega_l + \omega_{l'}, \omega_l, \omega_{l'}; \mathbf{G}) = \\
&\sum_{n_1\,\mathbf{q}_1, n_2\,\mathbf{q}_2} \frac{e^3}{im^2\omega_l\omega_{l'}\hbar V} \frac{\left(f_0(\varepsilon_{n_2}(\mathbf{q}_2)) - f_0(\varepsilon_{n_1}(\mathbf{q}_1))\right) \langle n_1\,\mathbf{q}_1| \, e^{i\mathbf{k}_l\cdot\boldsymbol{x}}\mathbf{p}\cdot\hat{e}_j \, |n_2\,\mathbf{q}_2\rangle}{i(\omega_{n_1\,\mathbf{q}_1, n_2\,\mathbf{q}_2} - \omega_l) + \gamma_{n_1\,\mathbf{q}_1, n_2\,\mathbf{q}_2}} \\
&\times \langle n_2\,\mathbf{q}_2| \, e^{-i(\mathbf{k}_l+\mathbf{G})\cdot\boldsymbol{x}} \, |n_1\,\mathbf{q}_1\rangle \, \delta_{i,k} \\
&- \sum_{n_1\,\mathbf{q}_1, n_2\,\mathbf{q}_2} \frac{ie^3}{4m^2\omega_l\omega_{l'}\hbar V} \frac{\left(f_0(\varepsilon_{n_2}(\mathbf{q}_2)) - f_0(\varepsilon_{n_1}(\mathbf{q}_1))\right) \langle n_1\,\mathbf{q}_1| \, e^{i(\mathbf{k}_l+\mathbf{k}_{l'})\cdot\boldsymbol{x}} \, |n_2\,\mathbf{q}_2\rangle}{i(\omega_{n_1\,\mathbf{q}_1, n_2\,\mathbf{q}_2} - \omega_l - \omega_{l'}) + \gamma_{n_1\,\mathbf{q}_1, n_2\,\mathbf{q}_2}} \\
&\times \big[2\,\langle n_2\,\mathbf{q}_2| \, e^{-i(\mathbf{k}_l+\mathbf{G}+\mathbf{k}_{l'})\cdot\boldsymbol{x}}\mathbf{p}\cdot\hat{e}_i \, |n_1\,\mathbf{q}_1\rangle \\
&- \hbar(\mathbf{k}_l + \mathbf{G} + \mathbf{k}_{l'})\cdot\hat{e}_i \, \langle n_2\,\mathbf{q}_2| \, e^{-i(\mathbf{k}_l+\mathbf{G}+\mathbf{k}_{l'})\cdot\boldsymbol{x}} \, |n_1\,\mathbf{q}_1\rangle \, \big] \delta_{j,k} \\
&- \sum_{n_1\,\mathbf{q}_1, n_2\,\mathbf{q}_2, n_3\,\mathbf{q}_3} \frac{e^3}{2m^3\omega_l\omega_{l'}\hbar^2 V} \\
&\big[2\,\langle n_2\,\mathbf{q}_2| \, e^{-i(\mathbf{k}_l+\mathbf{G}+\mathbf{k}_{l'})\cdot\boldsymbol{x}}\mathbf{p}\cdot\hat{e}_i \, |n_1\,\mathbf{q}_1\rangle \\
&- \hbar(\mathbf{k}_l + \mathbf{G} + \mathbf{k}_{l'})\cdot\hat{e}_i \, \langle n_2\,\mathbf{q}_2| \, e^{-i(\mathbf{k}_l+\mathbf{G}+\mathbf{k}_{l'})\cdot\boldsymbol{x}} \, |n_1\,\mathbf{q}_1\rangle \, \big] \\
&\times \left[\frac{\langle n_1\,\mathbf{q}_1| \, e^{i\mathbf{k}_l\cdot\boldsymbol{x}}\mathbf{p}\cdot\hat{e}_j \, |n_3\,\mathbf{q}_3\rangle \langle n_3\,\mathbf{q}_3| \, e^{i\mathbf{k}_{l'}\cdot\boldsymbol{x}}\mathbf{p}\cdot\hat{e}_k \, |n_2\,\mathbf{q}_2\rangle \left(f_0(\varepsilon_{n_2}(\mathbf{q}_2)) - f_0(\varepsilon_{n_3}(\mathbf{q}_3))\right)}{\left[i(\omega_{n_1\,\mathbf{q}_1, n_2\,\mathbf{q}_2} - \omega_l - \omega_{l'}) + \gamma_{n_1\,\mathbf{q}_1, n_2\,\mathbf{q}_2}\right]\left[i(\omega_{n_3\,\mathbf{q}_3, n_2\,\mathbf{q}_2} - \omega_{l'}) + \gamma_{n_3\,\mathbf{q}_3, n_2\,\mathbf{q}_2}\right]} \right. \\
&\left. - \frac{\langle n_1\,\mathbf{q}_1| \, e^{i\mathbf{k}_{l'}\cdot\boldsymbol{x}}\mathbf{p}\cdot\hat{e}_k \, |n_3\,\mathbf{q}_3\rangle \langle n_3\,\mathbf{q}_3| \, e^{i\mathbf{k}_l\cdot\boldsymbol{x}}\mathbf{p}\cdot\hat{e}_j \, |n_2\,\mathbf{q}_2\rangle \left(f_0(\varepsilon_{n_3}(\mathbf{q}_3)) - f_0(\varepsilon_{n_1}(\mathbf{q}_1))\right)}{\left[i(\omega_{n_1\,\mathbf{q}_1, n_2\,\mathbf{q}_2} - \omega_l - \omega_{l'}) + \gamma_{n_1\,\mathbf{q}_1, n_2\,\mathbf{q}_2}\right]\left[i(\omega_{n_1\,\mathbf{q}_1, n_3\,\mathbf{q}_3} - \omega_{l'}) + \gamma_{n_1\,\mathbf{q}_1, n_3\,\mathbf{q}_3}\right]} \right].
\end{aligned}
\tag{3.3.5}
$$

To evaluate the integrals I used the following

$$
\begin{aligned}
&\int\limits_V d\boldsymbol{x}\ \left[\psi^*_{n_2\,\mathbf{q}_2}(\boldsymbol{x}) \left(\boldsymbol{\nabla}\psi_{n_1\,\mathbf{q}_1}(\boldsymbol{x})\right) - \psi_{n_1\,\mathbf{q}_1}(\boldsymbol{x}) \left(\boldsymbol{\nabla}\psi^*_{n_2\,\mathbf{q}_2}(\boldsymbol{x})\right)\right] e^{i\mathbf{k}\cdot\boldsymbol{x}} \\
&= \frac{i}{\hbar}\left[2\,\langle n_2\,\mathbf{q}_2| \, e^{i\mathbf{k}\cdot\boldsymbol{x}'}\mathbf{p} \, |n_1\,\mathbf{q}_1\rangle + \hbar\mathbf{k}\,\langle n_2\,\mathbf{q}_2| \, e^{i\mathbf{k}\cdot\boldsymbol{x}''} \, |n_1\,\mathbf{q}_1\rangle\right].
\end{aligned}
\tag{3.3.6}
$$

For full derivation of this relation see appendix (A.2).

The general conductivity contains 3 terms. The first comes from the gauge part of the current density operator and the last two terms comes from the momentum part of the current density operator. The second term came from first order perturbation theory, from the $\mathcal{H}^{AA}$ part of the perturbation, and the last term came from the second order perturbation theory which contained a product of terms from $\mathcal{H}^A$.

3.3.2 The induced charge density and the conductivity

In this section I will reintroduce the charge density operator in more detail, show how it is related to the conductivity, which arises from the gauge part of current density, and relate it to the induced charge density tensor.

I begin with the average charge density

$$\rho_c(\boldsymbol{x},t) = \mathrm{tr}(\rho(t)D_{\mathrm{op}}(\boldsymbol{x})) = \sum_n \rho_c^{(n)} = \rho_c^{(0)}(\boldsymbol{x}) + \rho_c^{(1)}(\boldsymbol{x},t) + \cdots \,, \tag{3.3.7}$$

where $\rho_c(\boldsymbol{x},t)$ is the average charge density, D_{op} is the charge density operator (Eq. (3.2.1)) and n signifies the order of each term with respect to the field. The average charge density in the absence of an external field is $\rho_c^{(0)}(\boldsymbol{x})$, and $\rho_c^{(1)}(\boldsymbol{x},t)$ is the average induced charge. The induced charge density can be Fourier expanded in the field modes, namely

$$\rho_c^{(1)}(\boldsymbol{x},t) = \sum_l \left[\rho_c^{(1)}(\boldsymbol{x};\omega_l)e^{-i\omega_l t} + c.c.\right]. \tag{3.3.8}$$

The Fourier coefficients of the induced charge density are related to the electric field amplitudes via the induced charge density tensor

$$\rho_c^{(1)}(\boldsymbol{x};\omega_l) = \sum_{j=1}^{3} D_j(\boldsymbol{x};\omega_l)\left(\boldsymbol{\varepsilon}(\omega_l)\cdot\hat{e}_j\right), \tag{3.3.9}$$

where $D_j(\boldsymbol{x};\omega_l)$ is the induced charge density tensor in j-th direction. The induced charge density tensor has the periodicity of the lattice and therefore can be written as

$$\begin{aligned} D_j(\boldsymbol{x};\omega_l) &= \sum_{\mathbf{G}} D_j(\omega_l;\mathbf{G})e^{i\mathbf{G}\cdot\boldsymbol{x}}, \\ D_j(\omega_l;\mathbf{G}) &= \frac{1}{V}\int\limits_V d\boldsymbol{x}\, D_j(\boldsymbol{x};\omega_l)e^{-i\mathbf{G}\cdot\boldsymbol{x}}. \end{aligned} \tag{3.3.10}$$

The current density, which arises from $\boldsymbol{j}_{\rm op}^{\mathbf{A}}$ denoted by $\left\langle \boldsymbol{j}^{\mathbf{A}} \right\rangle (\boldsymbol{x}, t)$, is related to the charge density in the following way

$$\left\langle \boldsymbol{j}^{\mathbf{A}} \right\rangle (\boldsymbol{x}, t) = \mathrm{tr}\big(\rho(t)\boldsymbol{j}_{\rm op}^{\mathbf{A}}(\boldsymbol{x}, t)\big) = \frac{e}{m}\rho_c(\boldsymbol{x}, t)\mathbf{A}(\boldsymbol{x}, t). \tag{3.3.11}$$

The second order current density $\langle \boldsymbol{j} \rangle^{(2,\mathbf{A})} (\boldsymbol{x}, t)$ is thus related to the induced charge density

$$\langle \boldsymbol{j} \rangle^{(2,\mathbf{A})} (\boldsymbol{x}, t) = \mathrm{tr}\big(\rho^{(A)}\, \boldsymbol{j}_{\rm op}^{\mathbf{A}}(\boldsymbol{x}, t)\big) = \frac{e}{m}\rho_c^{(1)}(\boldsymbol{x}, t)\mathbf{A}(\boldsymbol{x}, t). \tag{3.3.12}$$

Using Eqs. (2.2.6, 3.3.1, 3.3.9) I get

$$\sigma_{ijk}^{(2,A)}(\boldsymbol{x}; \omega_l + \omega_{l'}, \omega_l, \omega_{l'}) = \frac{e}{im\omega_{l'}} D_j(\boldsymbol{x}; \omega_l)\delta_{i,k}, \tag{3.3.13}$$

where $\sigma_{ijk}^{(2,A)}$ is the conductivity which arises from $\boldsymbol{j}_{\rm op}^{\mathbf{A}}(\boldsymbol{x}, t)$. Using Eqs. (3.3.4, 3.3.13), I get

$$\sigma_{ijk}^{(2,A)}(\omega_l + \omega_{l'}, \omega_l, \omega_{l'}; \mathbf{G}) = \frac{e}{im\omega_{l'}} D_j(\omega_l; \mathbf{G})\delta_{i,k}. \tag{3.3.14}$$

Following this result, I identify the induced charge density tensor Fourier component to be

$$\begin{aligned} D_j(\omega_l; \mathbf{G}) = \frac{e^2}{m\omega_l \hbar V} \sum_{n_1\, \mathbf{q}_1, n_2\, \mathbf{q}_2} & \frac{\left(f_0(\varepsilon_{n_2}(\mathbf{q}_2)) - f_0(\varepsilon_{n_1}(\mathbf{q}_1))\right) \langle n_1\, \mathbf{q}_1 | \, e^{i\mathbf{k}_l \cdot \boldsymbol{x}} \mathbf{p} \cdot \hat{e}_j \, | n_2\, \mathbf{q}_2 \rangle}{i(\omega_{n_1\, \mathbf{q}_1, n_2\, \mathbf{q}_2} - \omega_l) + \gamma_{n_1\, \mathbf{q}_1, n_2\, \mathbf{q}_2}} \\ \times \langle n_2\, \mathbf{q}_2 | \, e^{-i(\mathbf{k}_l + \mathbf{G}) \cdot \boldsymbol{x}} \, | n_1\, \mathbf{q}_1 \rangle \, . & \end{aligned} \tag{3.3.15}$$

The second order general conductivity can be written as

$$
\begin{aligned}
&\sigma^{(2)}_{ijk}(\omega_l+\omega_{l'},\omega_l,\omega_{l'};\mathbf{G}) = \frac{e}{im\omega_{l'}} D_j(\omega_l;\mathbf{G})\delta_{ik} \\
&-\sum_{n_1\,\mathbf{q}_1,n_2\,\mathbf{q}_2} \frac{ie^3}{4m^2\omega_l\omega_{l'}\hbar V} \frac{\left(f_0(\varepsilon_{n_2}(\mathbf{q}_2))-f_0(\varepsilon_{n_1}(\mathbf{q}_1))\right)\langle n_1\,\mathbf{q}_1|\, e^{i(\mathbf{k}_l+\mathbf{k}_{l'})\cdot\boldsymbol{x}}\,|n_2\,\mathbf{q}_2\rangle}{i(\omega_{n_1\,\mathbf{q}_1,n_2\,\mathbf{q}_2}-\omega_l-\omega_{l'})+\gamma_{n_1\,\mathbf{q}_1,n_2\,\mathbf{q}_2}} \\
&\times \big[2\,\langle n_2\,\mathbf{q}_2|\, e^{-i(\mathbf{k}_l+\mathbf{G}+\mathbf{k}_{l'})\cdot\boldsymbol{x}}\mathbf{p}\cdot\hat{e}_i\,|n_1\,\mathbf{q}_1\rangle \\
&-\hbar(\mathbf{k}_l+\mathbf{G}+\mathbf{k}_{l'})\cdot\hat{e}_i\,\langle n_2\,\mathbf{q}_2|\, e^{-i(\mathbf{k}_l+\mathbf{G}+\mathbf{k}_{l'})\cdot\boldsymbol{x}}\,|n_1\,\mathbf{q}_1\rangle\,\big]\delta_{j,k} \\
&-\sum_{n_1\,\mathbf{q}_1,n_2\,\mathbf{q}_2,n_3\,\mathbf{q}_3} \frac{e^3}{2m^3\omega_l\omega_{l'}\hbar^2 V} \\
&\big[2\,\langle n_2\,\mathbf{q}_2|\, e^{-i(\mathbf{k}_l+\mathbf{G}+\mathbf{k}_{l'})\cdot\boldsymbol{x}}\mathbf{p}\cdot\hat{e}_i\,|n_1\,\mathbf{q}_1\rangle \\
&-\hbar(\mathbf{k}_l+\mathbf{G}+\mathbf{k}_{l'})\cdot\hat{e}_i\,\langle n_2\,\mathbf{q}_2|\, e^{-i(\mathbf{k}_l+\mathbf{G}+\mathbf{k}_{l'})\cdot\boldsymbol{x}}\,|n_1\,\mathbf{q}_1\rangle\,\big] \\
&\times\left[\frac{\langle n_1\,\mathbf{q}_1|\, e^{i\mathbf{k}_l\cdot\boldsymbol{x}}\mathbf{p}\cdot\hat{e}_j\,|n_3\,\mathbf{q}_3\rangle\,\langle n_3\,\mathbf{q}_3|\, e^{i\mathbf{k}_{l'}\cdot\boldsymbol{x}}\mathbf{p}\cdot\hat{e}_k\,|n_2\,\mathbf{q}_2\rangle\left(f_0(\varepsilon_{n_2}(\mathbf{q}_2))-f_0(\varepsilon_{n_3}(\mathbf{q}_3))\right)}{\left[i(\omega_{n_1\,\mathbf{q}_1,n_2\,\mathbf{q}_2}-\omega_l-\omega_{l'})+\gamma_{n_1\,\mathbf{q}_1,n_2\,\mathbf{q}_2}\right]\left[i(\omega_{n_3\,\mathbf{q}_3,n_2\,\mathbf{q}_2}-\omega_{l'})+\gamma_{n_3\,\mathbf{q}_3,n_2\,\mathbf{q}_2}\right]}\right. \\
&\left.-\frac{\langle n_1\,\mathbf{q}_1|\, e^{i\mathbf{k}_{l'}\cdot\boldsymbol{x}}\mathbf{p}\cdot\hat{e}_k\,|n_3\,\mathbf{q}_3\rangle\,\langle n_3\,\mathbf{q}_3|\, e^{i\mathbf{k}_l\cdot\boldsymbol{x}}\mathbf{p}\cdot\hat{e}_j\,|n_2\,\mathbf{q}_2\rangle\left(f_0(\varepsilon_{n_3}(\mathbf{q}_3))-f_0(\varepsilon_{n_1}(\mathbf{q}_1))\right)}{\left[i(\omega_{n_1\,\mathbf{q}_1,n_2\,\mathbf{q}_2}-\omega_l-\omega_{l'})+\gamma_{n_1\,\mathbf{q}_1,n_2\,\mathbf{q}_2}\right]\left[i(\omega_{n_1\,\mathbf{q}_1,n_3\,\mathbf{q}_3}-\omega_{l'})+\gamma_{n_1\,\mathbf{q}_1,n_3\,\mathbf{q}_3}\right]}\right].
\end{aligned}
\tag{3.3.16}
$$

4 Nonlinear interaction for spontaneous parametric down-conversion

In this section, I describe the evaluation of the conductivity relevant for the process of SPDC of x rays into UV/visible radiation. I denote the input x-ray beam, the output x-ray beam, and the optical beam as the pump $(\omega_p, \mathbf{k}_p)$, signal $(\omega_s, \mathbf{k}_s)$ and idler $(\omega_{id}, \mathbf{k}_{id})$ respectively. Due to the high absorption in the UV range, in a typical experiment only the signal photons are measured, and thus I focus my interest in the conductivity for the signal mode.

I can simplify the expressions by first assuming that the x-ray wavelengths are far above any electronic transitions and use the dipole approximation for the optical beam (but not for the x rays).

Secondly, by expressing the matrix elements using very localized of Wannier functions, I further simplify my expressions.

In addition, since the wavelengths of the x rays are also on the order of the distance between the atomic planes, the reciprocal lattice vector is used to comply with the requirement for momentum conservation (phase matching), given by the equation $\mathbf{k}_p + \mathbf{G} = \mathbf{k}_s + \mathbf{k}_{id}$. Thus the measured intensity is proportional to the Fourier coefficient that corresponds to the selected reciprocal lattice vector.

I begin the derivation with the general expression for the conductivity for the signal mode, using the following relation

$$\sigma^{(2)}_{ijk}(\omega_s; \mathbf{G}) = \sigma^{(2)}_{ijk}(\omega_p - \omega_{id}, \omega_p, -\omega_{id}; \mathbf{G}) + \sigma^{(2)}_{ikj}(-\omega_{id} + \omega_p, -\omega_{id}, \omega_p; \mathbf{G}), \quad (4.0.17)$$

such that

$$\langle \boldsymbol{j} \rangle^{(2)} (\boldsymbol{x}; \omega_p - \omega_{id} = \omega_s) \cdot \hat{e}_i = \sum_{jk} \sigma^{(2)}_{ijk}(\omega_s; \mathbf{G}) e^{i\mathbf{G}\cdot\boldsymbol{x}} (\boldsymbol{\varepsilon}(\omega_p) \cdot \hat{e}_j)(\boldsymbol{\varepsilon}^*(\omega_{id}) \cdot \hat{e}_k), \quad (4.0.18)$$

where $(\hat{e}_i, \hat{e}_j, \hat{e}_k)$ are unit vectors projected in the direction of the signal, pump and idler fields respectively.

4.1 The conductivity for the signal mode in the Bloch basis

Following the general result for the conductivity (Eqs.(3.3.5, 4.0.17)), I find that the conductivity for the signal mode is

$$\sigma^{(2)}_{ijk}(\omega_s;\mathbf{G}) =$$

$$\sum_{n_1\,\mathbf{q}_1,n_2\,\mathbf{q}_2} \frac{-e^3}{im^2\omega_p\omega_{id}\hbar V} \frac{\left(f_0(\varepsilon_{n_2}(\mathbf{q}_2)) - f_0(\varepsilon_{n_1}(\mathbf{q}_1))\right) \langle n_1\,\mathbf{q}_1| \, e^{i\mathbf{k}_p\cdot\boldsymbol{x}}\mathbf{p}\cdot\hat{e}_j \, |n_2\,\mathbf{q}_2\rangle}{i(\omega_{n_1\,\mathbf{q}_1,n_2\,\mathbf{q}_2} - \omega_p) + \gamma_{n_1\,\mathbf{q}_1,n_2\,\mathbf{q}_2}}$$

$$\times \langle n_2\,\mathbf{q}_2| \, e^{-i(\mathbf{k}_p+\mathbf{G})\cdot\boldsymbol{x}} \, |n_1\,\mathbf{q}_1\rangle \, \delta_{i,k}$$

$$+ \sum_{n_1\,\mathbf{q}_1,n_2\,\mathbf{q}_2} \frac{ie^3}{4m^2\omega_p\omega_{id}\hbar V} \frac{\left(f_0(\varepsilon_{n_2}(\mathbf{q}_2)) - f_0(\varepsilon_{n_1}(\mathbf{q}_1))\right) \langle n_1\,\mathbf{q}_1| \, e^{i(\mathbf{k}_p-\mathbf{k}_{id})\cdot\boldsymbol{x}} \, |n_2\,\mathbf{q}_2\rangle}{i(\omega_{n_1\,\mathbf{q}_1,n_2\,\mathbf{q}_2} - \omega_p + \omega_{id}) + \gamma_{n_1\,\mathbf{q}_1,n_2\,\mathbf{q}_2}}$$

$$\times \big[2 \, \langle n_2\,\mathbf{q}_2| \, e^{-i(\mathbf{k}_p+\mathbf{G}-\mathbf{k}_{id})\cdot\boldsymbol{x}}\mathbf{p}\cdot\hat{e}_i \, |n_1\,\mathbf{q}_1\rangle$$

$$- \hbar(\mathbf{k}_p + \mathbf{G} - \mathbf{k}_{id})\cdot\hat{e}_i \, \langle n_2\,\mathbf{q}_2| \, e^{-i(\mathbf{k}_p+\mathbf{G}-\mathbf{k}_{id})\cdot\boldsymbol{x}} \, |n_1\,\mathbf{q}_1\rangle \, \big]\delta_{j,k}$$

$$+ \sum_{n_1\,\mathbf{q}_1,n_2\,\mathbf{q}_2,n_3\,\mathbf{q}_3} \frac{e^3}{2m^3\omega_p\omega_{id}\hbar^2 V}$$

$$\big[2 \, \langle n_2\,\mathbf{q}_2| \, e^{-i(\mathbf{k}_p+\mathbf{G}-\mathbf{k}_{id})\cdot\boldsymbol{x}}\mathbf{p}\cdot\hat{e}_i \, |n_1\,\mathbf{q}_1\rangle$$

$$- \hbar(\mathbf{k}_p + \mathbf{G} - \mathbf{k}_{id})\cdot\hat{e}_i \, \langle n_2\,\mathbf{q}_2| \, e^{-i(\mathbf{k}_p+\mathbf{G}-\mathbf{k}_{id})\cdot\boldsymbol{x}''} \, |n_1\,\mathbf{q}_1\rangle \, \big]$$

$$\times \left[\frac{\langle n_1\,\mathbf{q}_1| \, e^{i\mathbf{k}_p\cdot\boldsymbol{x}}\mathbf{p}\cdot\hat{e}_j \, |n_3\,\mathbf{q}_3\rangle \, \langle n_3\,\mathbf{q}_3| \, e^{-i\mathbf{k}_{id}\cdot\boldsymbol{x}}\mathbf{p}\cdot\hat{e}_k \, |n_2\,\mathbf{q}_2\rangle \left(f_0(\varepsilon_{n_2}(\mathbf{q}_2)) - f_0(\varepsilon_{n_3}(\mathbf{q}_3))\right)}{\left[i(\omega_{n_1\,\mathbf{q}_1,n_2\,\mathbf{q}_2} - \omega_p + \omega_{id}) + \gamma_{n_1\,\mathbf{q}_1,n_2\,\mathbf{q}_2}\right]\left[i(\omega_{n_3\,\mathbf{q}_3,n_2\,\mathbf{q}_2} + \omega_{id}) + \gamma_{n_3\,\mathbf{q}_3,n_2\,\mathbf{q}_2}\right]} \right.$$

$$\left. - \frac{\langle n_1\,\mathbf{q}_1| \, e^{-i\mathbf{k}_{id}\cdot\boldsymbol{x}}\mathbf{p}\cdot\hat{e}_k \, |n_3\,\mathbf{q}_3\rangle \, \langle n_3\,\mathbf{q}_3| \, e^{i\mathbf{k}_p\cdot\boldsymbol{x}}\mathbf{p}\cdot\hat{e}_j \, |n_2\,\mathbf{q}_2\rangle \left(f_0(\varepsilon_{n_3}(\mathbf{q}_3)) - f_0(\varepsilon_{n_1}(\mathbf{q}_1))\right)}{\left[i(\omega_{n_1\,\mathbf{q}_1,n_2\,\mathbf{q}_2} - \omega_p + \omega_{id}) + \gamma_{n_1\,\mathbf{q}_1,n_2\,\mathbf{q}_2}\right]\left[i(\omega_{n_1\,\mathbf{q}_1,n_3\,\mathbf{q}_3} + \omega_{id}) + \gamma_{n_1\,\mathbf{q}_1,n_3\,\mathbf{q}_3}\right]} \right]$$

$$\sum_{n_1\,\mathbf{q}_1,n_2\,\mathbf{q}_2} \frac{-e^3}{im^2\omega_p\omega_{id}\hbar V} \frac{\left(f_0(\varepsilon_{n_2}(\mathbf{q}_2)) - f_0(\varepsilon_{n_1}(\mathbf{q}_1))\right) \langle n_1\,\mathbf{q}_1| \, e^{-i\mathbf{k}_{id}\cdot\boldsymbol{x}}\mathbf{p}\cdot\hat{e}_k \, |n_2\,\mathbf{q}_2\rangle}{i(\omega_{n_1\,\mathbf{q}_1,n_2\,\mathbf{q}_2} + \omega_{id}) + \gamma_{n_1\,\mathbf{q}_1,n_2\,\mathbf{q}_2}}$$

$$\times \langle n_2\,\mathbf{q}_2| \, e^{i(\mathbf{k}_{id}-\mathbf{G})\cdot\boldsymbol{x}} \, |n_1\,\mathbf{q}_1\rangle \, \delta_{i,j}$$

$$+ \sum_{n_1\,\mathbf{q}_1,n_2\,\mathbf{q}_2} \frac{ie^3}{4m^2\omega_p\omega_{id}\hbar V} \frac{\left(f_0(\varepsilon_{n_2}(\mathbf{q}_2)) - f_0(\varepsilon_{n_1}(\mathbf{q}_1))\right) \langle n_1\,\mathbf{q}_1| \, e^{i(\mathbf{k}_p-\mathbf{k}_{id})\cdot\boldsymbol{x}} \, |n_2\,\mathbf{q}_2\rangle}{i(\omega_{n_1\,\mathbf{q}_1,n_2\,\mathbf{q}_2} - \omega_p + \omega_{id}) + \gamma_{n_1\,\mathbf{q}_1,n_2\,\mathbf{q}_2}}$$

$$\times \big[2 \, \langle n_2\,\mathbf{q}_2| \, e^{-i(\mathbf{k}_p+\mathbf{G}-\mathbf{k}_{id})\cdot\boldsymbol{x}}\mathbf{p}\cdot\hat{e}_i \, |n_1\,\mathbf{q}_1\rangle$$

$$- \hbar(\mathbf{k}_p + \mathbf{G} - \mathbf{k}_{id})\cdot\hat{e}_i \, \langle n_2\,\mathbf{q}_2| \, e^{-i(\mathbf{k}_p+\mathbf{G}-\mathbf{k}_{id})\cdot\boldsymbol{x}} \, |n_1\,\mathbf{q}_1\rangle \, \big]\delta_{j,k}$$

$$
\begin{aligned}
&+ \sum_{n_1\,\mathbf{q}_1, n_2\,\mathbf{q}_2, n_3\,\mathbf{q}_3} \frac{e^3}{2m^3\omega_p\omega_{id}\hbar^2 V} \\
&\big[2\,\langle n_2\,\mathbf{q}_2|\, e^{-i(\mathbf{k}_p+\mathbf{G}-\mathbf{k}_{id})\cdot\boldsymbol{x}}\mathbf{p}\cdot\hat{e}_i\,|n_1\,\mathbf{q}_1\rangle \\
&-\hbar(\mathbf{k}_p+\mathbf{G}-\mathbf{k}_{id})\cdot\hat{e}_i\,\langle n_2\,\mathbf{q}_2|\, e^{-i(\mathbf{k}_p+\mathbf{G}-\mathbf{k}_{id})\cdot\boldsymbol{x}}\,|n_1\,\mathbf{q}_1\rangle\,\big] \\
&\times\left[\frac{\langle n_1\,\mathbf{q}_1|\, e^{-i\mathbf{k}_{id}\cdot\boldsymbol{x}}\mathbf{p}\cdot\hat{e}_k\,|n_3\,\mathbf{q}_3\rangle\,\langle n_3\,\mathbf{q}_3|\, e^{i\mathbf{k}_p\cdot\boldsymbol{x}}\mathbf{p}\cdot\hat{e}_j\,|n_2\,\mathbf{q}_2\rangle\,(f_0(\varepsilon_{n_2}(\mathbf{q}_2))-f_0(\varepsilon_{n_3}(\mathbf{q}_3)))}{[i(\omega_{n_1\,\mathbf{q}_1,n_2\,\mathbf{q}_2}-\omega_p+\omega_{id})+\gamma_{n_1\,\mathbf{q}_1,n_2\,\mathbf{q}_2}]\,[i(\omega_{n_3\,\mathbf{q}_3,n_2\,\mathbf{q}_2}-\omega_p)+\gamma_{n_3\,\mathbf{q}_3,n_2\,\mathbf{q}_2}]}\right. \\
&\left.-\frac{\langle n_1\,\mathbf{q}_1|\, e^{i\mathbf{k}_p\cdot\boldsymbol{x}}\mathbf{p}\cdot\hat{e}_j\,|n_3\,\mathbf{q}_3\rangle\,\langle n_3\,\mathbf{q}_3|\, e^{-i\mathbf{k}_{id}\cdot\boldsymbol{x}}\mathbf{p}\cdot\hat{e}_k\,|n_2\,\mathbf{q}_2\rangle\,(f_0(\varepsilon_{n_3}(\mathbf{q}_3))-f_0(\varepsilon_{n_1}(\mathbf{q}_1)))}{[i(\omega_{n_1\,\mathbf{q}_1,n_2\,\mathbf{q}_2}-\omega_p+\omega_{id})+\gamma_{n_1\,\mathbf{q}_1,n_2\,\mathbf{q}_2}]\,[i(\omega_{n_1\,\mathbf{q}_1,n_3\,\mathbf{q}_3}-\omega_p)+\gamma_{n_1\,\mathbf{q}_1,n_3\,\mathbf{q}_3}]}\right].
\end{aligned}
\tag{4.1.1}
$$

Next, I keep only terms with resonances close to the idler frequency (i.e. terms with ω_{id} in the denominator) and get

$$
\begin{aligned}
&\sigma_{ijk}(\omega_s;\mathbf{G}) = \\
&\sum_{n_1\,\mathbf{q}_1, n_2\,\mathbf{q}_2} \frac{-e^3}{im^2\omega_p\omega_{id}\hbar V}\,\frac{(f_0(\varepsilon_{n_2}(\mathbf{q}_2))-f_0(\varepsilon_{n_1}(\mathbf{q}_1)))\,\langle n_1\,\mathbf{q}_1|\, e^{-i\mathbf{k}_{id}\cdot\boldsymbol{x}}\mathbf{p}\cdot\hat{e}_k\,|n_2\,\mathbf{q}_2\rangle}{i(\omega_{n_1\,\mathbf{q}_1,n_2\,\mathbf{q}_2}+\omega_{id})+\gamma_{n_1\,\mathbf{q}_1,n_2\,\mathbf{q}_2}} \\
&\times\langle n_2\,\mathbf{q}_2|\, e^{i(\mathbf{k}_{id}-\mathbf{G})\cdot\boldsymbol{x}}\,|n_1\,\mathbf{q}_1\rangle\,\delta_{i,j} \\
&+ \sum_{n_1\,\mathbf{q}_1, n_2\,\mathbf{q}_2, n_3\,\mathbf{q}_3} \frac{e^3}{2m^3\omega_p\omega_{id}\hbar^2 V} \\
&\big[2\,\langle n_2\,\mathbf{q}_2|\, e^{-i(\mathbf{k}_p+\mathbf{G}-\mathbf{k}_{id})\cdot\boldsymbol{x}}\mathbf{p}\,|n_1\,\mathbf{q}_1\rangle-\hbar(\mathbf{k}_p+\mathbf{G}-\mathbf{k}_{id})\,\langle n_2\,\mathbf{q}_2|\, e^{-i(\mathbf{k}_p+\mathbf{G}-\mathbf{k}_{id})\cdot\boldsymbol{x}}\,|n_1\,\mathbf{q}_1\rangle\big]\cdot\hat{e}_i \\
&\times\left[\frac{\langle n_1\,\mathbf{q}_1|\, e^{i\mathbf{k}_p\cdot\boldsymbol{x}}\mathbf{p}\cdot\hat{e}_j\,|n_3\,\mathbf{q}_3\rangle\,\langle n_3\,\mathbf{q}_3|\, e^{-i\mathbf{k}_{id}\cdot\boldsymbol{x}}\mathbf{p}\cdot\hat{e}_k\,|n_2\,\mathbf{q}_2\rangle\,(f_0(\varepsilon_{n_2}(\mathbf{q}_2))-f_0(\varepsilon_{n_3}(\mathbf{q}_3)))}{[i(\omega_{n_1\,\mathbf{q}_1,n_2\,\mathbf{q}_2}-(\omega_p-\omega_{id}))+\gamma_{n_1\,\mathbf{q}_1,n_2\,\mathbf{q}_2}]\,[i(\omega_{n_3\,\mathbf{q}_3,n_2\,\mathbf{q}_2}+\omega_{id})+\gamma_{n_3\,\mathbf{q}_3,n_2\,\mathbf{q}_2}]}\right. \\
&\left.-\frac{\langle n_1\,\mathbf{q}_1|\, e^{-i\mathbf{k}_{id}\cdot\boldsymbol{x}}\mathbf{p}\cdot\hat{e}_k\,|n_3\,\mathbf{q}_3\rangle\,\langle n_3\,\mathbf{q}_3|\, e^{i\mathbf{k}_p\cdot\boldsymbol{x}}\mathbf{p}\cdot\hat{e}_j\,|n_2\,\mathbf{q}_2\rangle\,(f_0(\varepsilon_{n_3}(\mathbf{q}_3))-f_0(\varepsilon_{n_1}(\mathbf{q}_1)))}{[i(\omega_{n_1\,\mathbf{q}_1,n_2\,\mathbf{q}_2}-(\omega_p-\omega_{id}))+\gamma_{n_1\,\mathbf{q}_1,n_2\,\mathbf{q}_2}]\,[i(\omega_{n_1\,\mathbf{q}_1,n_3\,\mathbf{q}_3}+\omega_{id})+\gamma_{n_1\,\mathbf{q}_1,n_3\,\mathbf{q}_3}]}\right].
\end{aligned}
\tag{4.1.2}
$$

Since the x ray modes are well above any electronic transitions and keeping in mind that $\omega_p = \omega_s + \omega_{id}$, I can make the following approximation

$$
[i(\omega_{n_1\,\mathbf{q}_1,n_2\,\mathbf{q}_2}-(\omega_p-\omega_{id}))+\gamma_{n_1\,\mathbf{q}_1,n_2\,\mathbf{q}_2}]\approx -i\omega_s, \tag{4.1.3}
$$

and get

$$\begin{aligned}
&\sigma_{ijk}(\omega_s;\mathbf{G}) = \\
&\sum_{n_1\,\mathbf{q}_1,n_2\,\mathbf{q}_2} \frac{-e^3}{m^2\omega_p\omega_{id}\hbar V} \frac{(f_0(\varepsilon_{n_2}(\mathbf{q}_2)) - f_0(\varepsilon_{n_1}(\mathbf{q}_1)))}{(\omega_{n_2\,\mathbf{q}_2,n_1\,\mathbf{q}_1} - \omega_{id}) + i\gamma_{n_2\,\mathbf{q}_2,n_1\,\mathbf{q}_1}} \\
&\times \langle n_1\,\mathbf{q}_1|\, e^{-i\mathbf{k}_{id}\cdot\boldsymbol{x}}\mathbf{p}\cdot\hat{e}_k\, |n_2\,\mathbf{q}_2\rangle \langle n_2\,\mathbf{q}_2|\, e^{i(\mathbf{k}_{id}-\mathbf{G})\cdot\boldsymbol{x}}\, |n_1\,\mathbf{q}_1\rangle\, \delta_{i,j} \\
&- \sum_{n_1\,\mathbf{q}_1,n_2\,\mathbf{q}_2,n_3\,\mathbf{q}_3} \frac{e^3}{2m^3\omega_p\omega_{id}\omega_s\hbar^2 V} \\
&\big[2\,\langle n_2\,\mathbf{q}_2|\, e^{-i(\mathbf{k}_p+\mathbf{G}-\mathbf{k}_{id})\cdot\boldsymbol{x}}\mathbf{p}\cdot\hat{e}_i\, |n_1\,\mathbf{q}_1\rangle \\
&- \hbar(\mathbf{k}_p+\mathbf{G}-\mathbf{k}_{id})\cdot\hat{e}_i\, \langle n_2\,\mathbf{q}_2|\, e^{-i(\mathbf{k}_p+\mathbf{G}-\mathbf{k}_{id})\cdot\boldsymbol{x}}\, |n_1\,\mathbf{q}_1\rangle\, \big] \\
&\times \left[\frac{\langle n_1\,\mathbf{q}_1|\, e^{i\mathbf{k}_p\cdot\boldsymbol{x}}\mathbf{p}\cdot\hat{e}_j\, |n_3\,\mathbf{q}_3\rangle \langle n_3\,\mathbf{q}_3|\, e^{-i\mathbf{k}_{id}\cdot\boldsymbol{x}}\mathbf{p}\cdot\hat{e}_k\, |n_2\,\mathbf{q}_2\rangle\, (f_0(\varepsilon_{n_2}(\mathbf{q}_2)) - f_0(\varepsilon_{n_3}(\mathbf{q}_3)))}{[(\omega_{n_2\,\mathbf{q}_2,n_3\,\mathbf{q}_3} - \omega_{id}) + i\gamma_{n_2\,\mathbf{q}_2,n_3\,\mathbf{q}_3}]} \right. \\
&\left. - \frac{\langle n_1\,\mathbf{q}_1|\, e^{-i\mathbf{k}_{id}\cdot\boldsymbol{x}}\mathbf{p}\cdot\hat{e}_k\, |n_3\,\mathbf{q}_3\rangle \langle n_3\,\mathbf{q}_3|\, e^{i\mathbf{k}_p\cdot\boldsymbol{x}}\mathbf{p}\cdot\hat{e}_j\, |n_2\,\mathbf{q}_2\rangle\, (f_0(\varepsilon_{n_3}(\mathbf{q}_3)) - f_0(\varepsilon_{n_1}(\mathbf{q}_1)))}{[(\omega_{n_3\,\mathbf{q}_3,n_1\,\mathbf{q}_1} - \omega_{id}) + i\gamma_{n_3\,\mathbf{q}_3,n_1\,\mathbf{q}_1}]} \right].
\end{aligned} \tag{4.1.4}$$

In this expression I used the property $\omega_{n_1\,\mathbf{q}_1,n_2\,\mathbf{q}_2} = -\omega_{n_2\,\mathbf{q}_2,n_1\,\mathbf{q}_1}$, to explicitly show the resonance dependence on the idler mode. Furthermore, using the phase-matching condition, I find that $(\mathbf{k}_p+\mathbf{G}-\mathbf{k}_{id})\cdot\hat{e}_i = \mathbf{k}_s\cdot\hat{e}_i = 0$ since I am dealing with transverse modes and $\hat{e}_i$ is projected in the direction of the signal field. This leads to

$$\begin{aligned}
&\sigma_{ijk}(\omega_s;\mathbf{G}) = \\
&\sum_{n_1\,\mathbf{q}_1,n_2\,\mathbf{q}_2} \frac{-e^3}{m^2\omega_p\omega_{id}\hbar V} \frac{(f_0(\varepsilon_{n_2}(\mathbf{q}_2)) - f_0(\varepsilon_{n_1}(\mathbf{q}_1)))}{(\omega_{n_2\,\mathbf{q}_2,n_1\,\mathbf{q}_1} - \omega_{id}) + i\gamma_{n_2\,\mathbf{q}_2,n_1\,\mathbf{q}_1}} \\
&\times \langle n_1\,\mathbf{q}_1|\, e^{-i\mathbf{k}_{id}\cdot\boldsymbol{x}}\mathbf{p}\cdot\hat{e}_k\, |n_2\,\mathbf{q}_2\rangle \langle n_2\,\mathbf{q}_2|\, e^{i(\mathbf{k}_{id}-\mathbf{G})\cdot\boldsymbol{x}}\, |n_1\,\mathbf{q}_1\rangle\, \delta_{i,j} \\
&- \sum_{n_1\,\mathbf{q}_1,n_2\,\mathbf{q}_2,n_3\,\mathbf{q}_3} \frac{e^3}{m^3\omega_p\omega_{id}\omega_s\hbar^2 V} \langle n_2\,\mathbf{q}_2|\, e^{-i(\mathbf{k}_p+\mathbf{G}-\mathbf{k}_{id})\cdot\boldsymbol{x}}\mathbf{p}\cdot\hat{e}_i\, |n_1\,\mathbf{q}_1\rangle \\
&\times \left[\frac{\langle n_1\,\mathbf{q}_1|\, e^{i\mathbf{k}_p\cdot\boldsymbol{x}}\mathbf{p}\cdot\hat{e}_j\, |n_3\,\mathbf{q}_3\rangle \langle n_3\,\mathbf{q}_3|\, e^{-i\mathbf{k}_{id}\cdot\boldsymbol{x}}\mathbf{p}\cdot\hat{e}_k\, |n_2\,\mathbf{q}_2\rangle\, (f_0(\varepsilon_{n_2}(\mathbf{q}_2)) - f_0(\varepsilon_{n_3}(\mathbf{q}_3)))}{[(\omega_{n_2\,\mathbf{q}_2,n_3\,\mathbf{q}_3} - \omega_{id}) + i\gamma_{n_2\,\mathbf{q}_2,n_3\,\mathbf{q}_3}]} \right. \\
&\left. - \frac{\langle n_1\,\mathbf{q}_1|\, e^{-i\mathbf{k}_{id}\cdot\boldsymbol{x}}\mathbf{p}\cdot\hat{e}_k\, |n_3\,\mathbf{q}_3\rangle \langle n_3\,\mathbf{q}_3|\, e^{i\mathbf{k}_p\cdot\boldsymbol{x}}\mathbf{p}\cdot\hat{e}_j\, |n_2\,\mathbf{q}_2\rangle\, (f_0(\varepsilon_{n_3}(\mathbf{q}_3)) - f_0(\varepsilon_{n_1}(\mathbf{q}_1)))}{[(\omega_{n_3\,\mathbf{q}_3,n_1\,\mathbf{q}_1} - \omega_{id}) + i\gamma_{n_3\,\mathbf{q}_3,n_1\,\mathbf{q}_1}]} \right].
\end{aligned} \tag{4.1.5}$$

In this expression all the terms have similar denominator up to a change of indices and so by rearranging the sums in the second term I get

$$
\begin{aligned}
&\sigma_{ijk}(\omega_s;\mathbf{G}) = \\
&\sum_{n_1\,\mathbf{q}_1, n_2\,\mathbf{q}_2} \frac{-e^3}{m^2\omega_p\omega_{id}\hbar V} \frac{(f_0(\varepsilon_{n_2}(\mathbf{q}_2)) - f_0(\varepsilon_{n_1}(\mathbf{q}_1)))}{(\omega_{n_2\,\mathbf{q}_2,n_1\,\mathbf{q}_1} - \omega_{id}) + i\gamma_{n_2\,\mathbf{q}_2,n_1\,\mathbf{q}_1}} \\
&\times \langle n_1\,\mathbf{q}_1| \, e^{-i\mathbf{k}_{id}\cdot\boldsymbol{x}}\mathbf{p}\cdot\hat{e}_k \, |n_2\,\mathbf{q}_2\rangle \langle n_2\,\mathbf{q}_2| \, e^{i(\mathbf{k}_{id}-\mathbf{G})\cdot\boldsymbol{x}} \, |n_1\,\mathbf{q}_1\rangle \, \delta_{i,j} \\
&- \sum_{n_1\,\mathbf{q}_1, n_2\,\mathbf{q}_2, n_3\,\mathbf{q}_3} \frac{e^3}{m^3\omega_p\omega_{id}\omega_s\hbar^2 V} \frac{\langle n_1\,\mathbf{q}_1| \, e^{-i\mathbf{k}_{id}\cdot\boldsymbol{x}}\mathbf{p}\cdot\hat{e}_k \, |n_2\,\mathbf{q}_2\rangle \, (f_0(\varepsilon_{n_2}(\mathbf{q}_2)) - f_0(\varepsilon_{n_1}(\mathbf{q}_1)))}{[(\omega_{n_2\,\mathbf{q}_2,n_1\,\mathbf{q}_1} - \omega_{id}) + i\gamma_{n_2\,\mathbf{q}_2,n_1\,\mathbf{q}_1}]} \\
&\times \Bigg[\langle n_2\,\mathbf{q}_2| \, e^{-i(\mathbf{k}_p+\mathbf{G}-\mathbf{k}_{id})\cdot\boldsymbol{x}}\mathbf{p}\cdot\hat{e}_i \, |n_3\,\mathbf{q}_3\rangle \langle n_3\,\mathbf{q}_3| \, e^{i\mathbf{k}_p\cdot\boldsymbol{x}}\mathbf{p}\cdot\hat{e}_j \, |n_1\,\mathbf{q}_1\rangle \\
&- \langle n_2\,\mathbf{q}_2| \, e^{i\mathbf{k}_p\cdot\boldsymbol{x}}\mathbf{p}\cdot\hat{e}_j \, |n_3\,\mathbf{q}_3\rangle \langle n_3\,\mathbf{q}_3| \, e^{-i(\mathbf{k}_p+\mathbf{G}-\mathbf{k}_{id})\cdot\boldsymbol{x}}\mathbf{p}\cdot\hat{e}_i \, |n_1\,\mathbf{q}_1\rangle \Bigg].
\end{aligned}
\tag{4.1.6}
$$

This expression can be further simplified by using the completeness relation with respect to the sum over $(n_3\,\mathbf{q}_3)$, such that

$$
\sum_{n_3\,\mathbf{q}_3} |n_3\,\mathbf{q}_3\rangle \langle n_3\,\mathbf{q}_3| = \mathbb{1},
\tag{4.1.7}
$$

and get

$$
\begin{aligned}
&\sigma_{ijk}(\omega_s;\mathbf{G}) = \\
&\sum_{n_1\,\mathbf{q}_1, n_2\,\mathbf{q}_2} \frac{-e^3}{m^2\omega_p\omega_{id}\hbar V} \frac{(f_0(\varepsilon_{n_2}(\mathbf{q}_2)) - f_0(\varepsilon_{n_1}(\mathbf{q}_1)))}{(\omega_{n_2\,\mathbf{q}_2,n_1\,\mathbf{q}_1} - \omega_{id}) + i\gamma_{n_2\,\mathbf{q}_2,n_1\,\mathbf{q}_1}} \langle n_1\,\mathbf{q}_1| \, e^{-i\mathbf{k}_{id}\cdot\boldsymbol{x}}\mathbf{p}\cdot\hat{e}_k \, |n_2\,\mathbf{q}_2\rangle \\
&\Bigg\{ \langle n_2\,\mathbf{q}_2| \, e^{i(\mathbf{k}_{id}-\mathbf{G})\cdot\boldsymbol{x}} \, |n_1\,\mathbf{q}_1\rangle \, \delta_{i,j} \\
&+ \frac{1}{m\hbar\omega_s} \langle n_2\,\mathbf{q}_2| \left[e^{-i(\mathbf{k}_p+\mathbf{G}-\mathbf{k}_{id})\cdot\boldsymbol{x}}\mathbf{p}\cdot\hat{e}_i \, , \, e^{i\mathbf{k}_p\cdot\boldsymbol{x}}\mathbf{p}\cdot\hat{e}_j \right] |n_1\,\mathbf{q}_1\rangle \Bigg\}.
\end{aligned}
\tag{4.1.8}
$$

To simplify this expression, I solved the commutation relation found in the second term using the identity (see appendix A.3)

$$
\left[e^{i\mathbf{k}_1\cdot\boldsymbol{x}}(\mathbf{p}\cdot\hat{e}_i), e^{i\mathbf{k}_2\cdot\boldsymbol{x}}(\mathbf{p}\cdot\hat{e}_j)\right] = e^{i(\mathbf{k}_1+\mathbf{k}_2)\cdot\boldsymbol{x}} \left[(\hbar\mathbf{k}_2\cdot\hat{e}_i)\,(\mathbf{p}\cdot\hat{e}_j) - (\hbar\mathbf{k}_1\cdot\hat{e}_j)\,(\mathbf{p}\cdot\hat{e}_i) \right],
\tag{4.1.9}
$$

and find

$$\begin{aligned}&\left[e^{-i(\mathbf{k}_p+\mathbf{G}-\mathbf{k}_{id})\cdot\boldsymbol{x}}(\mathbf{p}\cdot\hat{e}_i),e^{i\mathbf{k}_p\cdot\boldsymbol{x}}(\mathbf{p}\cdot\hat{e}_j)\right]\\&=e^{i(\mathbf{k}_{id}-\mathbf{G})\cdot\boldsymbol{x}}\left[(\hbar\mathbf{k}_p\cdot\hat{e}_i)\left(\mathbf{p}\cdot\hat{e}_j\right)+\left(\hbar(\mathbf{k}_p+\mathbf{G}-\mathbf{k}_{id})\cdot\hat{e}_j\right)\left(\mathbf{p}\cdot\hat{e}_i\right)\right].\end{aligned}\tag{4.1.10}$$

The result can be further simplified by using

$$\begin{aligned}\mathbf{k}_p&=\mathbf{k}_s+(\mathbf{k}_{id}-\mathbf{G}); &\quad \mathbf{k}_s&=\mathbf{k}_p-(\mathbf{k}_{id}-\mathbf{G}),\\ \mathbf{k}_p\cdot\hat{e}_i&=(\mathbf{k}_{id}-\mathbf{G})\cdot\hat{e}_i; &\quad \mathbf{k}_s\cdot\hat{e}_j&=-(\mathbf{k}_{id}-\mathbf{G})\cdot\hat{e}_j,\end{aligned}\tag{4.1.11}$$

where in the last line I used the property that the fields are transverse, and I get

$$\begin{aligned}&\sigma_{ijk}(\omega_s;\mathbf{G})=\\&\sum_{n_1\,\mathbf{q}_1,n_2\,\mathbf{q}_2}\frac{-e^3}{m^2\omega_p\omega_{id}\hbar V}\frac{(f_0(\varepsilon_{n_2}(\mathbf{q}_2))-f_0(\varepsilon_{n_1}(\mathbf{q}_1)))}{(\omega_{n_2\,\mathbf{q}_2,n_1\,\mathbf{q}_1}-\omega_{id})+i\gamma_{n_2\,\mathbf{q}_2,n_1\,\mathbf{q}_1}}\left\langle n_1\,\mathbf{q}_1\right|e^{-i\mathbf{k}_{id}\cdot\boldsymbol{x}}\mathbf{p}\cdot\hat{e}_k\left|n_2\,\mathbf{q}_2\right\rangle\\&\Bigg\{\left\langle n_2\,\mathbf{q}_2\right|e^{i(\mathbf{k}_{id}-\mathbf{G})\cdot\boldsymbol{x}}\left|n_1\,\mathbf{q}_1\right\rangle\delta_{i,j}\\&+\frac{\hbar(\mathbf{k}_{id}-\mathbf{G})}{m\hbar\omega_s}\cdot\left\langle n_2\,\mathbf{q}_2\right|e^{i(\mathbf{k}_{id}-\mathbf{G})\cdot\boldsymbol{x}}\left[\hat{e}_i(\mathbf{p}\cdot\hat{e}_j)-\hat{e}_j(\mathbf{p}\cdot\hat{e}_i)\right]\left|n_1\,\mathbf{q}_1\right\rangle\Bigg\}.\end{aligned}\tag{4.1.12}$$

Since the idler frequency is assumed to be in the UV/visible range, I use the dipole approximation and get

$$\begin{aligned}&\sigma_{ijk}(\omega_s;\mathbf{G})=\\&\sum_{n_1\,\mathbf{q}_1,n_2\,\mathbf{q}_2}\frac{-e^3}{m^2\omega_p\omega_{id}\hbar V}\frac{(f_0(\varepsilon_{n_2}(\mathbf{q}_2))-f_0(\varepsilon_{n_1}(\mathbf{q}_1)))}{(\omega_{n_2\,\mathbf{q}_2,n_1\,\mathbf{q}_1}-\omega_{id})+i\gamma_{n_2\,\mathbf{q}_2,n_1\,\mathbf{q}_1}}\left\langle n_1\,\mathbf{q}_1\right|\mathbf{p}\cdot\hat{e}_k\left|n_2\,\mathbf{q}_2\right\rangle\\&\Bigg\{\left\langle n_2\,\mathbf{q}_2\right|e^{-i\mathbf{G}\cdot\boldsymbol{x}}\left|n_1\,\mathbf{q}_1\right\rangle\delta_{i,j}\\&+\frac{\hbar(\mathbf{k}_{id}-\mathbf{G})}{m\hbar\omega_s}\cdot\left\langle n_2\,\mathbf{q}_2\right|e^{-i\mathbf{G}\cdot\boldsymbol{x}}\left[\hat{e}_i(\mathbf{p}\cdot\hat{e}_j)-\hat{e}_j(\mathbf{p}\cdot\hat{e}_i)\right]\left|n_1\,\mathbf{q}_1\right\rangle\Bigg\}.\end{aligned}\tag{4.1.13}$$

For brevity of notation, which will be convenient for later use, I express the conductivity in the following way

$$\sigma_{ijk}(\omega_s;\mathbf{G}) = \frac{e}{im\omega_p} D_k(-\omega_{id};\mathbf{G})\delta_{i,j} + \frac{e^3}{Vm^3\omega_p\omega_s} B_{ijk}(\omega_{id},\mathbf{k}_{id};\mathbf{G}), \tag{4.1.14}$$

$$\begin{aligned} D_k(-\omega_{id};\mathbf{G}) = \left(\frac{i\hbar e^2}{mV}\right) \sum_{n_1\,\mathbf{q}_1,n_2\,\mathbf{q}_2} \langle n_1\,\mathbf{q}_1|\,\mathbf{p}\cdot\hat{e}_k\,|n_2\,\mathbf{q}_2\rangle \langle n_2\,\mathbf{q}_2|\,e^{-i\mathbf{G}\cdot\boldsymbol{x}}\,|n_1\,\mathbf{q}_1\rangle \\ \times \frac{-\left(f_0(\varepsilon_{n_2}(\mathbf{q}_2)) - f_0(\varepsilon_{n_1}(\mathbf{q}_1))\right)}{\hbar\omega_{id}(\hbar\omega_{n_2\,\mathbf{q}_2,n_1\,\mathbf{q}_1} - \hbar\omega_{id}) + i\hbar\gamma_{n_2\,\mathbf{q}_2,n_1\,\mathbf{q}_1}}, \end{aligned} \tag{4.1.15}$$

$$\begin{aligned} & B_{ijk}(\omega_{id},\mathbf{k}_{id};\mathbf{G}) = \\ & \sum_{n_1\,\mathbf{q}_1,n_2\,\mathbf{q}_2} \hbar(\mathbf{k}_{id}-\mathbf{G})\cdot\langle n_2\,\mathbf{q}_2|\,e^{-i\mathbf{G}\cdot\boldsymbol{x}}\,[\hat{e}_i(\mathbf{p}\cdot\hat{e}_j) - \hat{e}_j(\mathbf{p}\cdot\hat{e}_i)]\,|n_1\,\mathbf{q}_1\rangle \langle n_1\,\mathbf{q}_1|\,\mathbf{p}\cdot\hat{e}_k\,|n_2\,\mathbf{q}_2\rangle \\ & \times \frac{-\left(f_0(\varepsilon_{n_2}(\mathbf{q}_2)) - f_0(\varepsilon_{n_1}(\mathbf{q}_1))\right)}{\hbar\omega_{id}(\hbar\omega_{n_2\,\mathbf{q}_2,n_1\,\mathbf{q}_1} - \hbar\omega_{id}) + i\hbar\gamma_{n_2\,\mathbf{q}_2,n_1\,\mathbf{q}_1}}, \end{aligned} \tag{4.1.16}$$

where $D_k(-\omega_{id};\mathbf{G})$ is the induced charge density tensor at the idler mode, which arises from $\boldsymbol{j}^{\mathbf{A}}_{\text{op}}$, and $B_{ijk}(\omega_{id},\mathbf{k}_{id};\mathbf{G})$ is denoted as nonlinear dependence on the idler mode which arises from $\boldsymbol{j}^{\boldsymbol{p}}_{\text{op}}$.

Note that the first term vanishes for $i \neq j$, and that B_{ijk} is antisymmetric with respect to $(i \leftrightarrow j)$, and thus vanishes for $i = j$. This means that the first term, which is associated with the induced charge, contributes to the nonlinearity when the polarization of the pump is parallel to the polarization of the signal, while the second term contributes to the nonlinearity when the pump and signal polarizations are orthogonal to one another.

4.2 The conductivity for the signal mode in the Wannier basis

One of the goals of my research was to relate the nonlinear interaction to microscopic and inter unit cell information, hence I used the Wannier basis, which contains this information [34]. For this purpose, I first calculate the matrix elements contained in the conductivity, in terms of Wannier states and then approximate the Wannier functions to be very localized.

The Bloch basis $|n\,\mathbf{q}\rangle$, can be expressed by a superposition of localized Wannier functions. I relate between the two bases in the following way

$$\begin{aligned} |n\,\mathbf{q}\rangle &= \frac{1}{\sqrt{N}}\sum_{\mathbf{R}} e^{i\mathbf{q}\cdot\mathbf{R}}T(\mathbf{R})\,|W_n\rangle\,, \\ \psi_{n\,\mathbf{q}}(\boldsymbol{x}) = \langle \boldsymbol{x}|n\,\mathbf{q}\rangle &= \frac{1}{\sqrt{N}}\sum_{\mathbf{R}} e^{i\mathbf{q}\cdot\mathbf{R}}W_n(\boldsymbol{x}-\mathbf{R}), \end{aligned} \tag{4.2.1}$$

where N is the number of sites in the lattice, and $T(\mathbf{R}) = e^{\frac{-i\mathbf{p}\cdot\mathbf{R}}{\hbar}}$ is the translation operator, such that a Wannier function of band n at site $\mathbf{R}$, is given by

$$\langle \boldsymbol{x}|\,T(\mathbf{R})\,|W_n\rangle = \langle \boldsymbol{x}-\mathbf{R}|W_n\rangle = W_n(\boldsymbol{x}-\mathbf{R}). \tag{4.2.2}$$

Therefore, a matrix element of an operator $\hat{O}$ in the Bloch basis, can be expressed in the Wannier basis as follows

$$\langle n_1\,\mathbf{q}_1|\,\hat{O}\,|n_2\,\mathbf{q}_2\rangle = \frac{1}{N}\sum_{\mathbf{R}_1\,\mathbf{R}_2} e^{-i(\mathbf{q}_1\cdot\mathbf{R}_1-\mathbf{q}_2\cdot\mathbf{R}_2)}\,\langle W_{n_1}|\,T(-\mathbf{R}_1)\hat{O}T(\mathbf{R}_2)\,|W_{n_2}\rangle\,. \tag{4.2.3}$$

Using the results of appendix B, I find that the relevant matrix elements for the conductivity (Eq. (4.1.12)) are given by

$$\begin{aligned} \langle n_1\,\mathbf{q}_1|\,e^{i\mathbf{k}\cdot\boldsymbol{x}}\,|n_2\,\mathbf{q}_2\rangle &= \delta_{\mathbf{q}_1,\mathbf{q}_2+\mathbf{k}}\sum_{\mathbf{R}} e^{i(\mathbf{q}_1-\mathbf{k})\cdot\mathbf{R}}\,\langle W_{n_1}|\,e^{i\mathbf{k}\cdot\boldsymbol{x}}T(\mathbf{R})\,|W_{n_2}\rangle\,, \\ \langle n_1\,\mathbf{q}_1|\,e^{i\mathbf{k}\cdot\boldsymbol{x}}\mathbf{p}\,|n_2\,\mathbf{q}_2\rangle &= \delta_{\mathbf{q}_1,\mathbf{q}_2+\mathbf{k}}\sum_{\mathbf{R}} e^{i(\mathbf{q}_1-\mathbf{k})\cdot\mathbf{R}}\,\langle W_{n_1}|\,e^{i\mathbf{k}\cdot\boldsymbol{x}}\mathbf{p}T(\mathbf{R})\,|W_{n_2}\rangle\,, \end{aligned} \tag{4.2.4}$$

where the Kronecker delta in these expressions is

$$\delta_{\mathbf{k}_1,\mathbf{k}_2} = \frac{1}{N}\sum_{\mathbf{R}} e^{i(\mathbf{k}_1-\mathbf{k}_2)\cdot\mathbf{R}}. \tag{4.2.5}$$

This means that it is periodic by a reciprocal lattice vector, namely

$$\delta_{\mathbf{k}_1,\mathbf{k}_2} = \delta_{\mathbf{k}_1,\mathbf{k}_2+\mathbf{G}}. \tag{4.2.6}$$

A proof for the identity given by Eq. (4.2.5), can be found in appendix A.1. Using the results of Eq. (4.2.4), I find that the second order conductivity for the signal mode in the Wannier basis is

$$
\begin{aligned}
\sigma_{ijk}(\omega_s;\mathbf{G}) = \frac{-e^3}{m^2\omega_p\omega_{id}\hbar V} & \sum_{\mathbf{R}_1\,\mathbf{R}_2\,n_1\,n_2} \langle W_{n_1}| \, e^{-i\mathbf{k}_{id}\cdot\boldsymbol{x}}\mathbf{p}\cdot\hat{e}_k T(\mathbf{R}_1)\,|W_{n_2}\rangle \\
\times \Bigg\{ & \langle W_{n_2}| \, e^{i(\mathbf{k}_{id}-\mathbf{G})\cdot\boldsymbol{x}} T(\mathbf{R}_2)\,|W_{n_1}\rangle \, \delta_{i,j} \\
+ & \frac{\hbar(\mathbf{k}_{id}-\mathbf{G})}{m\hbar\omega_s}\cdot \langle W_{n_2}| \, e^{i(\mathbf{k}_{id}-\mathbf{G})\cdot\boldsymbol{x}} \left[\hat{e}_i(\mathbf{p}\cdot\hat{e}_j) - \hat{e}_j(\mathbf{p}\cdot\hat{e}_i)\right] T(\mathbf{R}_2)\,|W_{n_1}\rangle \Bigg\} \\
\times \sum_{\mathbf{q}} & \frac{\left(f_0(\varepsilon_{n_2}(\mathbf{q}+\mathbf{k}_{id})) - f_0(\varepsilon_{n_1}(\mathbf{q}))\right) e^{i\mathbf{q}\cdot(\mathbf{R}_1+\mathbf{R}_2)} e^{i\mathbf{k}_{id}\cdot\mathbf{R}_1}}{(\omega_{n_2\,\mathbf{q}+\mathbf{k}_{id},n_1\,\mathbf{q}} - \omega_{id}) + i\gamma_{n_2\,\mathbf{q}+\mathbf{k}_{id},n_1\,\mathbf{q}}}.
\end{aligned}
\tag{4.2.7}
$$

When assuming the dipole approximation with respect to the idler mode, I get

$$
\begin{aligned}
\sigma_{ijk}(\omega_s;\mathbf{G}) = \frac{-e^3}{m^2\omega_p\omega_{id}\hbar V} & \sum_{\mathbf{R}_1\,\mathbf{R}_2\,n_1\,n_2} \langle W_{n_1}| \, \mathbf{p}\cdot\hat{e}_k T(\mathbf{R}_1)\,|W_{n_2}\rangle \\
\times \Bigg\{ & \langle W_{n_2}| \, e^{-i\mathbf{G}\cdot\boldsymbol{x}} T(\mathbf{R}_2)\,|W_{n_1}\rangle \, \delta_{i,j} \\
+ & \frac{\hbar(\mathbf{k}_{id}-\mathbf{G})}{m\hbar\omega_s}\cdot \langle W_{n_2}| \, e^{-i\mathbf{G}\cdot\boldsymbol{x}} \left[\hat{e}_i(\mathbf{p}\cdot\hat{e}_j) - \hat{e}_j(\mathbf{p}\cdot\hat{e}_i)\right] T(\mathbf{R}_2)\,|W_{n_1}\rangle \Bigg\} \\
\times \sum_{\mathbf{q}} & \frac{\left(f_0(\varepsilon_{n_2}(\mathbf{q}+\mathbf{k}_{id})) - f_0(\varepsilon_{n_1}(\mathbf{q}))\right) e^{i\mathbf{q}\cdot(\mathbf{R}_1+\mathbf{R}_2)}}{(\omega_{n_2\,\mathbf{q}+\mathbf{k}_{id},n_1\,\mathbf{q}} - \omega_{id}) + i\gamma_{n_2\,\mathbf{q}+\mathbf{k}_{id},n_1\,\mathbf{q}}}.
\end{aligned}
\tag{4.2.8}
$$

By representing the conductivity in terms of Wannier functions, the sum over the Bloch wave vector is separated from the matrix elements, but the sum over the lattice vectors $\{\mathbf{R}_1, \mathbf{R}_2\}$ includes both the matrix elements and the spectral terms, which depend on the Bloch wave vector.

Though it implies from this expression, that if I could get rid of the sum over the lattice vectors, I could separate between the matrix elements and the spectral dependence of the interaction.

4.2.1 Approximating the Wannier states to be very localized

In the case of insulators and semiconductors, the Wannier functions are fairly localized, such that the overlap between neighboring functions at different sites is very weak. To further simplify the expression for the conductivity, I assume that the Wannier functions are very localized such that, there is no overlap between neighboring sites. This means that a matrix element of an operator $\hat{O}$, between two Wannier functions, separated by a lattice vector $\mathbf{R}$ is

$$\langle W_{n_1}|\,\hat{O}T(\mathbf{R})\,|W_{n_2}\rangle = \delta_{\mathbf{R},0}\,\langle W_{n_1}|\,\hat{O}\,|W_{n_2}\rangle \tag{4.2.9}$$

By making this assumption, I can separate the contribution of the intermolecular interactions and the band structure. As hinted in the previous section, by assuming that the Wannier functions are very localized, the summation over the matrix elements is reduced to a sum over only the band numbers. The rest of the terms depend on all quantum numbers hence have the meaning of the spectral dependence of the interaction.

I express the conductivity according to the definition given by Eq. (4.1.14), under the aforementioned approximation, and find that

$$D_k(-\omega_{id};\mathbf{G}) = \left(\frac{i\hbar e^2}{mV}\right)\sum_{n_1\,n_2}\langle W_{n_2}|\,e^{-i\mathbf{G}\cdot\boldsymbol{x}}\,|W_{n_1}\rangle\,\langle W_{n_1}|\,\mathbf{p}\cdot\hat{e}_k\,|W_{n_2}\rangle\,I_{n_2,n_1}(\varepsilon_{id},\mathbf{k}_{id}), \tag{4.2.10}$$

$$\begin{aligned} B_{ijk}(\omega_{id},\mathbf{k}_{id};\mathbf{G}) = \sum_{n_1\,n_2}&\hbar(\mathbf{k}_{id}-\mathbf{G})\cdot\langle W_{n_2}|\,e^{-i\mathbf{G}\cdot\boldsymbol{x}}\,[\hat{e}_i(\mathbf{p}\cdot\hat{e}_j)-\hat{e}_j(\mathbf{p}\cdot\hat{e}_i)]\,|W_{n_1}\rangle\\ &\times\langle W_{n_1}|\,\mathbf{p}\cdot\hat{e}_k\,|W_{n_2}\rangle\,I_{n_2,n_1}(\varepsilon_{id},\mathbf{k}_{id}),\end{aligned} \tag{4.2.11}$$

$$I_{n_1,n_2}(\varepsilon_{id},\mathbf{k}_{id}) = \frac{V}{(2\pi)^3}\int\limits_{B.Z.} d\mathbf{q}\,\frac{-\left(f_0(\varepsilon_{n_1}(\mathbf{q}+\mathbf{k}_{id}))-f_0(\varepsilon_{n_2}(\mathbf{q}))\right)}{\varepsilon_{id}\left[\left(\varepsilon_{n_1}(\mathbf{q}+\mathbf{k}_{id})-\varepsilon_{n_2}(\mathbf{q})\right)-\varepsilon_{id}\right)+i\hbar\gamma_{n_1\,\mathbf{q}+\mathbf{k}_{id},n_2\,\mathbf{q}}]}, \tag{4.2.12}$$

where I denote the spectral dependence of the interaction to be $I_{n_1,n_2}(\varepsilon_{id},\mathbf{k}_{id})$, and the idler energy is given by $\varepsilon_{id} = \hbar\omega_{id}$. The spectral dependence function

$I_{n_1,n_2}(\varepsilon_{id}, \mathbf{k}_{id})$, is expressed by an integral over the first Brillouin zone and was attained by converting the sum over the Bloch wave vector into an integral, namely

$$\sum_{\mathbf{q}} \Rightarrow \frac{V}{(2\pi)^3} \int\limits_{B.Z.} d\mathbf{q}. \tag{4.2.13}$$

At the end of section 4.1, I mentioned the polarization dependence of each term. The different polarization dependence of the two terms can be used to probe the contributions of the induced charge density, band transitions dependence, and inter-molecular interactions matrix elements. The functions $B_{ijk}(\omega_{id}, \mathbf{k}_{id}; \mathbf{G})$ and $D_k(-\omega_{id}; \mathbf{G})$ contain the information on the interaction dependence on the idler mode (the long wavelength), the band structure, and inter-molecular interactions matrix elements.

The information about the inter-molecular interactions is encoded in the matrix elements and the interaction dependence on the band structure is given by the function $I_{n_1,n_2}(\varepsilon_{id}, \mathbf{k}_{id})$. It is a measure of the number of band transitions ($n_1 \leftrightarrow n_2$) with separation of $\mathbf{k}_{id}$ and population difference of $f_0(\varepsilon_{n_1}(\mathbf{q} + \mathbf{k}_{id})) - f_0(\varepsilon_{n_2}(\mathbf{q}))$ that are closely related to the idler energy ε_{id}. Moreover, it is important to note that for maximally localized Wannier functions (as assumed here) there will only be contributions from interband transitions, when the dipole approximation is assumed with respect to the idler mode. This is because under the assumption that the Wannier functions are maximally localized, they can be taken to be real [35], and thus

$$\langle W_{n_1}| \mathbf{p} \cdot \hat{e}_k |W_{n_2}\rangle = - \langle W_{n_2}| \mathbf{p} \cdot \hat{e}_k |W_{n_1}\rangle \Rightarrow \langle W_n| \mathbf{p} \cdot \hat{e}_k |W_n\rangle = 0. \tag{4.2.14}$$

5 Model case of a semiconductor with two bands

In this section I focus on the nonlinear interaction in semiconductors. I begin with the spectral dependence of the nonlinear conductivity for the case of a semiconductor with two bands, proceed with an example case and conclude with an estimation on the contribution to the nonlinearity which arises from the matrix elements.

5.1 Spectral dependence

In the previous section, I showed that when the Wannier functions are localized, the spectral dependence can be described by the function $I_{n_1,n_2}(\varepsilon_{id}, \mathbf{k}_{id})$ (Eq. (4.2.12)). Therefore, to analyze the spectral dependence of the nonlinear conductivity in the case of a semiconductor, it is sufficient to explore the spectral dependence of $I_{n_1,n_2}(\varepsilon_{id}, \mathbf{k}_{id})$. To get more insight I consider a simple example of a semiconductor at zero temperature with two energy bands, where the valence band is fully occupied and the conduction band is completely vacant and in addition, I assume that the damping coefficients are equal to a constant γ.

I denote the band number for the valence band to be $n = 1$, and for the conductance $n = 2$. Under these assumptions, the Fermi-Dirac distribution is proportional to a delta function and can be written as

$$f_0(\varepsilon_n(\mathbf{q})) = \frac{\delta_{n,1}}{N}, \tag{5.1.1}$$

where the factor $\frac{1}{N}$, comes from normalization condition for the density matrix $\mathrm{tr}(\rho(t)) = 1$. The spectral function $I_{n_1,n_2}(\varepsilon_{id}, \mathbf{k}_{id})$ can thus be simplified by expressing it using two functions I denote as $I_+(\varepsilon_{id}, \mathbf{k}_{id})$ and $I_-(\varepsilon_{id}, \mathbf{k}_{id})$, which satisfy the equation

$$\begin{gathered} I_{n_1,n_2}(\varepsilon_{id}, \mathbf{k}_{id}) = \\ \delta_{n_1,2}\delta_{n_2,1} I_+(\varepsilon_{id}, \mathbf{k}_{id}) + \delta_{n_1,1}\delta_{n_2,2} I_-(\varepsilon_{id}, \mathbf{k}_{id}), \end{gathered} \tag{5.1.2}$$

and their expression is given by

$$
\begin{aligned}
I_{\pm}(\varepsilon_{id}, \mathbf{k}_{id}) &= \frac{v}{(2\pi)^3} \int\limits_{B.Z.} d\mathbf{q}\, \frac{1}{\varepsilon\left[(\Delta\varepsilon_{2,1}(\mathbf{q}, \pm\mathbf{k}_{id}) \mp \varepsilon) \pm i\hbar\gamma\right]} \\
&= v \int d\varepsilon\, \frac{g_{2,1}(\varepsilon, \pm\mathbf{k}_{id})}{\varepsilon_{id}\left[(\varepsilon \mp \varepsilon_{id}) \pm i\hbar\gamma\right]},
\end{aligned}
\tag{5.1.3}
$$

where the integration is performed over states between the two bands separated by a wave vector difference equals to $\mathbf{k}_{id}$ as illustrated in Fig. 3,

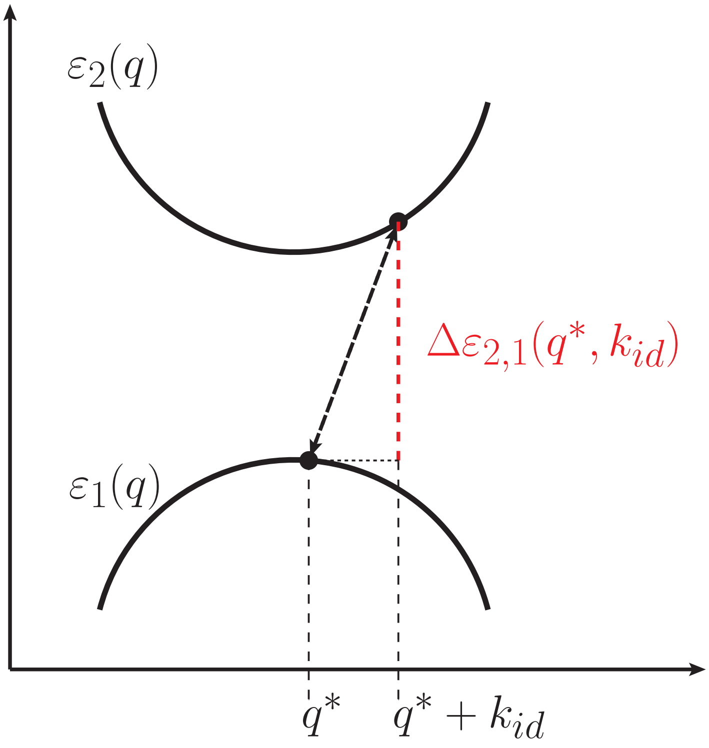

Figure 3: Schematic view of the energy difference between bands $(2 \leftrightarrow 1)$ at wave vector q^*, separated by k_{id}.

v is the volume of the primitive cell, $\Delta\varepsilon_{n_1,n_2}(\mathbf{q},\mathbf{k}) = \varepsilon_{n_1}(\mathbf{q}+\mathbf{k}) - \varepsilon_{n_2}(\mathbf{q})$ is the energy difference between bands $(n_1 \leftrightarrow n_2)$ at wave vector $\mathbf{q}$ that are separated by $\mathbf{k}$, and the weight function $g_{2,1}(\varepsilon, \pm\mathbf{k}_{id})$ in the integral is the joint density of states, which is defined as $g_{n_1,n_2}(\varepsilon,\mathbf{k}) = \frac{1}{(2\pi)^3} \int\limits_{S(\varepsilon)} \frac{dS}{\left|\boldsymbol{\nabla}_{\mathbf{q}}(\Delta\varepsilon_{n_1,n_2}(\mathbf{q},\mathbf{k}))\right|}$. Note that for $\mathbf{k} = 0$ the expression for $g_{n_1,n_2}(\varepsilon,\mathbf{k})$ reduces to the standard definition of the joint-density of states [36] and can be considered as such for a wave vector much smaller than a typical size of the first Brillouin zone ($|\mathbf{k}| \ll \frac{2\pi}{a}$). From Eq. (5.1.3) and from Fig. 3, it is clear that ε_{id} acts as a resonance in the integral form of the function $I_+(\varepsilon_{id},\mathbf{k}_{id})$ and therefore, is more sensitive to the joint-density of states than $I_-(\varepsilon_{id},\mathbf{k}_{id})$. This sensitivity is related to the contribution that arises from the number of energy transitions at the idler energy.

5.2 Example case

To further illustrate the spectral dependence given by $I_\pm(\varepsilon_{id},\mathbf{k}_{id})$, I consider the following simple energy dispersion

$$\begin{aligned}
&\varepsilon_1(\mathbf{k}) = V_{ss}|g_1(\mathbf{k})|,\\
&\varepsilon_2(\mathbf{k}) = \varepsilon_{\text{gap}} + V_{ss}(2-|g_1(\mathbf{k})|), \qquad (5.2.1)\\
&g_1(\mathbf{k}) = \cos\Big(\frac{\pi}{2}k_1\Big)\sin\Big(\frac{\pi}{2}k_2\Big)\sin\Big(\frac{\pi}{2}k_3\Big) + i\sin\Big(\frac{\pi}{2}k_1\Big)\cos\Big(\frac{\pi}{2}k_2\Big)\cos\Big(\frac{\pi}{2}k_1\Big).
\end{aligned}$$

where ε_{gap} is the gap energy, V_{ss} is the width of each band, and $g_1(\mathbf{k})$ is the band structure form function I used for this example [37], where in this form of the function $g_1(\mathbf{k})$, the vector is $\mathbf{k} = (k_x,k_y,k_z) = (\frac{2\pi}{a})(k_1,k_2,k_3)$. The dependence of the functions $I_\pm(\varepsilon_{id},\mathbf{k}_{id}\sim 0) \equiv I_\pm(\varepsilon_{id})$ on small idler energies is evaluated numerically under the assumption that the width of the levels are very narrow and therefore the damping coefficient γ is neglected. Furthermore, in order to see how $I_\pm(\varepsilon_{id})$ scale with the band gap energy and to investigate the dependence of the choice of bandwidth V_{ss}, I define dimensionless energy parameters

$$\begin{aligned}
&\tilde{\varepsilon}_{id} = \frac{\varepsilon_{id}}{\varepsilon_{\text{gap}}},\ \beta = \frac{2V_{ss}}{\varepsilon_{\text{gap}}},\\
&\widetilde{\Delta\varepsilon}(\mathbf{k}) = \frac{\varepsilon_2(\mathbf{k})-\varepsilon_1(\mathbf{k})}{\varepsilon_{\text{gap}}} = 1+\beta\left(1-|g_1(\mathbf{k})|\right),
\end{aligned} \qquad (5.2.2)$$

where $\tilde{\varepsilon}_{id}$, β and $\widetilde{\Delta\varepsilon}(\mathbf{k})$ are the idler energy, bandwidth energy, and interband transition energy relative to the band gap energy ε_{gap} respectively. With these definitions,

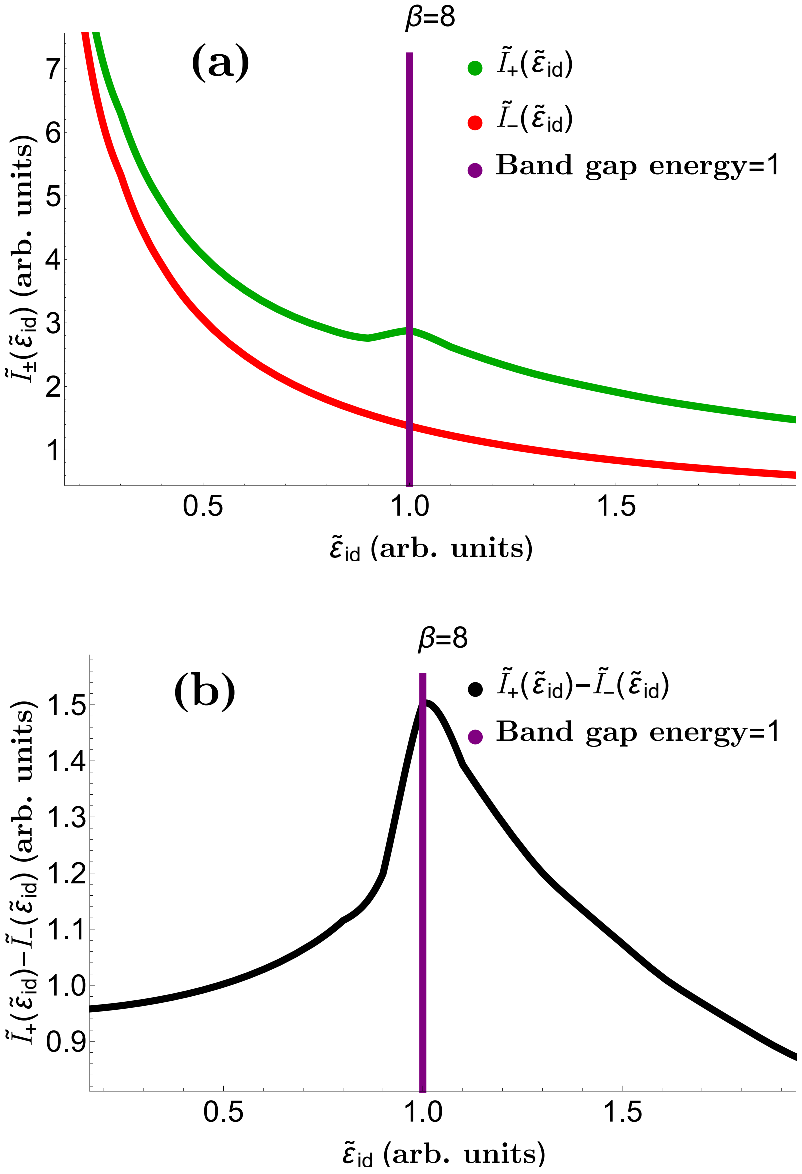

Figure 4: Band structure dependence of the nonlinear current density: (a) The term $\tilde{I}_+(\tilde{\varepsilon}_{id})$ (green) shows a clear peak at the band gap energy while the term $\tilde{I}_-(\tilde{\varepsilon}_{id})$ (red) decreases monotonically with the relative idler energy $\tilde{\varepsilon}_{id}$. (b) The difference between the $\tilde{I}_+(\tilde{\varepsilon}_{id})$ and the $\tilde{I}_-(\tilde{\varepsilon}_{id})$ term. The vertical purple line indicate band gap energy.

the functions $I_\pm(\varepsilon_{id})$ can be expressed by dimensionless functions times a scale factor

$$\begin{aligned} I_\pm(\varepsilon_{id}) &= \frac{\tilde{I}_\pm(\tilde{\varepsilon}_{id})}{\varepsilon_{\text{gap}}^2}, \\ \tilde{I}_\pm(\tilde{\varepsilon}_{id}) &= \frac{v}{(2\pi)^3} \int_{B.Z.} d\mathbf{k} \, \frac{1}{\tilde{\varepsilon}_{id} \left(\widetilde{\Delta\varepsilon}(\mathbf{k}) \mp \tilde{\varepsilon}_{id} \right)} \end{aligned} \tag{5.2.3}$$

where $\tilde{I}_\pm(\tilde{\varepsilon}_{id})$ are dimensionless, and will be used for this analysis. It is interesting to note that the difference function $I_+(\varepsilon_{id}) - I_-(\varepsilon_{id})$ can be related to the induced charge density when the dipole approximation is assumed with respect to the idler mode. In this case I find that

$$D_k(-\omega_{id}; \mathbf{G}) = f_{2,1}^{(k)}(\mathbf{G}) \left(I_+(\varepsilon_{id}) - I_-(\varepsilon_{id}) \right), \tag{5.2.4}$$

$$f_{2,1}^{(k)}(\mathbf{G}) = \left(\frac{i\hbar e^2}{mV} \right) \langle W_2 | \, e^{-i\mathbf{G}\cdot\boldsymbol{x}} \, | W_1 \rangle \, \langle W_1 | \, \mathbf{p} \cdot \hat{e}_k \, | W_2 \rangle \,, \tag{5.2.5}$$

where $f_{2,1}^{(k)}(\mathbf{G})$ encapsulates the inter-molecular interactions with respect to bands 2, 1 and the reciprocal lattice vector $\mathbf{G}$. $I_+(\varepsilon_{id}) - I_-(\varepsilon_{id})$ reflects the spectral dependence of the induced charge density on the joint density of states. I show the dependence of $\tilde{I}_\pm(\tilde{\varepsilon}_{id})$ and of their difference in Fig. 4. The prominent peak in $\tilde{I}_+(\tilde{\varepsilon}_{id})$ near the band gap energy is due to its strong dependence on the large number of inter-band transitions at the band gap, while $\tilde{I}_-(\tilde{\varepsilon}_{id})$ decreases monotonically. The difference $\tilde{I}_+(\tilde{\varepsilon}_{id}) - \tilde{I}_-(\tilde{\varepsilon}_{id})$ also exhibits a very distinctive peak near the band gap energy. It is possible to measure this peak if the spectral resolution of the detector is higher than the FWHM of the peak profile. This enhancement near the band gap energy demonstrates the sensitivity of the nonlinear response and of the induced charge to the joint density of states, and is also in agreement with a recent experiment, showing an enhancement just at the band gap energy [2].

To investigate how the bandwidth effects the model, I evaluated $\tilde{I}_\pm(\tilde{\varepsilon}_{id})$ for various values of $\beta = 2V_{ss}/\varepsilon_{\text{gap}}$. The functions $\tilde{I}_\pm(\tilde{\varepsilon}_{id})$ display the same behavior for all β differing only by a factor. This difference is displayed in Fig. 5 where the peaks of the functions decrease with growing values of β. This decrease is due to

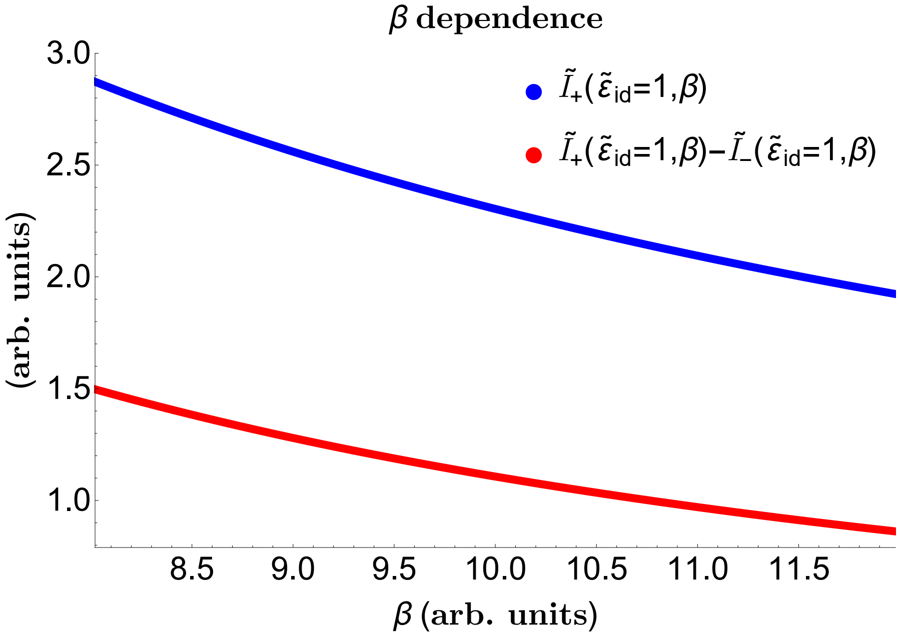

Figure 5: β dependence of the nonlinear current density: The functions $\tilde{I}_{+}(\tilde{\varepsilon}_{id})$ (blue) and the difference $(\tilde{I}_{+}(\tilde{\varepsilon}_{id}) - \tilde{I}_{-}(\tilde{\varepsilon}_{id}))$ (red) at the band gap energy $(\tilde{\varepsilon}_{id} = 1)$. Both decreases with the parameter β.

the broadening of the joint density of states, as β grows, which leads to a reduction in the density of transitions about the energy gap. The spectral dependence of the optical response on β, can be used to probe changes in the band structure due to an external field, and also the corresponding changes in $f_{2,1}^{(k)}(\mathbf{G})$.

5.2.1 Matrix elements in two-dimensional subspace

After describing the spectral dependence of the nonlinear conductivity, I estimate the contribution of the inter-molecular interactions in the case of two bands by working in a two-dimensional subspace spanned by the Wannier states of each band. Since the operator $e^{i\mathbf{G}\cdot\boldsymbol{x}}$ shares the same eigenstates as the position operator, I first find its matrix representation in the eigenbasis of the position operator and then rotate this matrix to the original basis (see appendix C for more detail.). Next, I express the matrix elements contained in $D_k(-\omega_{id};\mathbf{G})$ and $B_{ijk}(\omega_{id},\mathbf{k}_{id};\mathbf{G})$ in terms of the position and momentum matrix elements and obtain

$$D_k(-\omega_{id};\mathbf{G}) = -\left(\frac{i\hbar e^2}{mV}\right)\pi_k e^{-i\mathbf{G}\cdot\boldsymbol{a}}\sin(\mathbf{G}\cdot\boldsymbol{c})\left(I_+(\varepsilon_{id},\mathbf{k}_{id}) - I_-(\varepsilon_{id},\mathbf{k}_{id})\right), \tag{5.2.6}$$

$$\begin{aligned} B_{ijk}(\omega_{id},\mathbf{k}_{id};\mathbf{G}) =& \pi_k e^{-i\mathbf{G}\cdot\boldsymbol{a}}\cos(\mathbf{G}\cdot\boldsymbol{c})\left[\hbar(\mathbf{k}_{id}-\mathbf{G})\cdot(\hat{e}_i\pi_j - \hat{e}_j\pi_i)\right] \\ &\times\left(I_+(\varepsilon_{id},\mathbf{k}_{id}) + I_-(\varepsilon_{id},\mathbf{k}_{id})\right), \end{aligned} \tag{5.2.7}$$

where

$$i\pi_k = \langle W_2|\,\mathbf{p}\cdot\hat{e}_k\,|W_1\rangle = -\langle W_1|\,\mathbf{p}\cdot\hat{e}_k\,|W_2\rangle\,, \tag{5.2.8}$$

$$\boldsymbol{a} = \langle W_1|\,\boldsymbol{x}\,|W_1\rangle = \langle W_2|\,\boldsymbol{x}\,|W_2\rangle\,, \tag{5.2.9}$$

$$\boldsymbol{c} = \langle W_1|\,\boldsymbol{x}\,|W_2\rangle = \langle W_2|\,\boldsymbol{x}\,|W_1\rangle\,, \tag{5.2.10}$$

and the vectors $(\boldsymbol{\pi},\boldsymbol{a},\boldsymbol{c})$ are real. This form of the matrix elements is attained when assuming that the Wannier functions are real, and that $[x_i,x_j]=0$.

Generally speaking, even in the case of a simple semiconductor the estimation of the matrix elements requires numerical calculations. However, since the Wannier functions are commonly constructed using the linear combination of atomic orbital (LCAO) approach, in which Wannier functions are a constructed by a superposition of many atomistic wave functions [38], I can get a rough estimation of the magnitude of the nonlinear conductivity by approximating the Wannier functions to be hydrogen wave functions of levels 1s and 2p. For idler and pump photon energies at 1 eV and 10 keV respectively, I find that the first term of the conductivity is on the order of ($\approx 10^{-7}\ \frac{\mathrm{A}^3}{\mathrm{W}^2}$). The second term of the conductivity is on the order of ($\approx 10^{-11}\ \frac{\mathrm{A}^3}{\mathrm{W}^2}$).

6 Summary and outlook

My work shows that the contribution to the nonlinear interaction arises from both band structure properties and atomic-scale interactions. The results imply that it is possible to extract atomic-scale information on the valence electrons as predicted by previous publications [4, 6, 7, 9, 13, 15] but only if the band information can be separated from the Wannier function contribution. For example, when the Wannier functions are localized. Consequently, the spectral dependence of the nonlinearity is essential for the construction of the microscopic information of the electronic states. Moreover, the population difference between bands or within a band also plays a role in the spectral dependence. When considering more than two bands, there could be an effect of interference between several spectral contributions including interband and intraband transitions, provided that there is a population difference between these transitions.

In contrast to previous publications [7, 10], this theory predicts that the polarization of the signal is not only in the direction of the polarization of the pump. The two polarization components exhibits different spectral dependencies which can be investigated by measuring each component.

It is important to emphasize that since the nonlinear interaction I discuss is a parametric process in nature (the system does not change its state during the nonlinear interaction) it is inherently ultra-fast. It is therefore very likely that it would be possible to use the nonlinear x-ray and long wavelength interaction for the study of ultra-fast dynamics in solids. The theory implies that pump-prob measurements can be used to study the femtosecond and sub-femotosecond dynamics of interesting processes. Examples include the variation of the populations between bands, ultrafast charge transfer between electronic states, optically induced chemical potential variations, ultra-fast (optically induced) dynamics of band structures, and ultra-fast phase transitions.

This formalism can be combined with standard Ab initio methods for further studies of the nonlinear x ray and optical/UV mixing effects in many solid state systems.

Furthermore, effects which rely on nonlinear interactions can be used to reveal a very broad band spectroscopic information ranging from sub eV to several hundred of eV and structural information of the valence electrons by using a single apparatus. By using SPDC of x-rays to long wavelengths, the energy scan can be done by tuning the angle of the sample and the energy is selected by the detection system.

References

[1] R. Cohen and S. Shwartz, “Theory of nonlinear interactions between x rays and optical radiation in crystals,” *Physical Review Research*, vol. 1, no. 3, p. 033133, 2019.

[2] A. Schori, C. Bömer, D. Borodin, S. Collins, B. Detlefs, M. M. Sala, S. Yudovich, and S. Shwartz, “Parametric down-conversion of x rays into the optical regime,” *Physical review letters*, vol. 119, no. 25, p. 253902, 2017.

[3] S. Sofer, O. Sefi, E. Strizhevsky, H. Aknin, S. Collins, G. Nisbet, B. Detlefs, C. J. Sahle, and S. Shwartz, “Observation of strong nonlinear interactions in parametric down-conversion of x-rays into ultraviolet radiation,” *Nature Communications*, vol. 10, no. 1, pp. 1–8, 2019.

[4] H. Danino and I. Freund, “Parametric down conversion of x rays into the extreme ultraviolet,” *Physical Review Letters*, vol. 46, no. 17, p. 1127, 1981.

[5] K. Tamasaku, K. Sawada, and T. Ishikawa, “Determining x-ray nonlinear susceptibility of diamond by the optical fano effect,” *Physical review letters*, vol. 103, no. 25, p. 254801, 2009.

[6] K. Tamasaku, K. Sawada, E. Nishibori, and T. Ishikawa, “Visualizing the local optical response to extreme-ultraviolet radiation with a resolution of $\lambda/380$,” *Nature Physics*, vol. 7, no. 9, pp. 705–708, 2011.

[7] T. Glover, D. Fritz, M. Cammarata, T. Allison, S. Coh, J. Feldkamp, H. Lemke, D. Zhu, Y. Feng, R. Coffee, *et al.*, “X-ray and optical wave mixing,” *Nature*, vol. 488, no. 7413, pp. 603–608, 2012.

[8] B. Barbiellini, Y. Joly, and K. Tamasaku, “Explaining the x-ray nonlinear susceptibility of diamond and silicon near absorption edges,” *Physical Review B*, vol. 92, no. 15, p. 155119, 2015.

[9] J. R. Rouxel, M. Kowalewski, K. Bennett, and S. Mukamel, “X-ray sum frequency diffraction for direct imaging of ultrafast electron dynamics,” *Physical Review Letters*, vol. 120, no. 24, p. 243902, 2018.

[10] D. Borodin, A. Schori, J.-P. Rueff, J. Ablett, and S. Shwartz, “Evidence for collective nonlinear interactions in x ray into ultraviolet parametric down-conversion,” *Physical review letters*, vol. 122, no. 2, p. 023902, 2019.

[11] K. Tamasaku and T. Ishikawa, “Idler energy dependence of nonlinear diffraction in X $\rightarrow$ X + EUV parametric down-conversion,” *Acta Crystallographica Section A: Foundations of Crystallography*, vol. 63, no. 5, pp. 437–438, 2007.

[12] D. Borodin, S. Levy, and S. Shwartz, “High energy-resolution measurements of x-ray into ultraviolet parametric down-conversion with an x-ray tube source,” *Applied Physics Letters*, vol. 110, no. 13, p. 131101, 2017.

[13] I. Freund and B. Levine, “Optically modulated x-ray diffraction,” *Physical Review Letters*, vol. 25, no. 18, p. 1241, 1970.

[14] I. Freund and B. Levine, “Resonant dispersion of the nonlinear atomic scattering factor,” *Optics Communications*, vol. 3, no. 2, pp. 101–104, 1971.

[15] I. Freund, “Nonlinear x-ray diffraction. determination of valence electron charge distributions,” *Chemical Physics Letters*, vol. 12, no. 4, pp. 583–588, 1972.

[16] K. E. Dorfman and S. Mukamel, “Photon coincidence counting in parametric down-conversion: Interference of field-matter quantum pathways,” *Physical Review A*, vol. 86, no. 2, p. 023805, 2012.

[17] I. Freund, “Nonlinear diffraction,” *Physical Review Letters*, vol. 21, no. 19, p. 1404, 1968.

[18] S. Jha and C. Warke, “Nonlinear electromagnetic response of bloch electrons in a magnetic field,” *Il Nuovo Cimento B (1965-1970)*, vol. 53, no. 1, pp. 120–135, 1968.

[19] I. Freund and B. Levine, "Parametric conversion of x rays," *Physical Review Letters*, vol. 23, no. 15, p. 854, 1969.

[20] S. S. Jha and J. W. Woo, "Nonlinear response of bound electrons to x rays," *Physical Review B*, vol. 5, no. 10, p. 4210, 1972.

[21] S. Jha and J. Woo, "Nonlinear response of electrons in a solid to x-rays," *Il Nuovo Cimento B (1971-1996)*, vol. 10, no. 1, pp. 229–239, 1972.

[22] R. W. Boyd, *Nonlinear optics.* Academic press, 2003.

[23] G. Wysin, "Probability current and current operators in quantum mechanics," *Department of Physics, Kansas State University, Manhattan, KS*, vol. 66506, p. 2601, 2011.

[24] W. Louisell, A. Yariv, and A. Siegman, "Quantum fluctuations and noise in parametric processes. i.," *Physical Review*, vol. 124, no. 6, p. 1646, 1961.

[25] S. Harris, M. Oshman, and R. Byer, "Observation of tunable optical parametric fluorescence," *Physical Review Letters*, vol. 18, no. 18, p. 732, 1967.

[26] D. Magde and H. Mahr, "Study in ammonium dihydrogen phosphate of spontaneous parametric interaction tunable from 4400 to 16 000 Å," *Physical Review Letters*, vol. 18, no. 21, p. 905, 1967.

[27] S. Akhmanov, V. Fadeev, R. Khokhlov, and O. Chunaev, "Quantum noise in parametric light amplifiers," *ZhETF Pisma Redaktsiiu*, vol. 6, p. 575, 1967.

[28] D. Klyshko, "Coherent photon decay in a nonlinear medium," *Soviet Journal of Experimental and Theoretical Physics Letters*, vol. 6, p. 23, 1967.

[29] R. Byer and S. Harris, "Power and bandwidth of spontaneous parametric emission," *Physical Review*, vol. 168, no. 3, p. 1064, 1968.

[30] R. Smith, J. Skinner, J. Geusic, and W. Nilsen, "Observations of noncollinear phase matching in optical parametric noise emission," *Applied Physics Letters*, vol. 12, no. 3, pp. 97–100, 1968.

[31] D. Kleinman, "Theory of optical parametric noise," *Physical Review*, vol. 174, no. 3, p. 1027, 1968.

[32] P. Eisenberger and S. McCall, "X-ray parametric conversion," *Physical Review Letters*, vol. 26, no. 12, p. 684, 1971.

[33] K. Tamasaku and T. Ishikawa, "Interference between compton scattering and x-ray parametric down-conversion," *Physical review letters*, vol. 98, no. 24, p. 244801, 2007.

[34] N. Marzari, A. A. Mostofi, J. R. Yates, I. Souza, and D. Vanderbilt, "Maximally localized wannier functions: Theory and applications," *Reviews of Modern Physics*, vol. 84, no. 4, p. 1419, 2012.

[35] S. Ri and S. Ri, "Proof that the maximally localized wannier functions are real," *arXiv preprint arXiv:1407.6824*, 2014.

[36] N. W. Ashcroft and N. D. Mermin, *Solid state physics.* Cengage Learning, 1976.

[37] D. Chadi and M. L. Cohen, "Tight-binding calculations of the valence bands of diamond and zincblende crystals," *physica status solidi (b)*, vol. 68, no. 1, pp. 405–419, 1975.

[38] C. M. Zicovich-Wilson, R. Dovesi, and V. R. Saunders, "A general method to obtain well localized wannier functions for composite energy bands in linear combination of atomic orbital periodic calculations," *The Journal of Chemical Physics*, vol. 115, no. 21, pp. 9708–9719, 2001.

A Auxiliary identities

In this section I sum up a few identities used in various parts of the calculation.

A.1 Periodic Kronecker delta function

In this section, I will prove the following relation

$$\sum_{\mathbf{R}} e^{i\mathbf{k}\cdot\mathbf{R}} = N\delta_{\mathbf{k},0}. \tag{A.1.1}$$

Since the volume of the crystal is arbitrarily large, one can assume that $\mathbf{k}$ follow the Born-von Karman condition, namely that

$$\mathbf{k} = \sum_{i=1}^{3} \frac{m_i}{N_i}\mathbf{b}_i, \tag{A.1.2}$$

where $\{\mathbf{b}_i\}$ is the set of primitive vectors in the reciprocal lattice, N_i is the number of sites in the i-th direction of the lattice, and m_i is an integer, such that $m_i \leq N_i$. Furthermore, $\mathbf{R} = \mathbf{R}_{n_1,n_2,n_3} = \sum\limits_{j=1}^{3} n_j\mathbf{a}_j$ and $\sum\limits_{\mathbf{R}} = \prod\limits_{j=1}^{3}\sum\limits_{n_j=0}^{N_j-1}$ so the sum is simply

$$\sum_{\mathbf{R}} e^{i\mathbf{k}\cdot\mathbf{R}} = \prod_{j=1}^{3}\left[\sum_{n_j=0}^{N_j-1} \exp\left\{i\left(\frac{2\pi m_j n_j}{N_j}\right)\right\}\right] = \prod_{j=1}^{3}\left[\sum_{n_j=0}^{N_j-1}\left(e^{i\frac{2\pi m_j}{N_j}}\right)^{n_j}\right]. \tag{A.1.3}$$

To evaluate the sum in the product I will use

$$\sum_{n=0}^{N-1} d^n = \frac{d^N - 1}{d-1}, \tag{A.1.4}$$

and get

$$\sum_{\mathbf{R}} e^{i\mathbf{k}\cdot\mathbf{R}} = \prod_{j=1}^{3}\underbrace{\left[\frac{e^{i2\pi m_j} - 1}{e^{i\frac{2\pi m_j}{N_j}} - 1}\right]}_{N_j\delta_{m_j,0}} = N\delta_{\mathbf{k},0}. \tag{A.1.5}$$

Note: the delta is for $\mathbf{k}$ within the first Brillouin zone, since for $\mathbf{q} = \mathbf{k} + \mathbf{G}$, I get

$$\sum_{\mathbf{R}} e^{i(\mathbf{k}+\mathbf{G})\cdot\mathbf{R}} = \sum_{\mathbf{R}} e^{i\mathbf{k}\cdot\mathbf{R}} = N\delta_{\mathbf{k},0}. \tag{A.1.6}$$

A.2

I define

$$\mathbf{I}(2,1,\mathbf{k}) = \int\limits_V d\boldsymbol{x}\ \left[\psi^*_{n_2\,\mathbf{q}_2}(\boldsymbol{x})\left(\boldsymbol{\nabla}\psi_{n_1\,\mathbf{q}_1}(\boldsymbol{x})\right) - \psi_{n_1\,\mathbf{q}_1}(\boldsymbol{x})\left(\boldsymbol{\nabla}\psi^*_{n_2\,\mathbf{q}_2}(\boldsymbol{x})\right)\right] e^{i\mathbf{k}\cdot\boldsymbol{x}}, \tag{A.2.1}$$

$$\mathbf{I}(2,1,\mathbf{k}) = \int\limits_V d\boldsymbol{x}\,\psi^*_{n_2\,\mathbf{q}_2}(\boldsymbol{x})e^{i\mathbf{k}\cdot\boldsymbol{x}}\left(\boldsymbol{\nabla}\psi_{n_1\,\mathbf{q}_1}(\boldsymbol{x})\right) - \underbrace{\int\limits_V d\boldsymbol{x}\,\psi_{n_1\,\mathbf{q}_1}(\boldsymbol{x})e^{i\mathbf{k}\cdot\boldsymbol{x}}\left(\boldsymbol{\nabla}\psi^*_{n_2\,\mathbf{q}_2}(\boldsymbol{x})\right)}_{\mathbf{I}_{a,\mathbf{k}}}. \tag{A.2.2}$$

Using the relation $\mathbf{p} = -i\hbar\boldsymbol{\nabla}$ the first term can be expressed by a matrix element such that

$$\mathbf{I}(2,1,\mathbf{k}) = \frac{i}{\hbar}\left\langle n_2\,\mathbf{q}_2\right| e^{i\mathbf{k}\cdot\boldsymbol{x}}\mathbf{p}\left|n_1\,\mathbf{q}_1\right\rangle - \mathbf{I}_{a,\mathbf{k}}. \tag{A.2.3}$$

The second term can also be expressed by matrix elements

$$\mathbf{I}_{a,\mathbf{k}} = \int\limits_V d\boldsymbol{x}\,\psi_{n_1\,\mathbf{q}_1}(\boldsymbol{x})e^{i\mathbf{k}\cdot\boldsymbol{x}}\left(\boldsymbol{\nabla}\psi^*_{n_2\,\mathbf{q}_2}(\boldsymbol{x})\right), \tag{A.2.4}$$

integrating by parts and getting

$$\begin{aligned}
\mathbf{I}_{a,\mathbf{k}} &= -\int\limits_V d\boldsymbol{x}\,\psi^*_{n_2\,\mathbf{q}_2}(\boldsymbol{x})\boldsymbol{\nabla}\left(e^{i\mathbf{k}\cdot\boldsymbol{x}}\psi_{n_1\,\mathbf{q}_1}(\boldsymbol{x})\right)\\
&= -\int\limits_V d\boldsymbol{x}\,\psi^*_{n_2\,\mathbf{q}_2}(\boldsymbol{x})\left[i\mathbf{k}e^{i\mathbf{k}\cdot\boldsymbol{x}}\psi_{n_1\,\mathbf{q}_1}(\boldsymbol{x}) + e^{i\mathbf{k}\cdot\boldsymbol{x}}\boldsymbol{\nabla}\psi_{n_1\,\mathbf{q}_1}(\boldsymbol{x})\right]\\
&= -i\mathbf{k}\int\limits_V d\boldsymbol{x}\,\psi^*_{n_2\,\mathbf{q}_2}(\boldsymbol{x})e^{i\mathbf{k}\cdot\boldsymbol{x}}\psi_{n_1\,\mathbf{q}_1}(\boldsymbol{x}) - \int\limits_V d\boldsymbol{x}\,\psi^*_{n_2\,\mathbf{q}_2}(\boldsymbol{x})e^{i\mathbf{k}\cdot\boldsymbol{x}}\boldsymbol{\nabla}(\psi_{n_1\,\mathbf{q}_1}(\boldsymbol{x}))\\
&= \frac{-i}{\hbar}\left[\hbar\mathbf{k}\left\langle n_2\,\mathbf{q}_2\right| e^{i\mathbf{k}\cdot\boldsymbol{x}}\left|n_1\,\mathbf{q}_1\right\rangle + \left\langle n_2\,\mathbf{q}_2\right| e^{i\mathbf{k}\cdot\boldsymbol{x}}\mathbf{p}\left|n_1\,\mathbf{q}_1\right\rangle\right].
\end{aligned} \tag{A.2.5}$$

Note that I've discarded the surface term[1]. plugging it back to $\mathbf{I}(2,1,\mathbf{k})$ and getting

$$\mathbf{I}(2,1,\mathbf{k}) = \frac{i}{\hbar}\left[2\left\langle n_2\,\mathbf{q}_2\right| e^{i\mathbf{k}\cdot\boldsymbol{x}}\mathbf{p}\left|n_1\,\mathbf{q}_1\right\rangle + \hbar\mathbf{k}\left\langle n_2\,\mathbf{q}_2\right| e^{i\mathbf{k}\cdot\boldsymbol{x}}\left|n_1\,\mathbf{q}_1\right\rangle\right]. \tag{A.2.6}$$

---

[1] It can be shown that the surface term vanishes due to the periodicity of the Bloch wave functions (Born-Von Karman boundary conditions) and because the $\mathbf{k}$ vectors can be taken to be periodic with the bulk, namely $\mathbf{k} = \sum_{i=1}^{3} \frac{m_i}{N_i}\mathbf{b}_i$.

A.3

To evaluate the following expression

$$\Big[e^{i\mathbf{k}_1\cdot\boldsymbol{x}}(\mathbf{p}\cdot\hat{e}_i), e^{i\mathbf{k}_2\cdot\boldsymbol{x}}(\mathbf{p}\cdot\hat{e}_j)\Big], \tag{A.3.1}$$

I will use the identity

$$[AB, CD] = A[B,C]D + [A,C]BD + CA[B,D] + C[A,D]B, \tag{A.3.2}$$

and get

$$\begin{aligned}
&\Big[e^{i\mathbf{k}_1\cdot\boldsymbol{x}}(\mathbf{p}\cdot\hat{e}_i), e^{i\mathbf{k}_2\cdot\boldsymbol{x}}(\mathbf{p}\cdot\hat{e}_j)\Big] \\
&= e^{i\mathbf{k}_1\cdot\boldsymbol{x}}\Big[(\mathbf{p}\cdot\hat{e}_i), e^{i\mathbf{k}_2\cdot\boldsymbol{x}}\Big](\mathbf{p}\cdot\hat{e}_j) + \Big[e^{i\mathbf{k}_1\cdot\boldsymbol{x}}, e^{i\mathbf{k}_2\cdot\boldsymbol{x}}\Big](\mathbf{p}\cdot\hat{e}_i)(\mathbf{p}\cdot\hat{e}_j) \\
&+ e^{i\mathbf{k}_2\cdot\boldsymbol{x}}e^{i\mathbf{k}_1\cdot\boldsymbol{x}}[(\mathbf{p}\cdot\hat{e}_i),(\mathbf{p}\cdot\hat{e}_j)] + e^{i\mathbf{k}_2\cdot\boldsymbol{x}}\Big[e^{i\mathbf{k}_1\cdot\boldsymbol{x}},(\mathbf{p}\cdot\hat{e}_j)\Big](\mathbf{p}\cdot\hat{e}_i) \\
&= e^{i\mathbf{k}_1\cdot\boldsymbol{x}}\Big[(\mathbf{p}\cdot\hat{e}_i), e^{i\mathbf{k}_2\cdot\boldsymbol{x}}\Big](\mathbf{p}\cdot\hat{e}_j) - e^{i\mathbf{k}_2\cdot\boldsymbol{x}}\Big[(\mathbf{p}\cdot\hat{e}_j), e^{i\mathbf{k}_1\cdot\boldsymbol{x}}\Big](\mathbf{p}\cdot\hat{e}_i).
\end{aligned} \tag{A.3.3}$$

To proceed, I use the following identity

$$[\mathbf{p}, V(\boldsymbol{x})] = -i\hbar\boldsymbol{\nabla}V(\boldsymbol{x}), \tag{A.3.4}$$

and I find that

$$\Big[(\mathbf{p}\cdot\hat{e}_i), e^{i\mathbf{k}_2\cdot\boldsymbol{x}}\Big] = -i\hbar\left(\boldsymbol{\nabla}e^{i\mathbf{k}_2\cdot\boldsymbol{x}}\right)\cdot\hat{e}_i = (\hbar\mathbf{k}_2\cdot\hat{e}_i)\, e^{i\mathbf{k}_2\cdot\boldsymbol{x}}, \tag{A.3.5}$$

and so I get

$$\Big[e^{i\mathbf{k}_1\cdot\boldsymbol{x}}(\mathbf{p}\cdot\hat{e}_i), e^{i\mathbf{k}_2\cdot\boldsymbol{x}}(\mathbf{p}\cdot\hat{e}_j)\Big] = e^{i(\mathbf{k}_1+\mathbf{k}_2)\cdot\boldsymbol{x}}\left[(\hbar\mathbf{k}_2\cdot\hat{e}_i)(\mathbf{p}\cdot\hat{e}_j) - (\hbar\mathbf{k}_1\cdot\hat{e}_j)(\mathbf{p}\cdot\hat{e}_i)\right]. \tag{A.3.6}$$

B Matrix elements calculation in the Wannier basis

Here I review general remarks regarding the representation of matrix elements in the Wannier basis. A matrix element in the Bloch basis, can be expressed by a superposition of matrix elements in the Wannier basis.

$$\langle n_1\,\mathbf{q}_1|\,\hat{O}\,|n_2\,\mathbf{q}_2\rangle = \frac{1}{N}\sum_{\mathbf{R}_1\,\mathbf{R}_2} e^{-i(\mathbf{q}_1\cdot\mathbf{R}_1-\mathbf{q}_2\cdot\mathbf{R}_2)}\,\langle W_{n_1}|\,T(-\mathbf{R}_1)\hat{O}T(\mathbf{R}_2)\,|W_{n_2}\rangle\,. \tag{B.1}$$

If the operator being evaluated strictly depend on space ($\hat{O}=\hat{O}(\boldsymbol{x})$) I get

$$\begin{aligned}
&\langle n_1\,\mathbf{q}_1|\,\hat{O}\,|n_2\,\mathbf{q}_2\rangle\\
&=\frac{1}{N}\sum_{\mathbf{R}_1\,\mathbf{R}_2} e^{-i(\mathbf{q}_1\cdot\mathbf{R}_1-\mathbf{q}_2\cdot\mathbf{R}_2)}\,\langle W_{n_1}|\,T(-\mathbf{R}_1)\hat{O}(\boldsymbol{x})T(\mathbf{R}_2)\,|W_{n_2}\rangle\\
&=\frac{1}{N}\sum_{\mathbf{R}_1\,\mathbf{R}_2} e^{-i(\mathbf{q}_1\cdot\mathbf{R}_1-\mathbf{q}_2\cdot\mathbf{R}_2)}\,\langle W_{n_1}|\,T(-\mathbf{R}_1)\hat{O}(\boldsymbol{x})T(\mathbf{R}_1)T(-\mathbf{R}_1)T(\mathbf{R}_2)\,|W_{n_2}\rangle\\
&=\frac{1}{N}\sum_{\mathbf{R}_1\,\mathbf{R}_2} e^{-i(\mathbf{q}_1\cdot\mathbf{R}_1-\mathbf{q}_2\cdot\mathbf{R}_2)}\,\langle W_{n_1}|\,\hat{O}(\boldsymbol{x}+\mathbf{R}_1)T(\mathbf{R}_2-\mathbf{R}_1)\,|W_{n_2}\rangle
\end{aligned} \tag{B.2}$$

The matrix elements can be written in a different way, by saying that

$$\langle W_{n_1}|\,T(-\mathbf{R}_1)\hat{O}T(\mathbf{R}_2)\,|W_{n_2}\rangle = \sum_{\mathbf{R}_3}\delta_{\mathbf{R}_1-\mathbf{R}_2,\mathbf{R}_3}\,\langle W_{n_1}|\,T(-(\mathbf{R}_2+\mathbf{R}_3))\hat{O}T(\mathbf{R}_2)\,|W_{n_2}\rangle\,, \tag{B.3}$$

inserting this back to $\langle n_1\,\mathbf{q}_1|\,\hat{O}\,|n_2\,\mathbf{q}_2\rangle$ I get

$$\begin{aligned}
&\langle n_1\,\mathbf{q}_1|\,\hat{O}\,|n_2\,\mathbf{q}_2\rangle\\
&=\frac{1}{N}\sum_{\mathbf{R}_3}\sum_{\mathbf{R}_1\,\mathbf{R}_2}\delta_{\mathbf{R}_1-\mathbf{R}_2,\mathbf{R}_3}e^{-i(\mathbf{q}_1\cdot\mathbf{R}_1-\mathbf{q}_2\cdot\mathbf{R}_2)}\,\langle W_{n_1}|\,T(-(\mathbf{R}_2+\mathbf{R}_3))\hat{O}T(\mathbf{R}_2)\,|W_{n_2}\rangle\\
&\langle n_1\,\mathbf{q}_1|\,\hat{O}\,|n_2\,\mathbf{q}_2\rangle = \sum_{\mathbf{R}_3}e^{-i\mathbf{q}_1\cdot\mathbf{R}_3}\frac{1}{N}\sum_{\mathbf{R}_2}e^{-i(\mathbf{q}_1-\mathbf{q}_2)\cdot\mathbf{R}_2}\,\langle W_{n_1}|\,T(-(\mathbf{R}_2+\mathbf{R}_3))\hat{O}T(\mathbf{R}_2)\,|W_{n_2}\rangle\,.
\end{aligned} \tag{B.4}$$

There are 3 types of matrix elements of interest:

$$\begin{aligned}
&\textbf{1.}\ \langle n_1\,\mathbf{q}_1|\,e^{i\mathbf{k}\cdot\boldsymbol{x}}\,|n_2\,\mathbf{q}_2\rangle\,.\\
&\textbf{2.}\ \langle n_1\,\mathbf{q}_1|\,e^{i\mathbf{k}\cdot\boldsymbol{x}}\mathbf{p}\,|n_2\,\mathbf{q}_2\rangle\,.\\
&\textbf{3.}\ \langle n_1\,\mathbf{q}_1|\,\mathbf{p}\,|n_2\,\mathbf{q}_2\rangle\,.
\end{aligned} \tag{B.5}$$

I will consider each case separately,

Case 1:

$$\begin{aligned}
&\langle n_1\,\mathbf{q}_1|\,e^{i\mathbf{k}\cdot\boldsymbol{x}}\,|n_2\,\mathbf{q}_2\rangle\\
&=\sum_{\mathbf{R}_3}e^{-i\mathbf{q}_1\cdot\mathbf{R}_3}\frac{1}{N}\sum_{\mathbf{R}_2}e^{-i(\mathbf{q}_1-\mathbf{q}_2)\cdot\mathbf{R}_2}\,\langle W_{n_1}|\,T(-(\mathbf{R}_2+\mathbf{R}_3))e^{i\mathbf{k}\cdot\boldsymbol{x}}T(\mathbf{R}_2)\,|W_{n_2}\rangle\,,
\end{aligned} \tag{B.6}$$

I use

$$T(-\mathbf{R}_1)e^{i\mathbf{k}\cdot\boldsymbol{x}}T(\mathbf{R}_2) = e^{i\mathbf{k}\cdot(\boldsymbol{x}+\mathbf{R}_1)}T(\mathbf{R}_2-\mathbf{R}_1) = e^{i\mathbf{k}\cdot\mathbf{R}_1}e^{i\mathbf{k}\cdot\boldsymbol{x}}T(\mathbf{R}_2-\mathbf{R}_1), \tag{B.7}$$

$$\begin{aligned} T(-(\mathbf{R}_2+\mathbf{R}_3))e^{i\mathbf{k}\cdot\boldsymbol{x}}T(\mathbf{R}_2) &= e^{i\mathbf{k}\cdot(\boldsymbol{x}+(\mathbf{R}_2+\mathbf{R}_3))}T(\mathbf{R}_2-(\mathbf{R}_2+\mathbf{R}_3)) \\ &= e^{i\mathbf{k}\cdot(\mathbf{R}_2+\mathbf{R}_3)}e^{i\mathbf{k}\cdot\boldsymbol{x}}T(\mathbf{R}_2-(\mathbf{R}_2+\mathbf{R}_3)) \\ T(-(\mathbf{R}_2+\mathbf{R}_3))e^{i\mathbf{k}\cdot\boldsymbol{x}}T(\mathbf{R}_2) &= e^{i\mathbf{k}\cdot(\mathbf{R}_2+\mathbf{R}_3)}e^{i\mathbf{k}\cdot\boldsymbol{x}}T(-\mathbf{R}_3), \end{aligned} \tag{B.8}$$

and get

$$\begin{aligned} \langle n_1\,\mathbf{q}_1|\,e^{i\mathbf{k}\cdot\boldsymbol{x}}\,|n_2\,\mathbf{q}_2\rangle &= \sum_{\mathbf{R}_3} e^{-i\mathbf{q}_1\cdot\mathbf{R}_3}\frac{1}{N}\sum_{\mathbf{R}_2} e^{-i(\mathbf{q}_1-\mathbf{q}_2)\cdot\mathbf{R}_2}e^{i\mathbf{k}\cdot(\mathbf{R}_2+\mathbf{R}_3)}\,\langle W_{n_1}|\,e^{i\mathbf{k}\cdot\boldsymbol{x}}T(-\mathbf{R}_3)\,|W_{n_2}\rangle\,, \\ \langle n_1\,\mathbf{q}_1|\,e^{i\mathbf{k}\cdot\boldsymbol{x}}\,|n_2\,\mathbf{q}_2\rangle &= \sum_{\mathbf{R}_3} e^{-i(\mathbf{q}_1-\mathbf{k})\cdot\mathbf{R}_3}\frac{1}{N}\sum_{\mathbf{R}_2} e^{-i(\mathbf{q}_1-\mathbf{q}_2-\mathbf{k})\cdot\mathbf{R}_2}\,\langle W_{n_1}|\,e^{i\mathbf{k}\cdot\boldsymbol{x}}T(-\mathbf{R}_3)\,|W_{n_2}\rangle\,. \end{aligned} \tag{B.9}$$

If $\mathbf{k}=\mathbf{G}$ I get

$$\langle n_1\,\mathbf{q}_1|\,e^{i\mathbf{G}\cdot\boldsymbol{x}}\,|n_2\,\mathbf{q}_2\rangle = \delta_{\mathbf{q}_1,\mathbf{q}_2}\sum_{\mathbf{R}_3} e^{-i\mathbf{q}_1\cdot\mathbf{R}_3}\,\langle W_{n_1}|\,e^{i\mathbf{G}\cdot\boldsymbol{x}}T(-\mathbf{R}_3)\,|W_{n_2}\rangle\,. \tag{B.10}$$

If $\mathbf{k}\neq\mathbf{G}$ I get

$$\langle n_1\,\mathbf{q}_1|\,e^{i\mathbf{k}\cdot\boldsymbol{x}}\,|n_2\,\mathbf{q}_2\rangle = \delta_{\mathbf{q}_1,\mathbf{q}_2+\mathbf{k}}\sum_{\mathbf{R}_3} e^{-i(\mathbf{q}_1-\mathbf{k})\cdot\mathbf{R}_3}\,\langle W_{n_1}|\,e^{i\mathbf{k}\cdot\boldsymbol{x}}T(-\mathbf{R}_3)\,|W_{n_2}\rangle\,. \tag{B.11}$$

Case 2: In this case I get a very similar result, because the momentum operator commutes with the translation operator.

If $\mathbf{k}=\mathbf{G}$ I get

$$\langle n_1\,\mathbf{q}_1|\,e^{i\mathbf{G}\cdot\boldsymbol{x}}\mathbf{p}\,|n_2\,\mathbf{q}_2\rangle = \delta_{\mathbf{q}_1,\mathbf{q}_2}\sum_{\mathbf{R}_3} e^{-i\mathbf{q}_1\cdot\mathbf{R}_3}\,\langle W_{n_1}|\,e^{i\mathbf{G}\cdot\boldsymbol{x}}\mathbf{p}T(-\mathbf{R}_3)\,|W_{n_2}\rangle\,. \tag{B.12}$$

If $\mathbf{k}\neq\mathbf{G}$ I get

$$\langle n_1\,\mathbf{q}_1|\,e^{i\mathbf{k}\cdot\boldsymbol{x}}\mathbf{p}\,|n_2\,\mathbf{q}_2\rangle = \delta_{\mathbf{q}_1,\mathbf{q}_2+\mathbf{k}}\sum_{\mathbf{R}_3} e^{-i(\mathbf{q}_1-\mathbf{k})\cdot\mathbf{R}_3}\,\langle W_{n_1}|\,e^{i\mathbf{k}\cdot\boldsymbol{x}}\mathbf{p}T(-\mathbf{R}_3)\,|W_{n_2}\rangle\,. \tag{B.13}$$

Case 3:

$$\langle n_1\,\mathbf{q}_1|\,\mathbf{p}\,|n_2\,\mathbf{q}_2\rangle = \delta_{\mathbf{q}_1,\mathbf{q}_2}\sum_{\mathbf{R}_3} e^{-i\mathbf{q}_1\cdot\mathbf{R}_3}\,\langle W_{n_1}|\,\mathbf{p}T(-\mathbf{R}_3)\,|W_{n_2}\rangle\,. \tag{B.14}$$

C Matrix elements calculation in a reduced subspace

A matrix representation of an operator $\hat{O}$ in some basis, is given by

$$\hat{O}_{nm} = \langle n| \hat{O} |m\rangle , \tag{C.0.1}$$

where I denote $|n\rangle$ as the basis of choice.

In many quantum systems, the states are spanned in an infinite dimensional space, and in such a case, the matrix representation will be infinitely large, and might not be useful. However, I can limit the problem to a finite number of states, and then the matrix representation will be finite.

C.1 In k-dimensional subspace

In this section I will work in a k-dimensional subspace, and show how it is possible to represent a complicated operator.

I start with finding the representation of the operator $f(\hat{O})$, where $\hat{O}$ is an hermitian operator and f is an analytical function. Therefore, $f(\hat{O})$ can be expressed by a Taylor power series

$$f(\hat{O}) = \sum_{j=0}^{\infty} c_j \hat{O}^j. \tag{C.1.1}$$

It is sufficient to use the matrix representation of $\hat{O}$ for us to find the matrix representation of $f(\hat{O})$. Let U be the diagonalizing unitary matrix of $\hat{O}$, such that

$$U^{\dagger} \hat{O} U = \hat{\hat{O}}, \tag{C.1.2}$$

where $\hat{\hat{O}}$ is diagonal, such that

$$\begin{cases} \langle n| U^{\dagger} \hat{O} U |n\rangle = \langle n| \hat{\hat{O}} |n\rangle = \lambda_n, \\ \langle n| U^{\dagger} \hat{O} U |m\rangle = \langle n| \hat{\hat{O}} |m\rangle = 0, \quad \text{for } n \neq m. \end{cases} \tag{C.1.3}$$

This is also true for any power of $\hat{O}$, such that

$$\begin{cases} \langle n| U^\dagger \hat{O}^j U |n\rangle = \langle n| \hat{\hat{O}}^j |n\rangle = \lambda_n^j, \\ \langle n| U^\dagger \hat{O}^j U |m\rangle = \langle n| \hat{\hat{O}}^j |m\rangle = 0, \quad \text{for } n \neq m, \end{cases} \tag{C.1.4}$$

for this reason, it is clear that

$$\begin{cases} \langle n| U^\dagger f(\hat{O}) U |n\rangle = \langle n| f(\hat{\hat{O}}) |n\rangle = f(\lambda_n), \\ \langle n| U^\dagger f(\hat{O}) U |m\rangle = \langle n| f(\hat{\hat{O}}) |m\rangle = 0, \qquad \text{for } n \neq m. \end{cases} \tag{C.1.5}$$

This means that the matrix representation of $f(\hat{O})$ can be obtained by rotating back its diagonal form

$$\langle n| f(\hat{O}) |m\rangle = \langle n| U f(\hat{\hat{O}}) U^\dagger |m\rangle \,. \tag{C.1.6}$$

This means that if I work in a reduced subspace, equipped with the diagonalizing matrix U and the eigenvalues of $\hat{O}$, I can find a matrix representation of a function of $\hat{O}$.

C.2 Evaluting the matrix elements of the nonlinear conductivity in a reduced subspace of 2 dimensions

Here, I work out the matrix representation for the momentum and position when assuming just two bands.

I assume that the Wannier states are real, and therefore

$$\begin{aligned} \boldsymbol{x} &= \begin{pmatrix} x_{11} & x_{12} \\ x_{12} & x_{22} \end{pmatrix} \hat{x} + \begin{pmatrix} y_{11} & y_{12} \\ y_{12} & y_{22} \end{pmatrix} \hat{y} + \begin{pmatrix} z_{11} & z_{12} \\ z_{12} & z_{22} \end{pmatrix} \hat{z} \,, \\ \mathbf{p} &= \begin{pmatrix} 0 & -i\pi_1 \\ i\pi_1 & 0 \end{pmatrix} \hat{x} + \begin{pmatrix} 0 & -i\pi_2 \\ i\pi_2 & 0 \end{pmatrix} \hat{y} + \begin{pmatrix} 0 & -i\pi_3 \\ i\pi_3 & 0 \end{pmatrix} \hat{z} \,, \end{aligned} \tag{C.2.1}$$

note that

$$\begin{aligned} &\langle W_1| \boldsymbol{x} |W_2\rangle = \langle W_2| \boldsymbol{x} |W_1\rangle \,, \\ &\langle W_1| \mathbf{p} |W_2\rangle = - \langle W_2| \mathbf{p} |W_1\rangle \quad \langle W_1| \mathbf{p} |W_1\rangle = \langle W_2| \mathbf{p} |W_2\rangle = 0. \end{aligned} \tag{C.2.2}$$

Moreover, the position matrix elements are all real, while the momentum matrix elements are imaginary.

I can further simplify the expression for the position operator. Before doing so, I denote the diagonal matrix elements of the position operator in the following way

$$\begin{aligned} x_{11} &= a_1, \quad x_{22} = b_1, \quad x_{12} = c_1, \\ y_{11} &= a_2, \quad y_{22} = b_2, \quad y_{12} = c_2, \\ z_{11} &= a_3, \quad z_{22} = b_3, \quad z_{12} = c_3. \end{aligned} \tag{C.2.3}$$

So the position operator is now

$$\boldsymbol{x} \cdot \hat{e}_j = x_j = \begin{pmatrix} a_j & c_j \\ c_j & b_j \end{pmatrix}. \tag{C.2.4}$$

The position operator can be further simplified by evaluating

$$\langle W_1| \, x_i x_j \, |W_2\rangle ,$$

and demand that

$$\langle W_1| \, x_i x_j \, |W_2\rangle = \langle W_1| \, x_j x_i \, |W_2\rangle . \tag{C.2.5}$$

To do so, I use the completeness relation for our subspace

$$\begin{aligned} \langle W_1| \, x_i x_j \, |W_2\rangle &= \langle W_1| \, x_i \left(|W_1\rangle \langle W_1| + |W_2\rangle \langle W_2| \right) x_j \, |W_2\rangle \\ &= \langle W_1| \, x_i \, |W_1\rangle \langle W_1| \, x_j \, |W_2\rangle + \langle W_1| \, x_i \, |W_2\rangle \langle W_2| \, x_j \, |W_2\rangle \\ &= a_i c_j + c_i b_j, \end{aligned} \tag{C.2.6}$$

but on the other hand

$$\langle W_1| \, x_i x_j \, |W_2\rangle = a_j c_i + c_j b_i. \tag{C.2.7}$$

Demanding that the two matrix elements are identical, I get

$$a_i c_j + c_i b_j = a_j c_i + c_j b_i \Rightarrow \boxed{a_j = b_j}, \tag{C.2.8}$$

and the position operator now takes the form

$$\boldsymbol{x} \cdot \hat{e}_j = x_j = \begin{pmatrix} a_j & c_j \\ c_j & a_j \end{pmatrix}. \tag{C.2.9}$$

C.2.1 Diagonalizing position and momentum operators

The diagonalizing matrices for the position and momentum are the following

$$\begin{aligned} U_{\boldsymbol{x}} &= \frac{1}{\sqrt{2}}\begin{pmatrix} 1 & 1 \\ 1 & -1 \end{pmatrix}, \\ U_{\mathbf{p}} &= \frac{1}{\sqrt{2}}\begin{pmatrix} 1 & i \\ i & 1 \end{pmatrix}, \end{aligned} \tag{C.2.10}$$

such that

$$\begin{aligned} \tilde{\boldsymbol{x}} &= U_{\boldsymbol{x}}^{\dagger}\boldsymbol{x}U_{\boldsymbol{x}} = \begin{pmatrix} \boldsymbol{a}+\boldsymbol{c} & 0 \\ 0 & \boldsymbol{a}-\boldsymbol{c} \end{pmatrix} = \begin{pmatrix} \boldsymbol{\lambda}_{\boldsymbol{x}+} & 0 \\ 0 & \boldsymbol{\lambda}_{\boldsymbol{x}-} \end{pmatrix}, \\ \tilde{\mathbf{p}} &= U_{\mathbf{p}}^{\dagger}\mathbf{p}U_{\mathbf{p}} = \begin{pmatrix} \boldsymbol{\pi} & 0 \\ 0 & -\boldsymbol{\pi} \end{pmatrix}, \end{aligned} \tag{C.2.11}$$

where

$$\begin{aligned} &\boldsymbol{a} = (a_1, a_2, a_3)\,, \quad \boldsymbol{c} = (c_1, c_2, c_3)\,, \\ &\boldsymbol{\pi} = (\pi_1, \pi_2, \pi_3)\,, \end{aligned} \tag{C.2.12}$$

and so any function of the position operator in its diagonal form is

$$f(\tilde{\boldsymbol{x}}) = \begin{pmatrix} f(\boldsymbol{\lambda}_{\boldsymbol{x}+}) & 0 \\ 0 & f(\boldsymbol{\lambda}_{\boldsymbol{x}-}) \end{pmatrix}, \tag{C.2.13}$$

and thus

$$f(\boldsymbol{x}) = U_{\boldsymbol{x}} f(\tilde{\boldsymbol{x}}) U_{\boldsymbol{x}}^{\dagger} = \frac{1}{2}\begin{pmatrix} (f(\boldsymbol{\lambda}_{\boldsymbol{x}+}) + f(\boldsymbol{\lambda}_{\boldsymbol{x}-})) & (f(\boldsymbol{\lambda}_{\boldsymbol{x}+}) - f(\boldsymbol{\lambda}_{\boldsymbol{x}-})) \\ (f(\boldsymbol{\lambda}_{\boldsymbol{x}+}) - f(\boldsymbol{\lambda}_{\boldsymbol{x}-})) & (f(\boldsymbol{\lambda}_{\boldsymbol{x}+}) + f(\boldsymbol{\lambda}_{\boldsymbol{x}-})) \end{pmatrix}. \tag{C.2.14}$$

This means

$$\begin{aligned} e^{-i\mathbf{G}\cdot\boldsymbol{x}} &= \frac{1}{2}\begin{pmatrix} \left(e^{-i\mathbf{G}\cdot\boldsymbol{\lambda}_{\boldsymbol{x}+}} + e^{-i\mathbf{G}\cdot\boldsymbol{\lambda}_{\boldsymbol{x}-}}\right) & \left(e^{-i\mathbf{G}\cdot\boldsymbol{\lambda}_{\boldsymbol{x}+}} - e^{-i\mathbf{G}\cdot\boldsymbol{\lambda}_{\boldsymbol{x}-}}\right) \\ \left(e^{-i\mathbf{G}\cdot\boldsymbol{\lambda}_{\boldsymbol{x}+}} - e^{-i\mathbf{G}\cdot\boldsymbol{\lambda}_{\boldsymbol{x}-}}\right) & \left(e^{-i\mathbf{G}\cdot\boldsymbol{\lambda}_{\boldsymbol{x}+}} + e^{-i\mathbf{G}\cdot\boldsymbol{\lambda}_{\boldsymbol{x}-}}\right) \end{pmatrix} \\ &= e^{-i\frac{1}{2}\mathbf{G}\cdot(\boldsymbol{\lambda}_{\boldsymbol{x}+}+\boldsymbol{\lambda}_{\boldsymbol{x}-})}\begin{pmatrix} \cos\left(\frac{1}{2}\mathbf{G}\cdot(\boldsymbol{\lambda}_{\boldsymbol{x}+} - \boldsymbol{\lambda}_{\boldsymbol{x}-})\right) & -i\sin\left(\frac{1}{2}\mathbf{G}\cdot(\boldsymbol{\lambda}_{\boldsymbol{x}+} - \boldsymbol{\lambda}_{\boldsymbol{x}-})\right) \\ -i\sin\left(\frac{1}{2}\mathbf{G}\cdot(\boldsymbol{\lambda}_{\boldsymbol{x}+} - \boldsymbol{\lambda}_{\boldsymbol{x}-})\right) & \cos\left(\frac{1}{2}\mathbf{G}\cdot(\boldsymbol{\lambda}_{\boldsymbol{x}+} - \boldsymbol{\lambda}_{\boldsymbol{x}-})\right) \end{pmatrix}. \end{aligned} \tag{C.2.15}$$

note that

$$\begin{aligned}\frac{1}{2}(\boldsymbol{\lambda}_{\boldsymbol{x}+} + \boldsymbol{\lambda}_{\boldsymbol{x}-}) = \boldsymbol{a} = \langle W_1 | \, \boldsymbol{x} \, | W_1 \rangle = \langle W_2 | \, \boldsymbol{x} \, | W_2 \rangle \, , \\ \frac{1}{2}(\boldsymbol{\lambda}_{\boldsymbol{x}+} - \boldsymbol{\lambda}_{\boldsymbol{x}-}) = \boldsymbol{c} = \langle W_1 | \, \boldsymbol{x} \, | W_2 \rangle = \langle W_2 | \, \boldsymbol{x} \, | W_1 \rangle \, .\end{aligned} \tag{C.2.16}$$

Using these relations I get

$$e^{-i\mathbf{G}\cdot\boldsymbol{x}} = e^{-i\mathbf{G}\cdot\boldsymbol{a}} \begin{pmatrix} \cos(\mathbf{G}\cdot\boldsymbol{c}) & -i\sin(\mathbf{G}\cdot\boldsymbol{c}) \\ -i\sin(\mathbf{G}\cdot\boldsymbol{c}) & \cos(\mathbf{G}\cdot\boldsymbol{c}) \end{pmatrix} . \tag{C.2.17}$$

Now I can evaluate $e^{-i\mathbf{G}\cdot\boldsymbol{x}}\mathbf{p}\cdot\hat{e}_j = e^{-i\mathbf{G}\cdot\boldsymbol{x}}\mathbf{p}_j$ and find

$$\begin{aligned} e^{-i\mathbf{G}\cdot\boldsymbol{x}}\mathbf{p}_j = e^{-i\mathbf{G}\cdot\boldsymbol{x}} &= e^{-i\mathbf{G}\cdot\boldsymbol{a}} \begin{pmatrix} \cos(\mathbf{G}\cdot\boldsymbol{c}) & -i\sin(\mathbf{G}\cdot\boldsymbol{c}) \\ -i\sin(\mathbf{G}\cdot\boldsymbol{c}) & \cos(\mathbf{G}\cdot\boldsymbol{c}) \end{pmatrix} \begin{pmatrix} 0 & -i\pi_j \\ i\pi_j & 0 \end{pmatrix} \\ &= e^{-i\mathbf{G}\cdot\boldsymbol{a}} \begin{pmatrix} \pi_j\sin(\mathbf{G}\cdot\boldsymbol{c}) & -i\pi_j\cos(\mathbf{G}\cdot\boldsymbol{c}) \\ i\pi_j\cos(\mathbf{G}\cdot\boldsymbol{c}) & -\pi_j\sin(\mathbf{G}\cdot\boldsymbol{c}) \end{pmatrix} . \end{aligned} \tag{C.2.18}$$

תקציר

בעבודה זו, פיתחתי תאור תיאורטי עבור התגובה האופטית הלא ליניארית של גבישים לקרינת רנטגן ואור נראה, והתמקדתי בתאור התגובה עבור תהליך "המרת תדר פרמטרית" של קרינת רנטגן אל אור נראה. כמו כן, בחנתי את התלות האנרגטית של תגובה לא ליניארית זו, והערכתי את התרומה המגיעה מהאינטרקציה הבין אטומית עבור מקרה של שני פסי אנרגיה. הגישה התיאורטית מסתמכת על תורת ההפרעות בפורמליזם של מטריצת הצפיפות. מכיוון שגישה זו מסתמכת על פרמטרים סטטיסטיים, היא מאפשרת גישה לחקר תכונות סטטיסטיות כגון: תלות טמפרטורה, אנרגית פרמי, התפלגות אכלוס, וצפיפות מצבי האנרגיה בחומר.

תאורים מוקדמים של התגובה הלא ליניארית בתחום תדרים זה, לקחו בחשבון את המחזוריות של המבנה הגבישי, אך לא את מבנה הפסים של החומר. תחת אותן הנחות, הצליחו תיאוריות אלו לקשר בין התגובה הלא ליניארית למידע המיקרוסקופי בחומר אודות אלקטרוני הערכיות ברזולוציה אטומית.

בניגוד לכך, עבודה זו מעידה על כך שהאינטרקציה גם מכילה מידע הקשור לפוטנציאל המחזורי בחומר, למשל מבנה הפסים, ומתארת את התנאים הנדרשים כדי להפריד בין שתי תרומות אלו. כמו כן, התיאוריה חוזה שקיימת תלות קיטוב חדשה, אשר ניתן להשתמש בה כדי לחקור תרומות שונות של האינטרקציה, ובכך לספק מידע נוסף על החומר.

היות והתיאוריה מעידה שמקור האינטרקציה נובע גם מתרומה מתכונות של מבנה הפסים, וגם מאינטרקציות בסקלות אטומיות, היא יכולה לסלול את הדרך לשימוש באפקטים לא ליניארים בקרני רנטגן ואורכי גל ארוכים יותר כדי לחשוף מידע ספקטרוסקופי רחב יחד עם מידע מבני אודות אלקטרוני הערכיות.

עבודה זו נעשתה בהדרכתו של

פרופ׳ שרון שוורץ

מן המחלקה לפיזיקה של אוניברסיטת בר־אילן

אוניברסיטת בר־אילן

תגובה אופטית לא ליניארית של חומרים מחזוריים בתחום קרני הרנטגן

רון כהן

עבודה זו הוגשה כחלק מהדרישות לשם קבלת תואר מוסמך
במחלקה לפיזיקה של אוניברסיטת בר־אילן

רמת גן תש״פ